AD-A181 488 DYNAMIC ANALYSIS OF THE FLEXIBLE BOOM IN THE N-ROSS SATELLITE(U) NAVAL POSTGRADUATE SCHOOL MONTEREY CA C S KANG MAR 87 1/2

UNCLASSIFIED F/G 22/1 NL

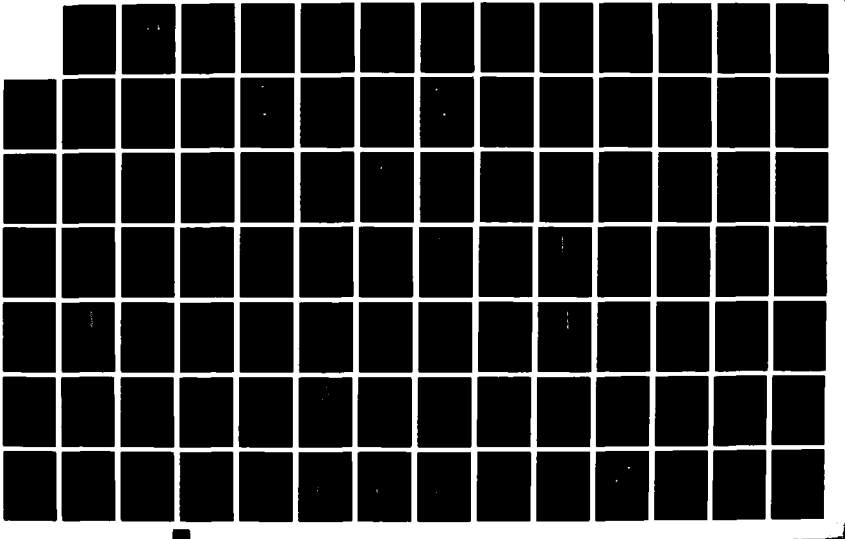

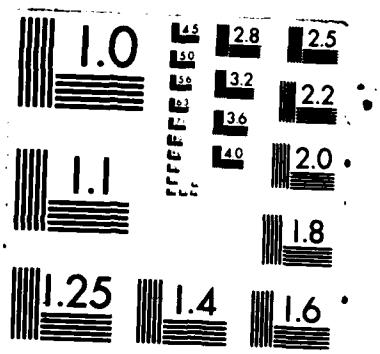
1.0
1.1
1.25
1.4
1.6
1.8
2.0
2.2
2.5
2.8
3.2
3.6
4.0
4.5
5.0
5.6
6.3

(2)

NAVAL POSTGRADUATE SCHOOL

Monterey, California

THESIS

DYNAMIC ANALYSIS OF THE FLEXIBLE BOOM
IN THE N-ROSS SATELLITE

by

Kang, Choong Soon

March 1987

Thesis Advisor Young S. Shin
Co-Advisor Kilsoo Kim

SECURITY CLASSIFICATION OF THIS PAGE

AD-A181 488

REPORT DOCUMENTATION PAGE

1a REPORT SECURITY CLASSIFICATION UNCLASSIFIED	1b RESTRICTIVE MARKINGS
2a SECURITY CLASSIFICATION AUTHORITY	3 DISTRIBUTION/AVAILABILITY OF REPORT Approved for public release; distribution is unlimited
2b DECLASSIFICATION/DOWNGRADING SCHEDULE	
4 PERFORMING ORGANIZATION REPORT NUMBER(S)	5 MONITORING ORGANIZATION REPORT NUMBER(S)
6a NAME OF PERFORMING ORGANIZATION Naval Postgraduate School 6b OFFICE SYMBOL (If applicable) Code 69	7a NAME OF MONITORING ORGANIZATION Naval Postgraduate School
6c ADDRESS (City, State, and ZIP Code) Monterey, California 93943-5000	7b ADDRESS (City, State, and ZIP Code) Monterey, California 93943-5000
8a NAME OF FUNDING/SPONSORING ORGANIZATION Space & Naval Warfare Systems Command 8b OFFICE SYMBOL (If applicable)	9 PROCUREMENT INSTRUMENT IDENTIFICATION NUMBER
8c ADDRESS (City, State, and ZIP Code) Washington, D.C. 20363-5100	10 SOURCE OF FUNDING NUMBERS PROGRAM ELEMENT NO / PROJECT NO / TASK NO / WORK UNIT ACCESSION NO

11 TITLE (Include Security Classification)

Dynamic Analysis of the Flexible Boom in the N-ROSS Satellite

12 PERSONAL AUTHOR(S)

Kang, Choong Soon

13a TYPE OF REPORT	13b TIME COVERED	14 DATE OF REPORT (Year, Month, Day)	15 PAGE COUNT
Masters and Engineer's Thesis	FROM _____ TO _____	1987, March	148

16 SUPPLEMENTARY NOTATION

17 COSATI CODES			18 SUBJECT TERMS (Continue on reverse if necessary and identify by block number)
FIELD	GROUP	SUB-GROUP	Spacecraft, Flexible body, Dynamics

19 ABSTRACT (Continue on reverse if necessary and identify by block number)

Accurate ocean data is essential for successful fleet operation. The N-ROSS Satellite, which is being developed for this mission, will carry a Low Frequency Microwave Radiometer (LFMR). The LFMR consists of large flexible reflector and boom and spins at 15 r.p.m. The effects of the flexibility of the boom, the spin-up procedure and the structural damping on the pointing error of the LFMR are investigated by performing the dynamic simulation using the Dynamic Simulation Language. Two cases of boom material, Aluminum Alloy and the Graphite epoxy composite material, are analyzed and the results are compared. The simulation and analysis results are presented in graphical forms.

20 DISTRIBUTION/AVAILABILITY OF ABSTRACT	21 ABSTRACT SECURITY CLASSIFICATION
☒ UNCLASSIFIED/UNLIMITED ☐ SAME AS RPT ☐ DTIC USERS	UNCLASSIFIED
22a NAME OF RESPONSIBLE INDIVIDUAL Young S. Shin and Kilsoo Kim	22b TELEPHONE (Include Area Code) (408)646-2568/2288 / 22c OFFICE SYMBOL 69Sg/69Ki

DD FORM 1473, 84 MAR 83 APR edition may be used until exhausted
All other editions are obsolete

SECURITY CLASSIFICATION OF THIS PAGE
UNCLASSIFIED

Approved for public release; distribution is unlimited.

Dynamic Analysis of The Flexible Boom In The N-ROSS Satellite

by

Kang, Choong Soon
Major, Republic of Korea Air Force
B.S., Korea Airforce Academy, 1978

Submitted in partial fulfillment of the
requirements for the degrees of

MASTER OF SCIENCE IN MECHANICAL ENGINEERING
and
MECHANICAL ENGINEER

from the

NAVAL POSTGRADUATE SCHOOL
March 1987

Author: _____
Kang, Choong Soon

Approved by: _____
Young S. Shin, Thesis Advisor

_____
Kilsoo Kim, Co-Advisor

_____
Anthony Healy, Chairman,
Department of Mechanical Engineering

_____
G. E. Schacher,
Dean of Science and Engineering

ABSTRACT

Accurate ocean data is essential for successful fleet operation. The N-ROSS Satellite, which is being developed for this mission, will carry a Low Frequency Microwave Radiometer (LFMR). The LFMR consists of large flexible reflector and boom and spins at 15 r.p.m. The effects of the flexibility of the boom, the spin-up procedure and the structural damping on the pointing error of the LFMR are investigated by performing the dynamic simulation using the Dynamic Simulation Language. Two cases of boom material, Aluminum Alloy and the Graphite/epoxy composite material, are analyzed and the results are compared. The simulation and analysis results are presented in graphical forms.

TABLE OF CONTENTS

LIST OF TABLES

LIST OF FIGURES

ACKNOWLEDGEMENTS

I would like to express my appreciation to my thesis advisor, Professor Young Sik Shin and Dr. Kil Soo Kim for their invaluable guidance, advice and enthusiastic support towards the completion of this thesis.

I would also like to thank Professor Liang Wey Chang for his kindness and constructive comments about formulating the equations of motion and simulating discussions on this thesis.

My special appreciation is extended to the Korean Government for offering the opportunity to study in Naval Post Graduates School. I wish to thank a lot of American fellow students whose help was sometimes imperative for understanding the computer simulations.

I also express my sincere gratitude to my wife, Young Seop and my son, Dong In for their patience with long hours and her assistance and encouragement in my frustrations.

I. INTRODUCTION

A. BACKGROUND

Accurate ocean weather prediction is essential for successful fleet operations. The NANY needs superior data collection capability to obtain the data density and reliability necessary to produce consistently accurate forecasts and oceanographic data. However present prediction models are limited by the quality and quantity of input data which come mainly from ships. The obvious approach to satisfy these purpose can be derived from satellite observations. Therefore, the NAVY planned the construction of the Navy Remote Ocean Sensing System (N - ROSS). [Ref. 1] This system consists of satellites which scan the earth surface and provide the fleet with timely worldwide knowledge of ocean data such as seasurface wind speed, wind direction, seasurface temperature, ice edge detection, ocean wave height and ocean photograpy. [Ref. 2] To satisfy the mission requirements the N - ROSS Satellite will carry several sensors. Among these sensors the Low Frequency Microwave Radiometer (LFMR) is the most important and the most interesting from the dynamics of the spacecraft point of view. The function of the LFMR is scanning the earth surface and measure the seasurface temperature. To increase the scanning area the deployable reflector spins at 15 r.p.m. The sizes of this LFMR reflector and boom are relatively large compared to the N - ROSS Satellite itself. So the weight of this boom should be light, which makes the boom flexible. By this reason, there exist certain extent of deflection at the tip of the LFMR boom and this boom vibrates when this boom is spinning. Deflection and vibration due to this elastic deformation induce pointing error of the reflector in elevation and azimuth angle. However there is strict pointing error requirement of the LFMR. [Ref. 2] Therefore analysis of the flexible LFMR boom which supports the sensor payload is imperative for this research.

B. STATEMENT OF PROBLEM

The traditional approach to dynamics of a boom system is based on the assumption that the systems are composed of rigid bodies. Until recently, only a rigid body motion was assumed for the analysis. However, the flexible system includes a small elastic deformation as well as a large motion. These small elastic deformations include bending, twisting and axial extension. Development of a dynamic model

including flexibility demands more accuracy for the system responses. Without considering these small motion of a boom, we cannot expect a certain accuracy to maintain a spacecraft attitude and pointing control. [Ref. 3] Recently, efforts have been made to control maneuvers of mechanical systems which can not be adequately modeled using a rigid body assumption for all or some of the system components, especially in the fields of satellites, [Ref. 4: pp. 257-264]

Therefore, the development of a good dynamic model of a flexible system, an efficient dynamic equations formulation method and a good dynamic simulation schem are essential for the analysis of and identification of potential problems in the flexible LFMR system.

C. THESIS OUTLINE

In Chapter II, the development of an analytic model for the Lower Frequency Microwave Radiometer (LFMR) reflector boom in 3-dimensional motion is described. The large motion due to rotation is described by an equivalent rigid boom motion and elastic deflection of a flexible boom relative to the equivalent rigid boom motion is expressed using the mode superposition technique. The dynamical equations for this model are formulated using the Lagrange's method.

In Chapter III, The computer implementations for the solution of the obtained equations are explained. For the modal analysis of the system, NAsa STRuctural ANalysis (NASTRAN) computer program was used and Dynamic Simulation Language (DSL) was applied to solve the simultaneous, nonlinear, ordinary differential equations. The LINPACK subroutines DGEFA and DGESL are also used in the dynamic simulation.

In Chapter IV, simulation results are presented to investigate the deflection and pointing error of the LFMR. Comparisons are made by changing the torque input condition. The problems considered are 1) the effects of spin-up procedure on the pointing error of the LFMR reflector; 2) the effect of damping on the settling time of pointing error; 3) the equilibrium configuration of LFMR booms due to constant rotating speeds For the comparison purpose, two kinds of material, aluminum alloy and composite material, were assumed as the LFMR boom materials.

In chapter V, Conclusions are made from the research and some recommendations for future work in the area of the dynamic analysis of the flexible LFMR reflector boom system are given.

II. FORMULATIONS OF DYNAMIC EQUATIONS

A. INTRODUCTION

In this Chapter, the dynamical equations of motion for the LFMR system which rotates in three dimensional space is developed. The 2-dimensional planar motion of the same boom was also studies and are presented in Appendix A. A simple dynamic model of the LFMR system is developed for this analysis. The Lagrangian approach and the mode superposition technique are used for the formulation of the dynamic equations of the flexible LFMR system.

B. DESCRIPTIONS OF THE MODEL

The LFMR shown in Fig. 2.1 consists of four structures: a reflector, an upper reflector boom, a lower reflector boom and an electronics box. The reflector is attached to the top of the upper reflector boom. The upper reflector boom and the lower reflector boom is connected by a boom hinge. The electronics box is attached to the bottom end of the lower boom.

For our analysis, the deployable reflector is modeled as a concentrated mass at the tip of the upper reflector. We assume the boom hinge which connects the two booms is stiff and firm and there is no relative motion between the booms after the deployment of the LFMR boom. Therefore we consider the whole system (reflector, booms, boom hinge) as a one body system.

The LFMR system is connected to the Main Bus of the N - ROSS Satellite by a Spacecraft Boom. The attitude of the N - ROSS Satellite is controlled by a Attitude Determination And Control System (ADACS) very accurately. [Ref. 5] Therefore, it is assumed that the spin axis and the base is remain fixed in the reference frame fixed to the N - ROSS Satellite. The N - ROSS Spacecraft moves on a circular orbit with the spin axis always pointing the earth center. Hence, the gravitational force is in equilibrium with the centrifugal force in the orbit plane: the LFMR system is in zero-g environment. Therefore, in the dynamic model of the present studies, the reference frame fixed to the N - ROSS Spacecraft is assumed the Newtonian (inertial) reference frame and the LFMR system is in zero-g environment.

From the above assumptions the dynamic model of the LFMR system is defined as shown in Figure 2.2. The global coordinates X, Y, Z is fixed in the inertial reference

frame and a moving coordinate x, y, z (local coordinates), which is a body fixed coordinate system, is defined as shown in Figure 2.2. The body fixed coordinate system (local coordinates) is attached to the base O. The local z-axes and the global Z-axes are the common axis of rotation. The local x, y-axes and the global X, Y-axes are in the same plane with angle difference θ.

C. LAGRANGE'S EQUATION

For any system there must be same numbers of independent coordinates as the degrees of the freedom of the system to completely describe the motion of the system. The choice of coordinates is important in dynamic analysis. Such independent coordinates are called *generalized coordinates* and are denoted by the letter q_r. For a system with a set of n independent generalized coordinates q_r (r = 1, 2, 3, ... , n), Lagrange's equations are expressed as [Ref. &7]

$$\frac{d}{dt}\left[\frac{\partial T}{\partial \dot{q}_k}\right] - \frac{\partial T}{\partial q_k} + \frac{\partial U}{\partial q_k} = Q_k \qquad \text{(eqn 2.1)}$$

(k = 1, 2, 3, ... , n)

where T is the kinetic energy, U is the potential energy and Q_k is the generalized forces which is defined as follows

$$Q_i = \sum_i F_j \frac{\delta R_j}{\delta q_i} \qquad \text{(eqn 2.2)}$$

The dot over a variable means derivative with respect to time. F_j is the force acting on particle j and R_j is the instantaneous position of particle *j* and may be expressed in terms of generalized coordinates

$$R_j = R_j (q_1, q_2, q_3, ..., q_n) \qquad \text{(eqn 2.3)}$$

and δR_j is the virtual displacement of the particle.

To describe the motion of the LFMR boom system which composed of a large slow motion due to rotation and a small fast motion due to elastic vibration, two kinds of generalized coordinates are defined. One is θ for rotation of boom and others are q_h

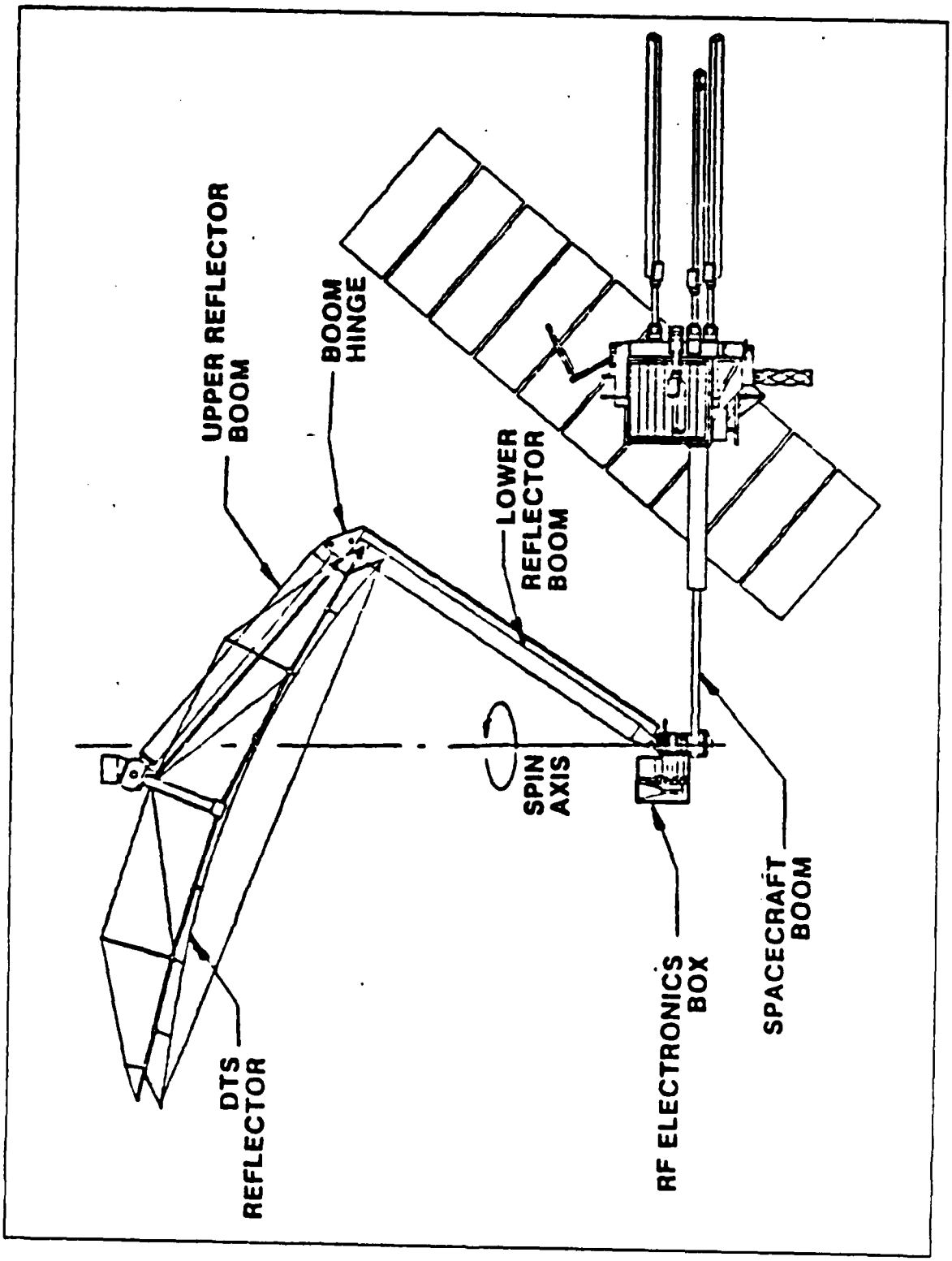

Figure 2.1 N-ROSS Baseline Configuration.

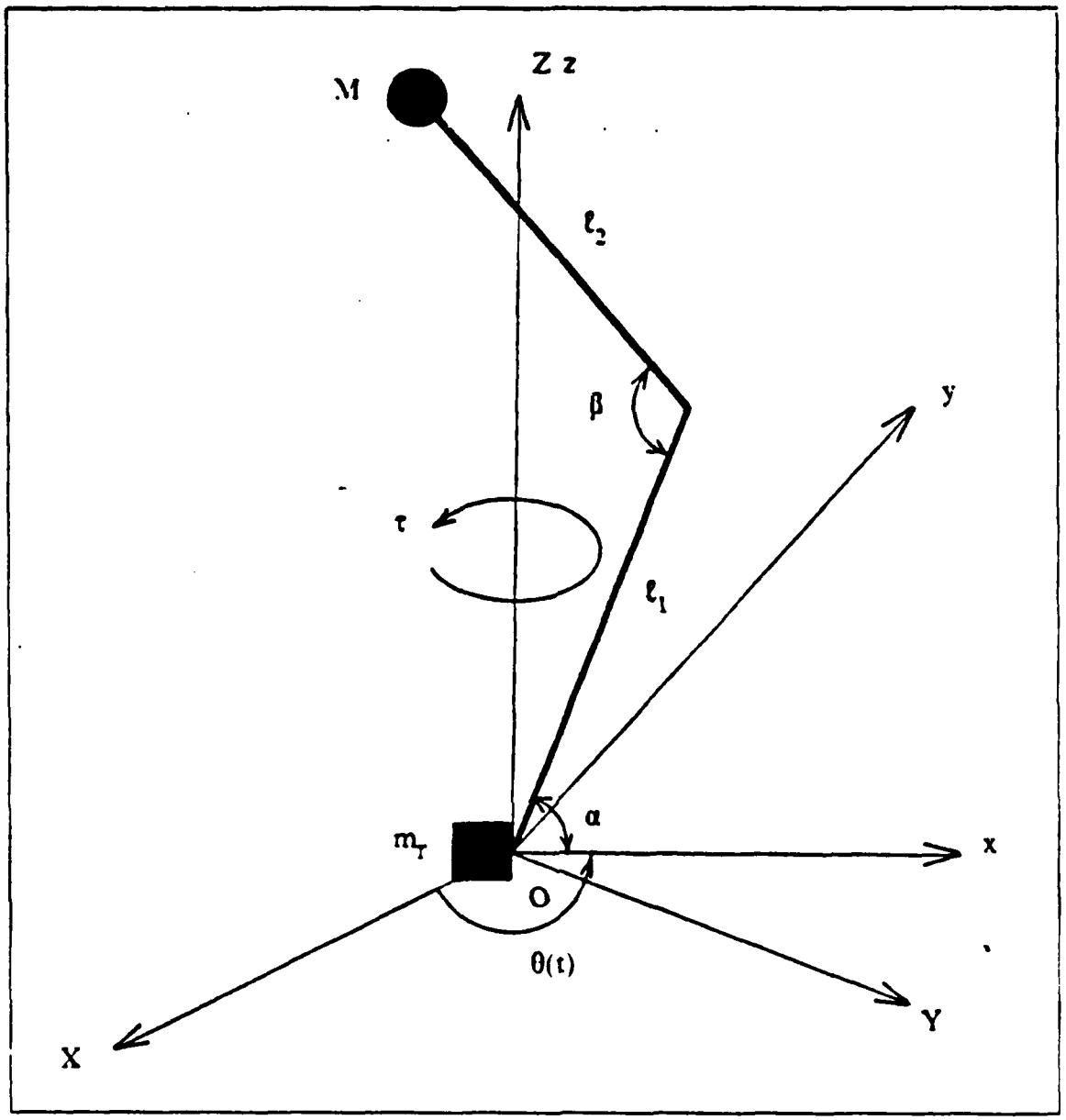

Figure 2.2 Modeling of LFMR boom system.

(h = 1, 2, 3, ... , n) for *h-th* mode generalized displacement, where n is number of modes.

Now Lagrange's equation 2.1 is rewritten as

$$\frac{d}{dt}\left[\frac{\partial T}{\partial \dot{\theta}}\right] - \frac{\partial T}{\partial \theta} + \frac{\partial U}{\partial \theta} = Q_r \qquad \text{(eqn 2.4)}$$

and

$$\frac{d}{dt}\left[\frac{\partial T}{\partial \dot{q}_h}\right] - \frac{\partial T}{\partial q_h} + \frac{\partial U}{\partial q_h} = Q_h \qquad \text{(eqn 2.5)}$$

(h = 1, 2, 3, ... , n)

The external force acting on the LFMR system is assumed the torque τ by a torque motor at the root of the boom. The contribution of this torque to the generalized forces is $Q_r = \tau$ and this torque does not contribute to Q_h. Damping forces are assumed equal to the modal damping value in this analysis. Since the modal damping values can be measured easily. Therefore the contribution of damping forces to the generalized forces Q_h can be obtained using a dissipation function.

$$D = \frac{1}{2} \sum_i 2 \zeta_i \omega_i M_i \dot{q}_i^2(t) \qquad \text{(eqn 2.6)}$$

with $$Q_h = -\frac{\partial D}{\partial \dot{q}_h}$$

$$= -2 \zeta_h \omega_h M_h \dot{q}_h$$

where

ζ_h : modal damping ratio of *h-th* mode

ω_h : the natural frequency of *h-th* mode

M_h : the modal mass of *h-th* mode

Then equation 2.4 and 2.5 finally written as

$$\frac{d}{dt}\left[\frac{\partial T}{\partial \dot{\theta}}\right] - \frac{\partial T}{\partial \theta} + \frac{\partial U}{\partial \theta} = \tau \qquad \text{(eqn 2.7)}$$

and

$$\frac{d}{dt}\left[\frac{\partial T}{\partial \dot{q}_h}\right] - \frac{\partial T}{\partial q_h} + \frac{\partial U}{\partial q_h} = -2 \zeta_h \omega_h M_h \dot{q}_h \qquad \text{(eqn 2.8)}$$

(h = 1, 2, 3, ... , n)

D. POSITION AND VELOCITY

During the rotational motion of the LFMR system, the boom deforms. The deformed positions of a generic point in the system can be expressed the vector sum of a vector $\mathbf{R_0}(x)$ from the origin to the undeformed position of the point and a vector $\mathbf{W}(x,t)$ which is deflection, as shown in Figure 2.3. The notations show in the Figure 2.3 represent the following parameters:

M :	tip mass
m_T :	mass of electronics box
ℓ_1 :	length of lower boom
ℓ_2 :	length of upper boom
β :	angle between two links
τ :	applied torque
$\theta(t)$:	angular displacement
$\dot{\theta}(t)$:	angular velocity
$\mathbf{R_0}(x)$:	position vector of the point on the boom in the local x-direction
$\mathbf{R}(x,t)$:	position vector of the point on the boom after deformation
$\mathbf{W}(x,t)$:	deformation vector of boom
i :	unit vector of local x-direction
j :	unit vector of local y-direction
k :	unit vector of local z-direction
i_0 :	unit vector of global X-direction
j_0 :	unit vector of global Y-direction
k_0 :	unit vector of global Z-direction

Then the position vector $\mathbf{R}(x,t)$ is expressed as

$$\mathbf{R}(x,t) = \mathbf{R_0}(x) + \mathbf{W}(x,t) \qquad \text{(eqn 2.9)}$$

The undeformed position $\mathbf{R_0}(x)$ is represented by its components,

$$\mathbf{R_0}(x) = \mathbf{R_x}(x) + \mathbf{R_z}(x) \qquad \text{(eqn 2.10)}$$

$$= R_x(x)\,\mathbf{i} + R_z(x)\,\mathbf{k}$$

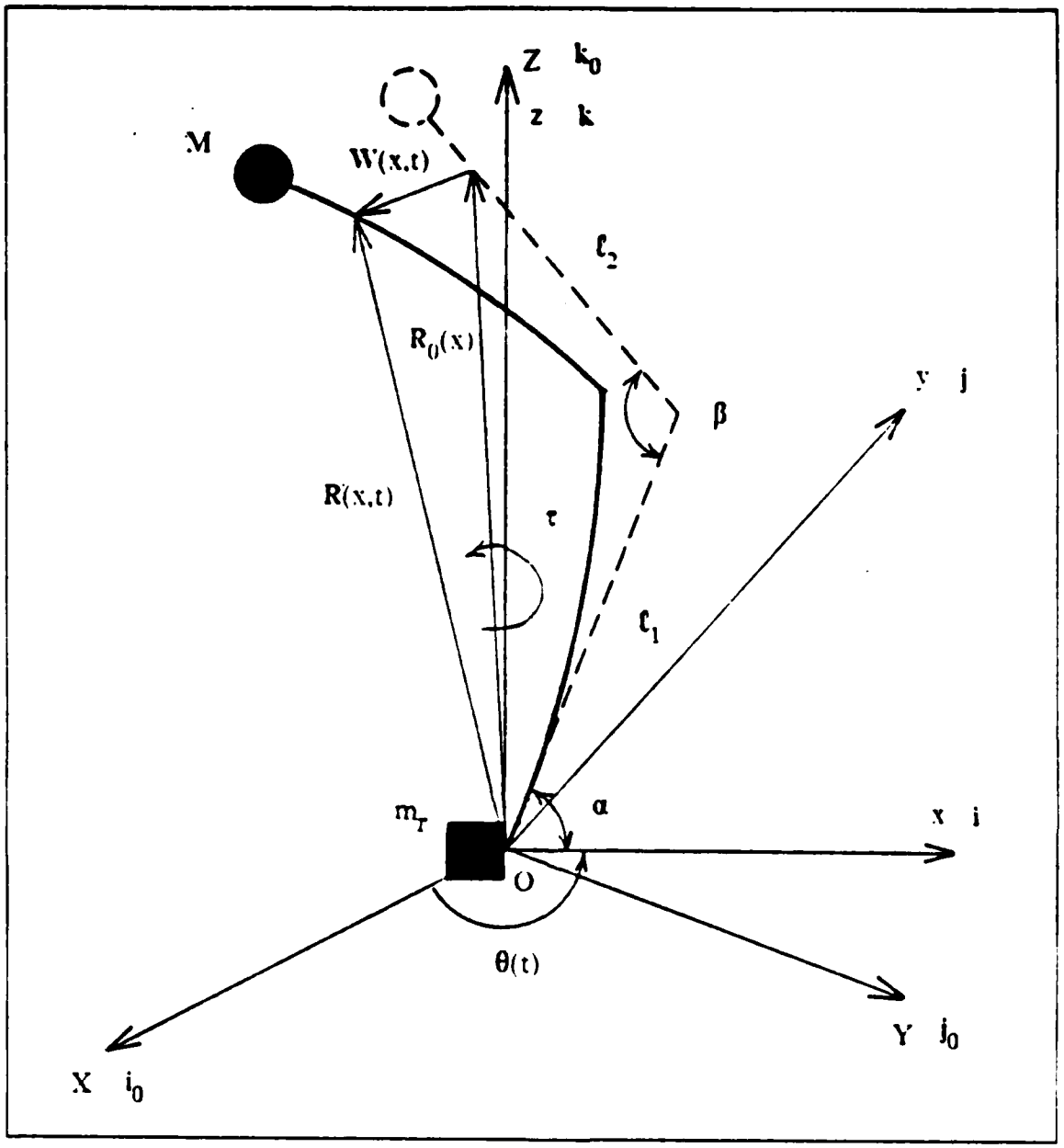

Figure 2.3 Parameters of the boom system.

The elastic deflection W(x,t) is expressed as the modal sum as follows:

$$W(x,t) = \sum_i [\, \varphi_i^x(x)\, i + \varphi_i^y(x)\, j + \varphi_i^z(x)\, k \,]\, q_i(t) \qquad \text{(eqn 2.11)}$$

where

$\varphi_i^x(x)$ i is *i-th* mode shape function in extension

$\varphi_i^y(x)$ j is *i-th* mode shape function in translation

From the equation 2.10 and equation 2.11, equation 2.9 can be rewritten in the form of

$$\mathbf{R}(x,t) = R_x(x)\,\mathbf{i} + R_z(x)\,\mathbf{k} + \sum_i [\,\varphi_i^x(x)\,\mathbf{i} + \varphi_i^y(x)\,\mathbf{j} + \varphi_i^z(x)\,\mathbf{k}\,]\,q_i(t) \qquad \text{(eqn 2.12)}$$

$$= [\,R_x(x) + \varphi^x(x)\,q_i(t)\,]\,\mathbf{i} + [\,\sum_i \varphi^y(x)\,q_i(t)\,]\,\mathbf{j} + [\,R_z(x) + \sum_i \varphi_i^z(x)\,q_i(t)\,]\,\mathbf{k}$$

The velocity of the point in the Newtonian reference frame is obtained by taking the time derivative of equation 2.12 and applying the relation between the time derivative of unit vector i and j,

$$\dot{\mathbf{i}} = \dot{\theta}\,\mathbf{k} \times \mathbf{i} = \dot{\theta}\,\mathbf{j}$$
$$\dot{\mathbf{j}} = \dot{\theta}\,\mathbf{k} \times \mathbf{j} = -\dot{\theta}\,\mathbf{i}$$
$$\dot{\mathbf{k}} = \dot{\theta}\,\mathbf{k} \times \mathbf{k} = 0$$

the velocity is

$$\mathbf{R}(x.t) = [\,-\dot{\theta}\sum_i \varphi_i^y(x)\,q_i(t) + \sum_i \varphi_i^x(x)\,\dot{q}_i(t)\,]\,\mathbf{i} + [\,\dot{\theta}\,R_x(x) + \dot{\theta}\sum_i \varphi_i^x(x)\,q_i(t) + \sum_i \varphi_i^y(x)\,\dot{q}_i(t)\,]\,\mathbf{j} + [\,\sum_i \varphi_i^z(x)\,\dot{q}_i(t)\,]\,\mathbf{k} \qquad \text{(eqn 2.13)}$$

E. KINETIC ENERGY

The kinetic energy of the system can be expressed by the summation of three different kinetic energies. One is the kinetic energy of the boom itself, another is the kinetic energy of the tip mass and the other is the kinetic energy of the R.F electronic box attached to the origin of the boom.

The kinetic energy of the boom itself is

$$T_{bm} = \frac{1}{2}\int_0^{\ell} \dot{\mathbf{R}}(x,t) \bullet \dot{\mathbf{R}}(x,t)\, dm \qquad \text{(eqn 2.14)}$$

$$= \frac{1}{2}\int_0^{\ell} \dot{\mathbf{R}}(x,t) \bullet \dot{\mathbf{R}}(x,t)\, \rho dx$$

where

dm :	differential mass of the boom
dx :	differential length of the boom
ρ :	mass per unit length
ℓ :	total length of the boom
$\dot{\mathbf{R}}(x,t)$:	absolute velocity of the points on the boom

The kinetic energy of the tip mass is

$$T_{tm} = \frac{1}{2} M\, \dot{\mathbf{R}}(\ell,t) \bullet \dot{\mathbf{R}}(\ell,t) \qquad \text{(eqn 2.15)}$$

where

M :	tip mass
$\dot{\mathbf{R}}(\ell,t)$:	the absolute velocity at the tip position

The kinetic energy of the R.F electronic box is

$$T_{rf} = \frac{1}{2} I_{r_{zz}} \dot{\theta}^2 \qquad \text{(eqn 2.16)}$$

where

$I_{r_{zz}}$:	mass moment of inertia for the electronic box
$\dot{\theta}$:	time derivative of angular displacement

Thus the total kinetic energy of the system is

$$T = T_{bm} + T_{tm} + T_{rf} \qquad \text{(eqn 2.17)}$$

$$= \frac{1}{2}\int_0^{\ell} \dot{\mathbf{R}}(x,t) \bullet \dot{\mathbf{R}}(x,t)\, dm$$

$$+ \frac{1}{2} M\, \dot{\mathbf{R}}(\ell,t) \bullet \dot{\mathbf{R}}(\ell,t)$$

$$+ \frac{1}{2} I_{r_{zz}}\, \dot{\theta}^2$$

F. POTENTIAL ENERGY

The potential energy U of the flexible boom system can be composed of the gravitational potential energy U_g due to rotation of the system and the strain energy (or elastic energy) U_s of the boom due to deformation. But in our model analysis, we exclude gravitational acceleration and only consider the strain energy. The potential energy was determined by the work done by the static weight in the deflection. This work is, of course , stored in the flexible flexible boom system as strain energy.

In this thesis, we apply mide summation method to expand the deflection in terms of the normal modes of the system. The deflection of a boom without any external forces, satisfies the lollowing equation of motion. [Ref. 7]

$$[\, EIW''(x,t)\,]'' + \rho W(x,t) = 0 \qquad \text{(eqn 2.18)}$$

where

ρ : mass per unit length

EI : flexural rigidity

and ' represent the derivative with respect to x. The normal modes $\varphi_i(x)$ of the boom must satisfy the equation

$$[\, EI\varphi_i''(x)\,]'' - \omega_i^2 \rho\, \varphi_i(x) = 0 \qquad \text{(eqn 2.19)}$$

and its boundary conditions. The normal modes $\varphi_i(x)$ also satisfy the orthogonality relation

$$\int_0^{\ell} \varphi_i(x)\, \varphi_j(x)\, dm = 0 \qquad (\text{for} \quad j \neq i) \qquad \text{(eqn 2.20)}$$

$$= M_i \qquad (\text{for} \quad j = i)$$

where M_i is the generalized modal mass of the *i-th* mode.

As expressed in Appendix A, the deflection of the boom in the equation A.4 for the general form is

$$W(x,t) = \sum_i \varphi_i(x)\, q_i(t) \qquad \text{(eqn 2.21)}$$

and the generalized coordinate $q_i(t)$ can be determined by applying Lagrange's equation after setting up the kinetic and potential energies.

Now the potential energy can be expressed as

$$U = \frac{1}{2} \int_0^{\ell} EIW''^2(x,t)\, dx \qquad \text{(eqn 2.22)}$$

$$= \frac{1}{2} \sum_i \sum_j q_i\, q_j \int_0^{\ell} EI\varphi_i''(x)\, \varphi_j''(x)\, dx$$

Multiplying the both sides of equation 2.19 by $\varphi_j(x)$ and after integration for the whole boom, equation 2.19 becomes

$$\int_0^{\ell} \varphi_j(x)\, [\, EI\, \varphi_i''(x)\,]\, dx \qquad \text{(eqn 2.23)}$$

$$= \omega_i^2 \int_0^{\ell} \varphi_i(x)\, \varphi_j(x)\, dm$$

After integration by parts and using the boundary conditions, equation 2.23 becomes

$$\int_0^{\ell} EI\, [\, \varphi_i''(x)\, \varphi_j''(x)\,]\, dx \qquad \text{(eqn 2.24)}$$

$$= \omega_i^2 \int_0^{\ell} \varphi_i(x)\, \varphi_j(x)\, dm$$

From the orthogonality condition, the equation 2.20 and from equation 2.24, the strain energy in equation 2.22 becomes

$$U = \frac{1}{2} \sum_i \omega_i^2 M_i q_i(t)^2 \qquad \text{(eqn 2.25)}$$

G. DERIVATIONS OF EQUATIONS OF MOTION

From the equation 2.13, the dot product of $\mathbf{R}(x,t)$ is

$$\dot{\mathbf{R}}(x,t)\bullet\dot{\mathbf{R}}(x,t) = [\, -\dot{\theta} \sum_i \varphi_i^{y}(x)\, q_i(t) + \sum_i \varphi_i^{x}(x)\, \dot{q}_i(t)\,]^2 \qquad \text{(eqn 2.26)}$$

$$+ [\, \dot{\theta}\, R_x(x) + \dot{\theta} \sum_i \varphi_i^{x}(x)\, q_i(t) + \sum_i \varphi_i^{y}(x)\, \dot{q}_i(t)\,]^2$$

$$+ [\, \sum_i \varphi_i^{z}(x)\, \dot{q}_i(t)\,]^2$$

$$= \dot{\theta}^2 [\, \sum_i \varphi_i^{y}(x)\, q_i(t)\,]^2 + [\, \sum_i \varphi_i^{x}(x)\, \dot{q}_i(t)\,]^2$$

$$- 2\dot{\theta} \sum_i \varphi_i(x)\, q_i(t) \sum_i \varphi_i^{x}(x)\, \dot{q}_i(t)$$

$$+ R_x(x)^2 \dot{\theta}^2 + \dot{\theta}^2 [\, \sum_i \varphi_i^{x}(x)\, q_i(t)\,]^2 + [\, \sum_i \varphi_i^{y}(x)\, \dot{q}_i(t)\,]^2$$

$$+ 2 R_x(x) \dot{\theta}^2 q_i(t) + 2\dot{\theta} \sum_i \varphi_i^{x}(x)\, q_i(t) \sum \varphi_i^{y}(x)\, \dot{q}_i(t)$$

$$+ 2 R_x(x) \dot{\theta} \sum_i \varphi_i^{y}(x)\, \dot{q}_i(t) + [\, \sum_i \varphi_i^{z}(x)\, \dot{q}_i(t)\,]^2$$

$$= \dot{\theta}^2 [\, \{\, \sum_i \varphi_i^{y}(x)\, q_i(t)\,\}^2 + \{\, \sum_i \varphi_i^{x}(x)\, q_i(t)\,\}^2 + \{\, \sum_i \varphi_i^{z}(x)\, q_i(t)\,\}^2\,]$$

$$+ [\, \{\, \sum_i \varphi_i^{x}(x)\, q_i(t)\,\}^2 + \{\, \sum_i \varphi_i^{y}(x)\, q_i(t)\,\}^2 + \{\, \sum_i \varphi_i^{z}(x)\, q_i(t)\,\}^2\,]$$

$$- 2\dot{\theta} \sum_i \varphi_i^y(x)\, q_i(t) \sum_i \varphi_i^x(x)\, \dot{q}_i(t) + R_x^2(x)\, \dot{\theta}^2$$

$$+ 2 R_x(x)\, \dot{\theta}^2 \sum_i \varphi_i^x(x)\, q_i(t) + 2\dot{\theta} \sum_i \varphi_i^x(x)\, q_i(t) \sum_i \varphi_i^y(x)\, \dot{q}_i(t)$$

$$+ 2 R_x(x)\, \dot{\theta} \sum_i \varphi_i^y(x)\, \dot{q}_i(t) - \dot{\theta}^2 \{ \sum_i \varphi_i^z(x)\, q_i(t) \}^2$$

Substituting equation 2.26 into the equation 2.17 and apply orthogonal relationship

$$\int_0^\ell \{ \varphi_i^x(x)\, \varphi_j^x(x) + \varphi_i^y(x)\, \varphi_j^y(x) + \varphi_i^z(x)\, \varphi_j^z(x) \}\, dm \qquad \text{(eqn 2.27)}$$

$$+ M \{ \varphi_i^x(\ell)\, \varphi_j^x(\ell) + \varphi_i^y(\ell)\, \varphi_j^y(\ell) + \varphi_i^z(\ell)\, \varphi_j^z(\ell) \} = 0 \quad (\text{for } i \neq j)$$

$$= M_i \quad (\text{for } i = j)$$

then the kinetic energy is

$$T = \frac{1}{2} \dot{\theta}^2 \sum q_i^2(t)\, M_i + \frac{1}{2} \sum_i \dot{q}_i(t)^2\, M_i \qquad \text{(eqn 2.28)}$$

$$- \dot{\theta} \sum_i \sum_j q_i(t)\, \dot{q}_j(t) [\int_0^\ell \varphi_i^y(x)\, \varphi_j^x(x)\, dm + M\, \varphi_i^y(\ell)\, \varphi_j^x(\ell)]$$

$$+ \frac{1}{2} \dot{\theta}^2 [\int_0^\ell R_x^2(x)\, dm + M\, R_x(\ell)$$

$$- \dot{\theta}^2 \sum_i q_i(t) [\int_0^\ell R_x(x)\, \varphi_i^x(x)\, dm + M R_x(\ell)\, \varphi_i^x(\ell)$$

$$+ \dot{\theta} \sum_i \sum_j q_i(t)\, \dot{q}_j(t) [\int_0^\ell \varphi_i^x(x)\, \varphi_j^y(x)\, dm + M\, \varphi_i^x(\ell)\, \varphi_j^y(\ell)]$$

$$+ \dot{\theta} \sum_i \dot{q}_i(t) [\int_0^\ell R_x(x)\, \varphi_i^y(x)\, dm + M\, R_x(\ell)\, \varphi_i^y(\ell)]$$

$$- \dot{\theta}^2 [\int_0^\ell \{ \sum_i \varphi_i^z(x)\, q_i(t) \}^2 + M \{ \sum_i \varphi_i^z(\ell)\, q_i(t) \}^2]$$

$$+ \frac{1}{2} I_{r_{zz}}\, \dot{\theta}^2$$

By applying the kinetic energy and potential energy expressions (eqn 2.25) and (eqn 2.28), to the Lagrange's equations 2.7 and 2.8 then equations of motion will be reduced as follows. The detailed derivation process can be formed in Appendix B.

$$\ddot{\theta}\Big[\sum_i q_i^2(t)\,M_i + \int_0^{\ell} R_x^2(x)\,dm + M\,R_x^2(\ell) \qquad \text{(eqn 2.29)}$$

$$+ 2\sum_i q_i(t)\Big\{\int_0^{\ell} R_x(x)\,\varphi_i^x(x)\,dm + M\,R_x(\ell)\,\varphi_i^x(\ell)\Big\}$$

$$- 2\Big\{\int_0^{\ell}\Big(\sum_i \varphi_i^z(x)\,q_i(t)\Big)^2 + M\Big(\sum_i \varphi_i^z(\ell)\,q_i(t)\Big)^2 + I_{r_{zz}}\Big]$$

$$+ 2\dot{\theta}\sum_i \dot{q}_i(t)\Big[q_i(t)\,M_i + \int_0^{\ell} R_x(x)\,\varphi_i^x(x)\,dm + M\,R_x(\ell)\,\varphi_i^x(\ell)\Big\}$$

$$- 2\sum_j q_j(t)\Big\{\int_0^{\ell}\varphi_i^z(x)\,\varphi_j^z(x)\,dm - M\,\varphi_i^z(\ell)\,\varphi_j^z(\ell)\Big\}\Big]$$

$$- \sum_i \ddot{q}_i(t)\Big[\sum q_j(t)\Big\{\int_0^{\ell}\varphi_i^x(x)\quad\varphi_j^y(x)\,dm + M\,\varphi_i^x(\ell)\,\varphi_j^x(\ell)$$

$$- \int_0^{\ell}\varphi_i^y(x)\,\varphi_j^x(x)\,dm - M\,\varphi_i^y(\ell)\,\varphi_j^x(\ell)\Big\}$$

$$- \int_0^{\ell} R_x(x)\,\varphi_i^y(x)\,dm - M\,R_x(\ell)\,\varphi_i^y(\ell)\Big] = \tau$$

$$\ddot{q}_h(t)\,M_h + \ddot{\theta}\Big[\sum_i q_i(t)\Big\{\int_0^{\ell}\varphi_i^x(x)\,\varphi_h^y(x)\,dm + M\,\varphi_i^x(\ell)\,\varphi_h^y(\ell) \qquad \text{(eqn 2.30)}$$

$$- \int_0^{\ell}\varphi_i^y(x)\,\varphi_h^x(x)\,dm - M\,\varphi_i^y(\ell)\,\varphi_h^x(\ell)\Big\}$$

$$+ \int_0^{\ell} R_x(x)\,\varphi_h^y(x)\,dm + M\,R_x(\ell)\,\varphi_h^y(\ell)\Big]$$

$$+ 2\dot{\theta}\sum_i \dot{q}_i(t)\Big[\int_0^{\ell}\varphi_i^x(x)\,\varphi_h^y(x)\,dm + M\,\varphi_i^x(\ell)\,\varphi_h^y(\ell)$$

$$- \int_0^{\ell}\varphi_i^y(x)\,\varphi_h^x(x)\,dm - M\,\varphi_i^y(\ell)\,\varphi_h^x(\ell)\Big]$$

$$- \theta^2 [\, q_i(t)\, M_i - \int_0^{\ell} R_x(x)\, \varphi_i^x(x)\, dm - M R_x(\ell)\, \varphi_i^x(\ell)$$

$$+ 2 \sum_i q_i(t) \{ \int_0^{\ell} \varphi_i^z(x)\, \varphi_h^x(x)\, dm + M\, \varphi_i^z(\ell)\, \varphi_h^z(\ell) \}]$$

$$+ \omega^2{}_h\, M_h\, q_h(t) = 0$$

$$(h = 1, 2, 3, \ldots\ldots, n)$$

Now let's define the following quantities:

$$M_\theta = [\sum_i q_i^2(t)\, M_i + \int_0^{\ell} R_x^2(x)\, dm + M\, R_x^2(\ell)$$

$$+ 2 \sum_i q_i(t) \{ \int_0^{\ell} R_x(x)\, \varphi_i^x(x)\, dm + M\, R_x(\ell)\, \varphi_i^x(\ell) \}$$

$$- 2 \{ \int_0^{\ell} (\sum_i \varphi_i^z(x)\, q_i(t))^2 + M (\sum_i \varphi_i^z(\ell)\, q_i(t))^2 + I_{r_{zz}}]$$

$$M_{\theta q_i} = 2 [\, q_i(t)\, M_i + \int_0^{\ell} R_x(x)\, \varphi_i^x(x)\, dm + M\, R_x(\ell)\, \varphi_i^x(\ell) \}$$

$$- 2 \sum_j q_j(t) \{ \int_0^{\ell} \varphi_i^z(x)\, \varphi_j^z(x)\, dm - M\, \varphi_i^z(\ell)\, \varphi_j^z(\ell) \}]$$

$$M_{q_i} = - [\sum_i q_j(t) \{ \int_0^{\ell} \varphi_i^x(x) \quad \varphi_j^y(x)\, dm + M\, \varphi_i^x(\ell)\, \varphi_j^x(\ell)$$

$$- \int_0^{\ell} \varphi_i^y(x)\, \varphi_j^x(x)\, dm - M\, \varphi_i^y(\ell)\, \varphi_j^x(\ell) \}$$

$$- \int_0^{\ell} R_x(x)\, \varphi_i^y(x)\, dm - M\, R_x(\ell)\, \varphi_i^y(\ell)]$$

$$M_{\theta h} = [\sum_i q_i(t) \{ \int_0^{\ell} \varphi_i^x(x)\, \varphi_h^y(x)\, dm + M\, \varphi_i^x(\ell)\, \varphi_h^y(\ell)$$

$$- \int_0^{\ell} \varphi_i^y(x)\, \varphi_h^x(x)\, dm - M\, \varphi_i^y(\ell)\, \varphi_h^x(\ell) \}$$

$$+ \int_0^{\ell} R_x(x)\, \varphi_h^y(x)\, dm + M\, R_x(\ell)\, \varphi_h^y(\ell)]$$

$$M_{\theta q_h} = 2 \left[\int_0^{\ell} \varphi_i^{x}(x)\, \varphi_h^{y}(x)\, dm + M\, \varphi_i^{x}(\ell)\, \varphi_h^{y}(\ell) \right.$$

$$\left. - \int_0^{\ell} \varphi_i^{y}(x)\, \varphi_h^{x}(x)\, dm - M\, \varphi_i^{y}(\ell)\, \varphi_h^{x}(\ell) \right]$$

$$F_{c_h} = \dot{\theta}^2 \left[q_i(t)\, M_i - \int_0^{\ell} R_x(x)\, \varphi_i^{x}(x)\, dm - M R_x(\ell)\, \varphi_i^{x}(\ell) \right.$$

$$\left. + 2 \sum_i q_i(t) \left\{ \int_0^{\ell} \varphi_i^{z}(x)\, \varphi_h^{x}(x)\, dm + M\, \varphi_i^{z}(\ell)\, \varphi_h^{z}(\ell) \right\} \right]$$

$$F_{e_h} = M\, \omega_h^{2}\, q_h(t)$$

Then equation 2.29 becomes

$$M_{\theta} \ddot{\theta} + M_{\theta q_i} \dot{\theta} \sum \dot{q}_i(t) + M_{q_i} \ddot{q}_i(t) = \tau \qquad \text{(eqn 2.31)}$$

and quation 2.30 becomes

$$M_{\theta h} \ddot{\theta} + M_{\theta q_h} \dot{\theta} \sum \dot{q}_i(t) + M_h \ddot{q}_i(t) - F_{c_h} + F_{e_h} = 0 \qquad \text{(eqn 2.32)}$$

$$(h = 1, 2, 3, \ldots\ldots, n)$$

III. COMPUTER IMPLEMENTATION

A. INTRODUCTION

To solve the equations of motion, two computer program, Dynamic Simulation Language (DSL) and NAsa STRuctural ANalysis (NASTRAN) program are used. NASTRAN is a general purpose digital computer program for the analysis of large complex structures. [Ref. 8] This finite element computer program was used in the modal analysis which determine the mode shapes, generalized modal mass, generalized stiffness, natural frequency of the LFMR model. Then these properties directly inputed to the DSL program to get a set of solutions.

DSL is an IBM/VS FORTRAN-based simulation language for digital simulation of continuous system. [Ref. 9] It is one of the most effective for the solution of continuous modeling and simulation problem with computational power (automatic double precision and accurate timing), whether the problem is time based or not.

For the integration method to solve simultaneous nonlinear second order coupled ordinary differential equations, Runge-Kutta method was chosen. Runge-Kutta fifth order integration method (RK5) is self-starting, stable and automatically determine the step-size but this needs excessive computer time.

Two different cases are analyzed. One is the LFMR boom made of Aluminum Alloy and the other is the LFMR boom made of Isotropic Graphite Epoxy composite material (T300/5028 $(0/90/45/-45)_S$). The mass distribution of the two cases are the same. Therefore the boom model of graphite epoxy composite material was stiffer since the mass density was linear.

B. MODAL ANALYSIS

As previously mentioned, we consider our model as a one body system and we don't need any compatibility conditions which is necessary in multibody dynamics. For the modal analysis we equally divide the whole boom with fourteen grid points. Figure 3.1 shows Finite element model of LFMR boom. As the number of grid points increases we can get more accurate results. But Degrees of Freedom (DOF) of the system also increases. Fourteen grid point is sufficient for our our analysis.

In the modal analysis of the boom , Modified Given's method (MGIV) was applied and for the purpose of simplifying the equation of motion we normalized the

mode shape such that the generalized modal mass equal to unity. From the relationship of the generalized stiffness, generalized modal mass and natural frequency, the generalized stiffness K_i is

$$K_i = \omega_i^2 M_i$$

and reduces to

$$K_i = \omega_i^2$$

Only the first 2 modes were needed in the 3-dimensional dynamic analysis with sufficient accuracy.

NASTRAN program is shown in Appendix C and some outputs are tabulated in Table 1 and 2 for 3-dimensional motion. Figures 3.2 and 3.3 show the first and the second mode shapes for three dimensional motion. In Figures 3.2 and 3.3, the left side figure is the projection to x-z plane and right side figure is projection to y-z plane.

The first mode shape shows there is no in-plane vibration and the second mode shape shows there is no out-of-plane vibration.

TABLE 1

REAL EIGENVALUES OF ALUMINUM ALLOY (3 D)

mode no.	radians ω_i	cycles ω_i	generalized mass(M_i)	generalized stiffness(K_i)
1	3.384515E+00	5.386623E−01	1.000000E+00	1.145494E+01
2	3.568821E+00	5.679954E−01	1.000000E+00	1.273648E+01

C. DSL PROGRAMING

DSL was implemented for the solution of a set of simultaneous, nonlinear, second order, ordinary differential equations. DSL offers a new simulation tool that speeds problem analysis and solution for a wide variety of application. It is adopted for simulation because it requires less skillful time for problem analysis and provides quicker, more comprehensive plotting through GRAFAEL and sophiscated line or print plot. These advantages can translate directly into higher productivity and cost savings.

TABLE 2
REAL EIGENVALUES OF COMPOSITE MATERIAL (3 D)

mode no.	radians ω_i	cycles ω_i	generalized mass(M_i)	generalized stiffness(K_i)
1	4.287485E+00	6.823744E−01	1.000000E+00	1.838253E+01
2	4.461334E+00	7.100433E−01	1.000000E+00	1.990350E+01

DSL is a high-level continuous simulation language which incorporates VS FORTRAN as a subset. Because of its tremendous flexibility, DSL facilitates the solution of nearly all prlblems involving time-dependent differential equations. Thus DSL readily assists in the dynamic analysis of transient behavior of dynamic systems. Also DSL is easily learned and applied to many problems in science, engineering, mathematics and management. Coding is simple, execution is rapid and results can be displayed graphically. For any one involved in simulation modeling DSL offers increased power for faster problem solving and the user choice of nine integration method (fixed-step, variable-step, variable-step & variable-order method).

In our model analysis, Runge-Kutta fifth order method (RK5) was used because it is self-starting, stable and provides good accuracy. To code the equations of motion, the equation 2.31 and 2.32 have to be rewritten as follows:

$$M_\theta \ddot{\theta} + M_{q_i} \ddot{q}_i(t) = \tau - M_{\theta_i} \dot{\theta} \sum \dot{q}_i(t) \qquad \text{(eqn 3.1)}$$

and equation 2.30 becomes

$$M_{\theta h} \ddot{\theta} + M_h \ddot{q}_i(t) = F_{c_h} - F_{e_h} - M_{\theta q_h} \dot{\theta} \sum \dot{q}_i(t) \qquad \text{(eqn 3.2)}$$

$$(h = 1, 2, 3, \ldots\ldots, n)$$

Two ways solving these systems of equations are shown. One uses matrix algebra and utilizes subroutines from the library LINPACK, the other uses subroutine REGULRA provided by DSL. For our system analysis we select matrix algebra because it is easy to use for large numbers of variables.

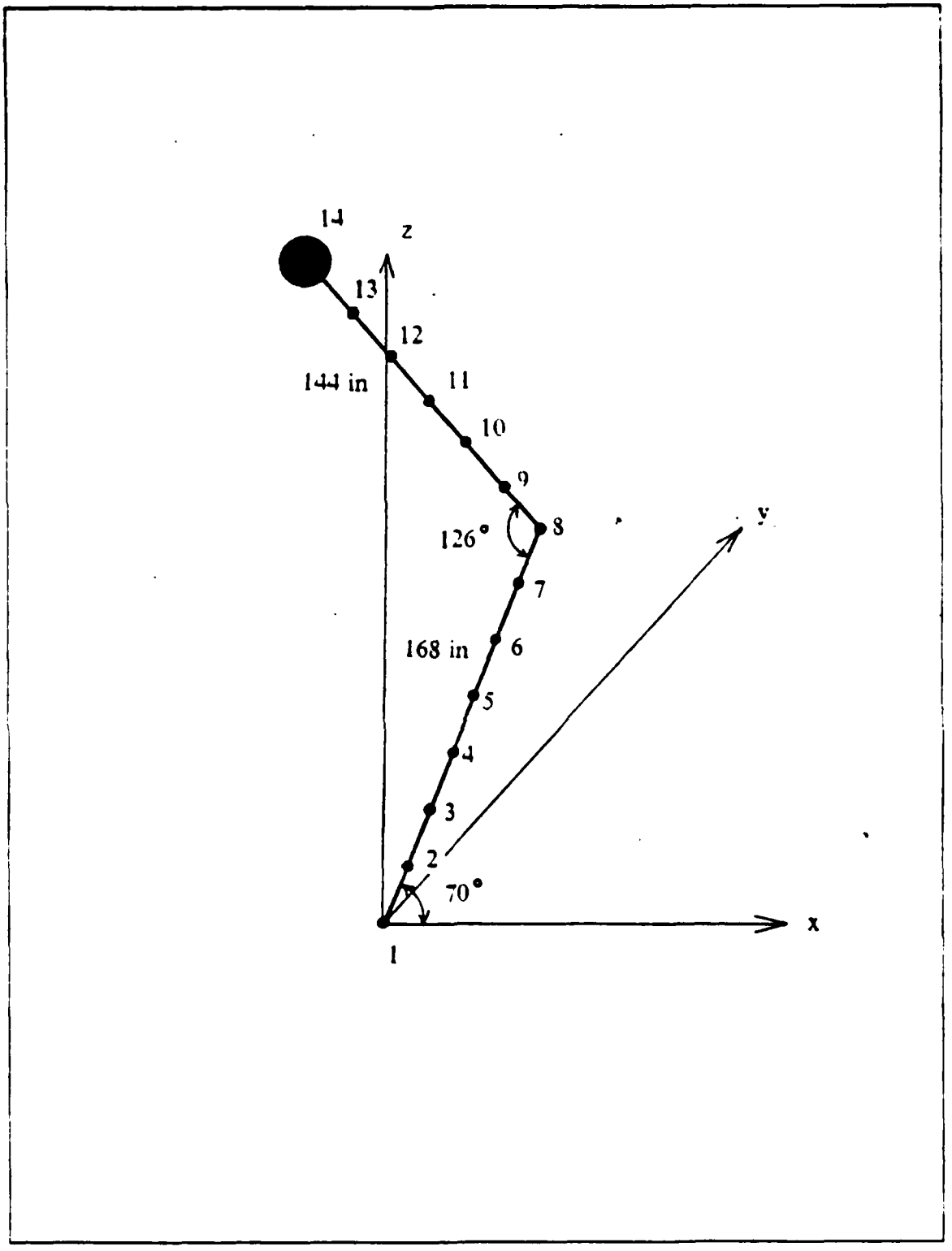

Figure 3.1 Finite element model of LFMR boom.

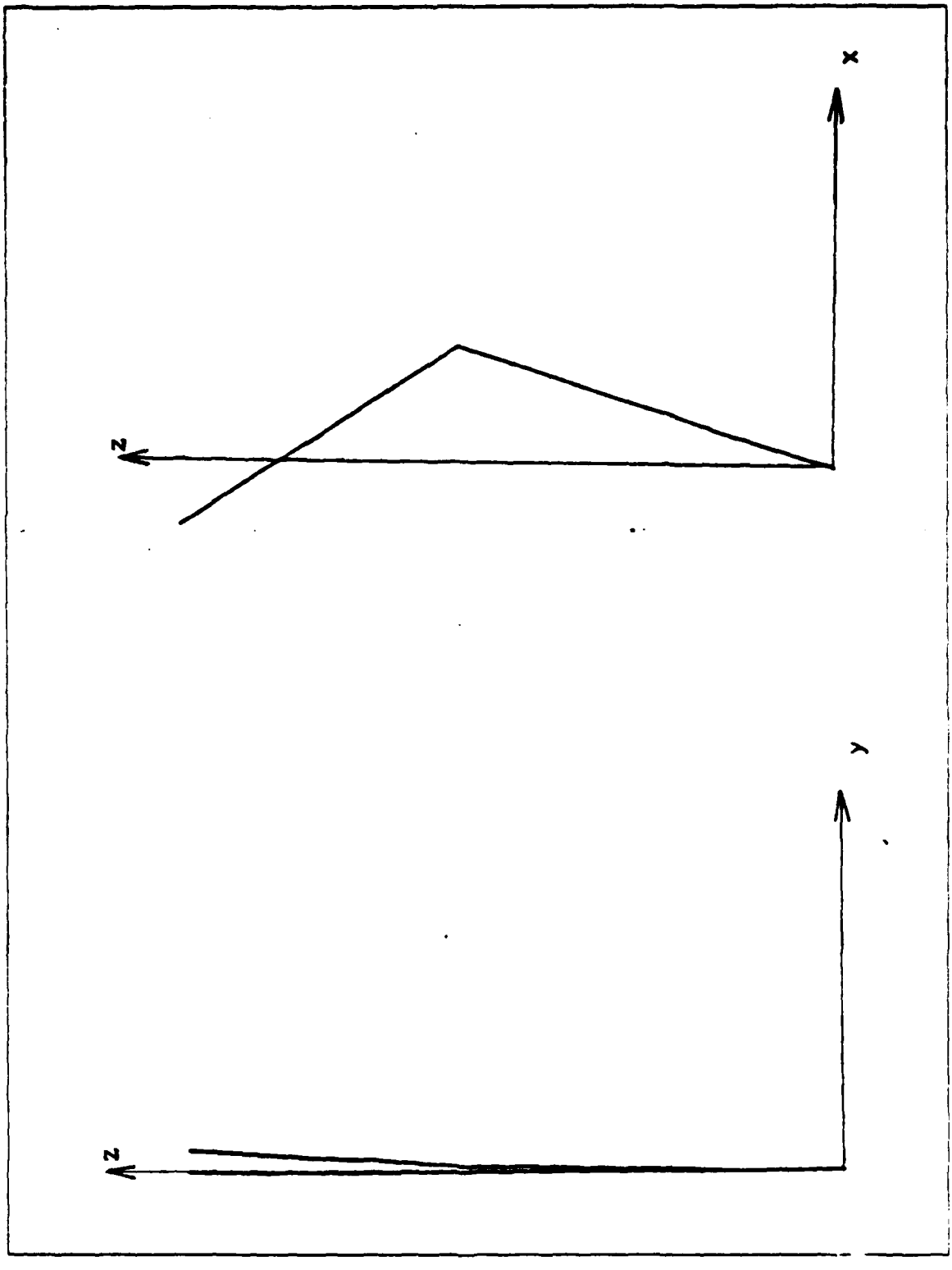

Figure 3.2 First mode shape.

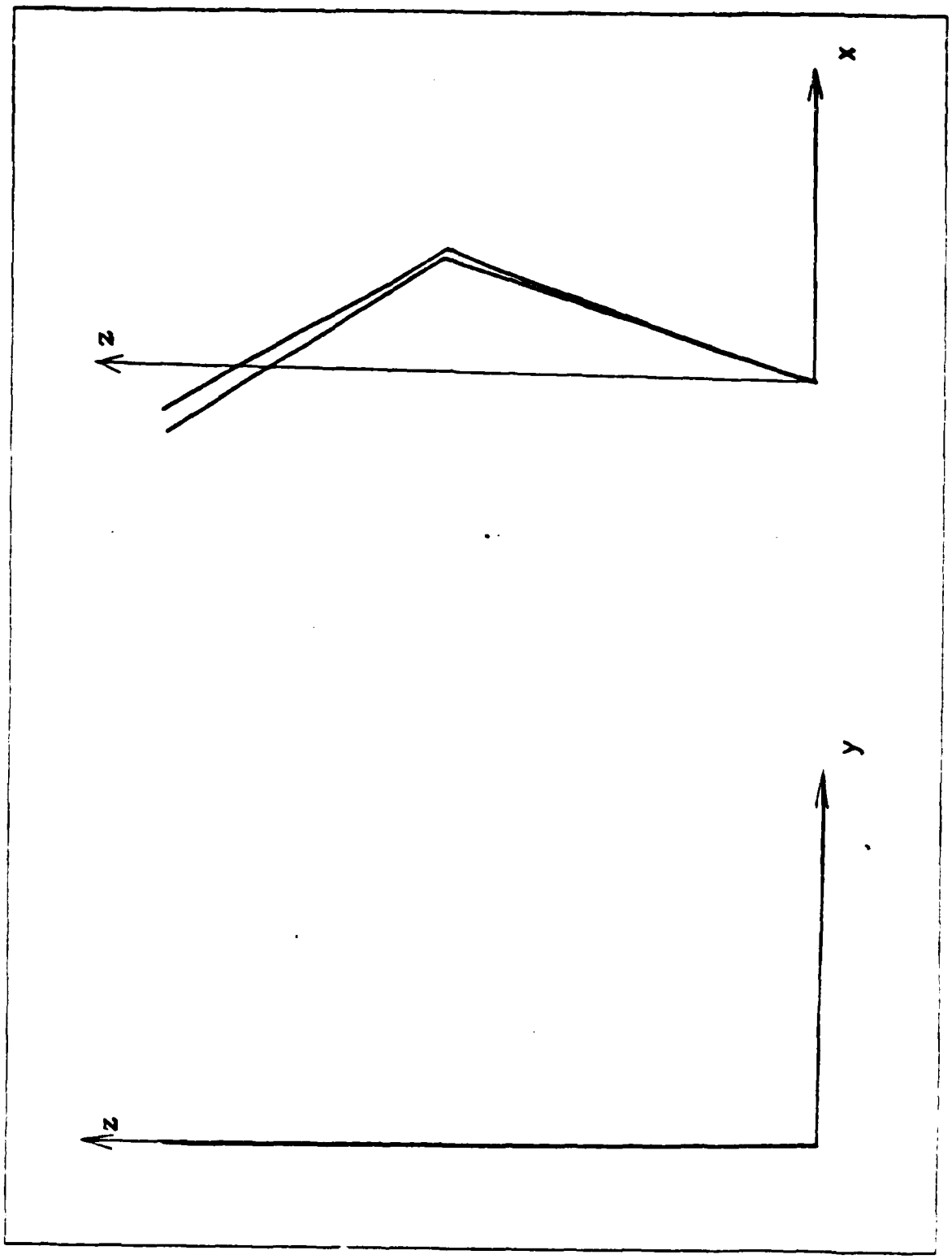

Figure 3.3 Second mode shape.

Using matrix notation, the equations 3.1 and 3.2 may be rewritten as

$$[M]\{\ddot{X}\} = \{f\}$$

where the matrices M, X, and f are defined as follows:

$$[M] = \begin{bmatrix} M_\theta & M_{q_1} & \cdots & M_{q_n} \\ M_{\theta 1} & M_1 & 0 \cdots & 0 \\ M_{\theta 2} & 0 & M_2 & 0 \cdots 0 \\ \vdots & & & \vdots \\ M_{\theta n} & 0 & \cdots & M_n \end{bmatrix}$$

$$\{\ddot{X}\} = \begin{Bmatrix} \ddot{\theta} \\ \ddot{q}_1 \\ \ddot{q}_2 \\ \vdots \\ \ddot{q}_n \end{Bmatrix}$$

$$\{f\} = \begin{Bmatrix} \tau - M_\theta q_i \\ F_{c_1} - F_{e_1} - M_{\theta q_1} \dot{\theta}\, \dot{q}_1 \\ \vdots \\ F_{c_n} - F_{e_n} - M_{\theta q_n} \dot{\theta}\, \dot{q}_n \end{Bmatrix}$$

Then

$$\{\ddot{X}\} = [M]^{-1}\{f\}$$

and by successive integration of $\{\ddot{X}\}$, the solution vector may be obtained. Since the elements of the [M] and { f } matrices are time dependent, the $\{\ddot{X}\}$ vector must be computed at each integration step. A matrix decomposition subroutine (DGEFA) using Gaussian elimination and a subroutine which uses this decomposition to solve a matrix equation (DGESL) are called directly from the LINPACK library. Because DGESL returns the solution vector $\{\ddot{X}\}$ in the right-hand-side vector f, the vector name $\{\ddot{X}\}$ does not appear explicitly in the program.

The coefficients of [M] and { f } matrices are calculated in each time step. θ, q_i (i = 1, 2, 3, ... , n), deflection and slope at the tip position in each direction were calculated at each time interval of interest. The graphs of these variables vs. time were also obtained. The computer program for dynamic analysis is coded in Appendix D.

IV. RESULTS AND DISCUSSIONS

Computer simulation was done in four areas for double link boom system in three dimensional motion to investigate the equilibrium configuration and the vibration amplitude of the tip position. The effects of the spin up procedure on the pointing error of the reflector is studied; the first analysis was the comparison of the three different torque histories by maintaining magnitude of torque until rotating speed of boom reaches to 15 r.p.m. Secondly the magnitude of appllied torque was changed in three cases for one of three torque applying methods above. The effects of structural damping of the boom on the settling time is also studied by changing the modal damping values. The magnitude of the deflection and slope at the equilibrium configuration at three different rotating speeds are investigated by simulating free motions of the system with the three different initial rotating speed and undeformed configuration. Also some comparisons were made for double link flexible boom system in planar motion in Appendix B.

A. MATERIAL PROPERTIES AND PARAMETERS

For the comparison of the computer simulation results, two kinds of material were chosen. One is Aluminum alloy 6061-T6 (99% Al-1% Mg) and the other is an Isotropic Graphite-Epoxy Composite material (T300/5208 $(0/90/45/-45)_S$). [Ref. 10] Same mass, same length of each link, same outer diameter was used for these two materials. Size of the electronic box is 1 ft. cube. The properties of the materials and some geometric parameters are given in Table 3 and Table 4 respectivly.

B. EFFECTS OF TORQUE APPLYING PROCEDURE

Three cases of torque applying method were chosen without damping for comparison. To maintain 15 r.p.m of rotating speed, we select the maximum magnitude of torque is 10 lbs-in. This value may be appropriate to maintain 15 r.p.m in 20 to 30 seconds.

In the first case, 10 lbs-in torque was abruptly applied from the begining. This method is unlikely in the real situation but we chose this case for comparison purpose. In the second case, torque was parabolically applied until reaching 15 r.p.m then cut off abruptly to 0. Finally torque was applied same manner as case two but linearly decreased to 0. Figure 4.1 shows three different spin-up schemes.

TABLE 3
BOOM PROPERTIES

PROPERTY	ALUMINUM ALLOY	COMPOSITE
specific weight (γ)	0.0980 lb in^3	0.0588 lb in^3
modulus of elasticity (E)	10.1E+06 psi	10.1E+06 psi
modulus of rigidity (G)	3.7E+06 psi	4.1E+06 psi
poisson's ratio (ν)	0.360	0.250
outer diameter (r_1)	3.0 in	3.0 in
inner diameter (r_2)	2.7312 in	2.5362 in
thickness (t)	0.1344 in	0.2319 in
cross area (A)	1.2101^2	2.0168 in^2
mass per unit length (ρ)	3.0690E-04 lb in	3.0690E-04 lb in
area moment of inertia (I)	1.2447 in^4	1.9451 in^4
polar moment of inertia (J)	2.4894 in^4	3.8902 in^4

In these three cases angular displacement θ was changed parabolically as shown in Figure 4.2 while torque is applied, then linearly increased as torque was cut off. The cases B and C are almost indentical and overlapped in the Figure 4.2. Angular displacement was equally increased with time for aluminum alloy and composite material because total system mass is same. As shown in Figure 4.3, angular velocity $\dot{\theta}$ varied linearly with some oscillation in the begining for the first case because torque was suddenly applied, then it gradually decreased until reaching 15 r.p.m. After cutting off applied torque, $\dot{\theta}$ oscillates periodically because the boom deflects to the positive x-direction and the concentrated mass center moves to the rotating axes. this means radius of rotation decreased and moment of inertia also decreased. From the conservation of angular momentum,

$$H_0 = m r^2 \dot{\theta} = \text{constant}$$

TABLE 4
GEOMETRIC PARAMETERS

PARAMETER	VALUE
ℓ_1 ; length of lower boom	168 in
ℓ_2 ; length of upper boom	144 in
α ; angle between ℓ_1 and x-axes	70°
β ; angle between ℓ_1 and ℓ_2	126°
M ; tip mass	37.5 lbs
m_T ; mass of R.F electronic box	50 lbs

So as the tip position changes, $\dot{\theta}$ varies with reciprocal of r^2. Therefore angular velocity oscillates periodically.

In case two and three, $\dot{\theta}$ increased smoothly without oscillation until reaching 15 r.p.m then it had relatively small oscillation as soon as torque was removed gradually. Figure 4.5 shows the angular velocity of the Aluminum Alloy boom in magnified scale. For the composite material as shown in Figure 4.4, magnitude of oscillation was much smaller than that of aluminum alloy so it looks no oscillation. But magnified angular velocity of constant part shows obvious oscillation in Figure 4.6. Figures 4.7 - 4.10 show the variations of the generalized coordinates q_1 and q_2 respectively.

During rotation deflection in x-direction was dominated and deflection center reaches to its equilibrium position in x, z-direction then oscillates harmonically as shown in Figures 4.11 and 4.12 but displacement in y-direction was rapidly increased at the begining then decreased gradually to 0 and as soon as applied torque was removed it oscillates harmonically as shown in Figures 4.13 and Figure 4.14.

Characteristics of displacement and slope at the tip position is very similar to its generalized coordinates, and the generalized coordinates q_2 in Figures 4.9 and 4.10 was dominated for the system deflection. Displacement in z-direction was shown in Figure 4.15 and 16 for two material booms. Displacement and slope change as shown in Figures 4.17 - 4.22 was apparently different from case A and case B but after cutting

off the torque its characteristics of deformation was not much different. For the case three deflection and slope increases smoothly while torque is applying then as torque was removed it reaches its equilibrium position and oscillates with small fluctuation error.

Figures 4.11 -4.24 show displacement and slope at the tip position in each direction for aluminum alloy boom and composite material boom.

As we mentioned previously, we are mainly interested in the pointing error at the tip position in both elevation and azimuth. For the composite material boom, all 3 cases were satisfied the pointing error requirement (elevation and azimuth angle error : 0.0328°). But for the Aluminum Alloy boom, torque applying case A and case B were not satisfied the elevation angle error requirement. Figures 4.19-4.22 show the characteristics of elevation and azimuth angle variation, and in Figures 4.23 and 4.24, the effects of torque applying procedure are compared. From these results, pointing error at the equilibrium position depends on torque removing procedure. As we see in Figures 4.23 and 4.24, pointing error in case A and case B is almost same but it is very different in case C and pointing error varies more sensitively with flexible material as torque removing procedure varies. Consequently, if we apply the torque more gently and remove slowly with sufficient time, the pointing error both deflection and the slope can be reduced to much smaller values.

C. EFFECTS OF CHANGING MAGNITUDE OF TORQUE

In this section we investigate the effects of the maximum magnitude of applied torque. For the simple comparison, we select second case of torque applying method used in previous section. Magnitudes of torque chosen are 10 lbs-in, 20 lbs-in and 40 lbs-in as shown in Figure 4.25. As the magnitude of applied torque increases 4 times, applying time was reduced to almost one third. All characteristics are same as the second case of previous section for 3 cases shown in Figures 4.26-4.36 but magnitude of pointing error increased linearly as the maximum torque increases as shown in Figures 4.37 and 4.38. Figures 4.26-4.43 show angular displacement, angular velocity, generalized coordinates, displacement and pointing error for the boom made of Aluminum Alloy.

D. EFFECTS OF DAMPING COEFFICIENT

In this section, we will investigate the damping effects for settling down the vibration of the boom. As we mentioned before, in the 3 cases of torque applying

procedure, the second case did not satisfy the pointing error requirement in elevation angle. We will not mention about the first case because it is unlikely to be used in real situations. For the comparison purpose, we arbitrary choose 3 modal damping coefficient such as 0.2 %, 0.5 % and 1.0 %. To see the results more clearly, we simulate the model in 200 seconds. Figure 4.39 shows the spin-up procedure used in this analysis. Figure 4.40 shows vibration settling down ratio during the first 200 seconds. In this Figure, it is hard to recognize the effects of all 3 cases but in Figure 4.41, we can clearly see the vibration settling down for each case.

Two trials were made for investigation. Firstly, we tried to find how much vibration was settled down in 200 seconds for each damping coefficient. Secondly, we found how much time was required to meet the pointing error requirement for each case. Figure 4.42 shows elevation angle pointing error decreasing ratio in 200 seconds. Each value stands for magnitude of pointing error ratio to its initial value which is the magnitude of pointing error without damping. As shown in Figure 4.42 pointing error decreased exponentially as damping coefficient increases linearly. Figure 4.43 shows desired time to meet pointing error requirement for each damping coefficient. As damping coefficient increases linearly, desired time decreased exponentially.

E. THE EQUILIBRIUM CONFIGURATION AT DIFFERENT ROTATING SPEEDS

Initial conditions were given for 3 cases such as 5 r.p.m, 10 r.p.m and 15 r.p.m with damping coefficient of 2 %. From this result, we could investigate the magnitude of deflection in each direction and slope at the tip position. Figure 4.45 shows angular velocity (rotating speed) variation with time. As the initial rotating speed increases, magnitude of oscillation was also increased and the rotating speed at the equilibrium state also increased. As we mentioned in section B, angular momentum is constant in the system since no external torque is applying. Therefore as the boom deflects to the positive x-direction, radius of rotation decreases so angular velocity increases consequently. Figure 4.45 shows elevation angle change and its magnitude of fluctuation change. As the magnitude of initial speed increases linearly, elevation angle change and magnitude of fluctuation increases exponentially. This result is shown in Figure 4.47. Magnitude of deflection in x-direction and z-direction was also increased as the rotating speed increased as shown in Figures 4.47 and 4.48 respectively. This effects was more sensitive for the flexible material boom. The oscillation of azimuth angle centered at 0.

F. FIGURES

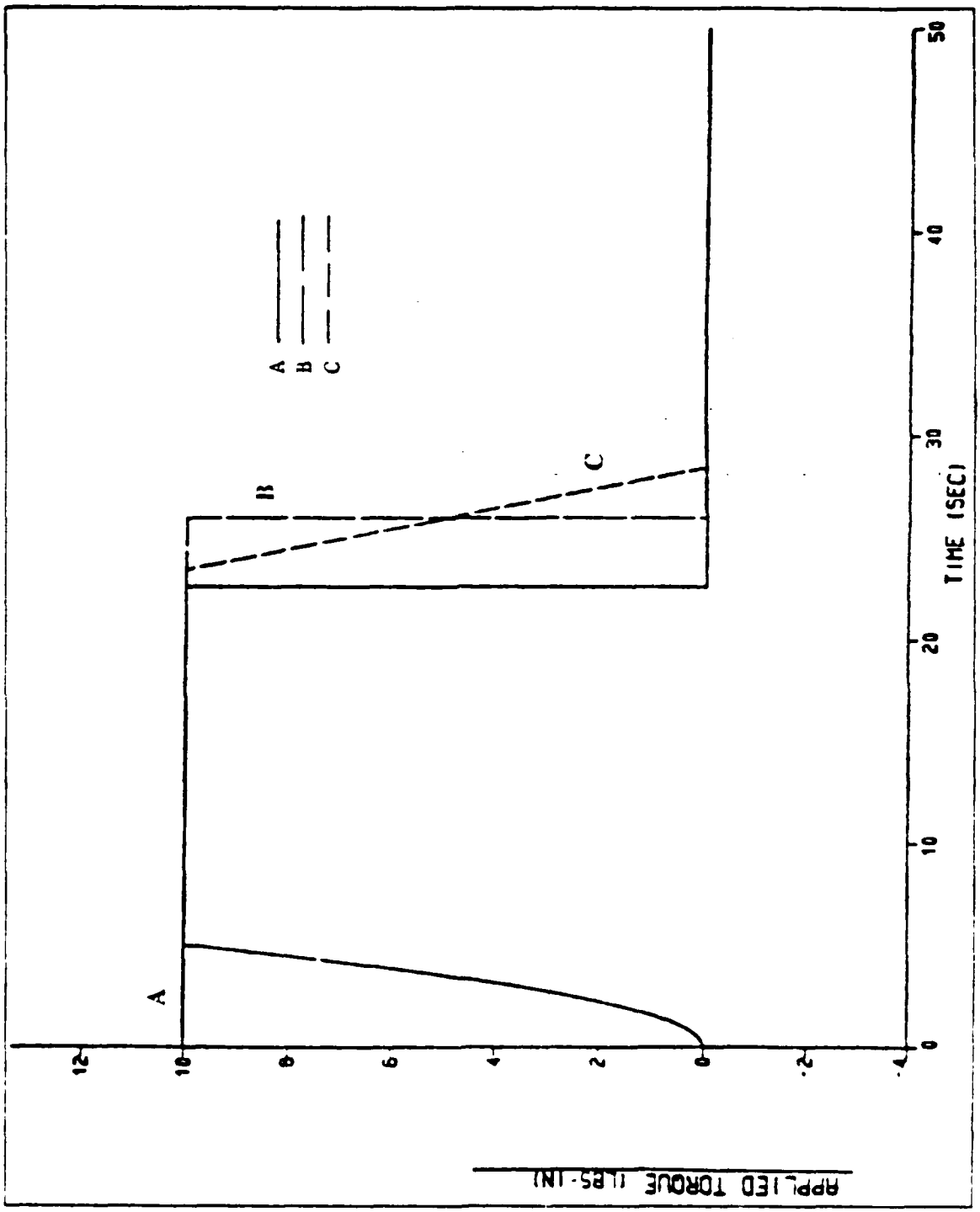

Figure 4.1 Applied torque vs. time.

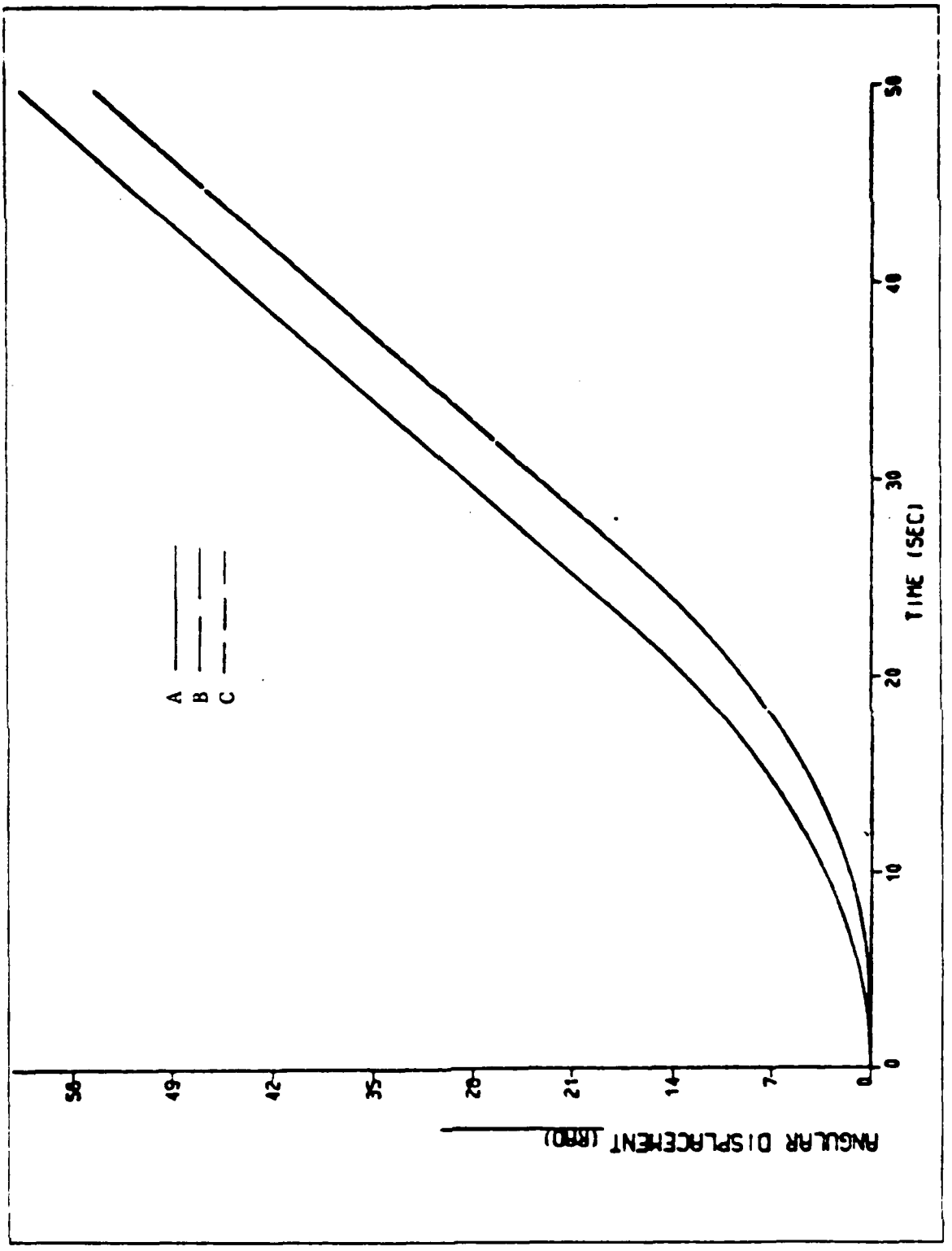

Figure 4.2 Angular displacement vs. time.

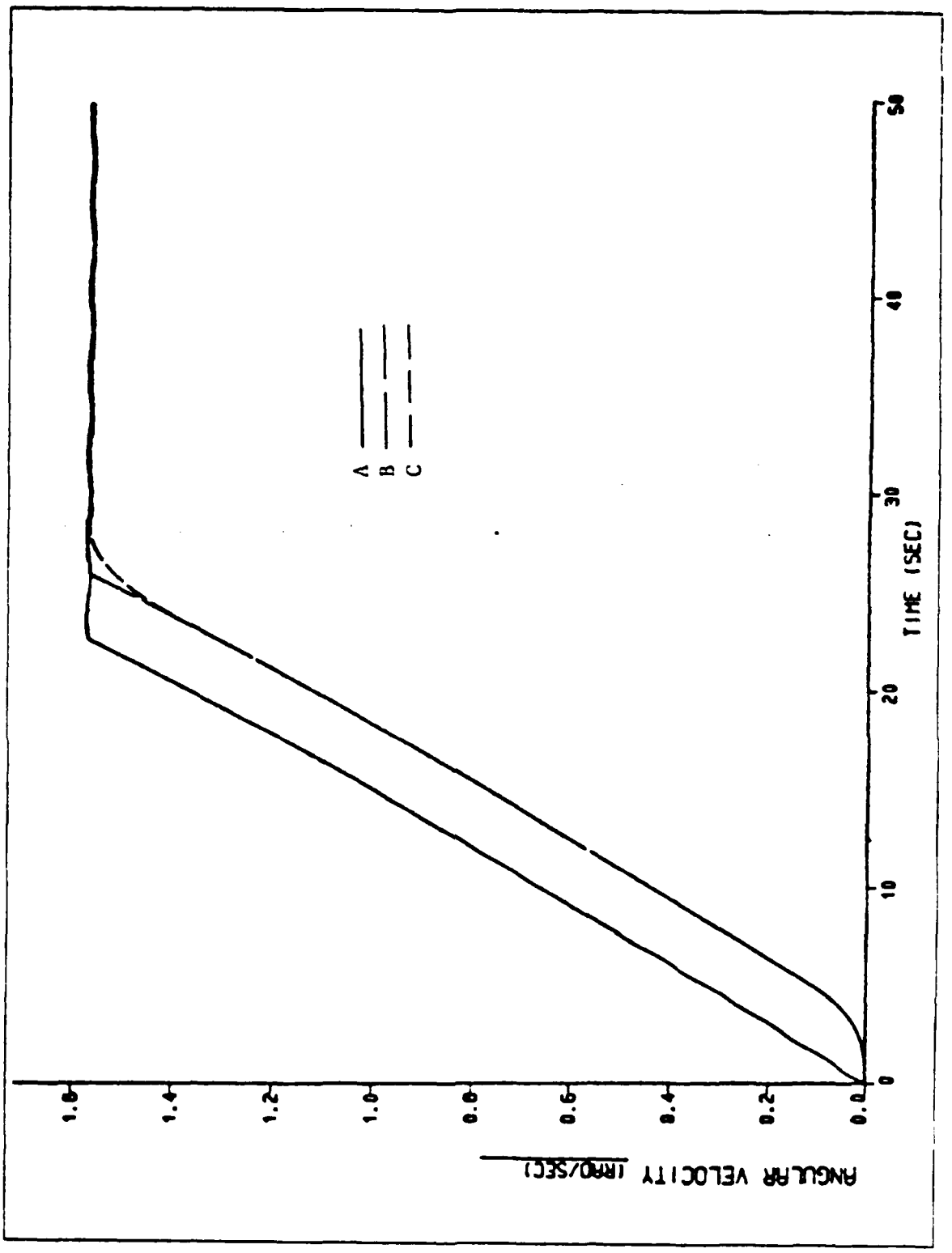

Figure 4.3 Angular velocity vs. time (AL.).

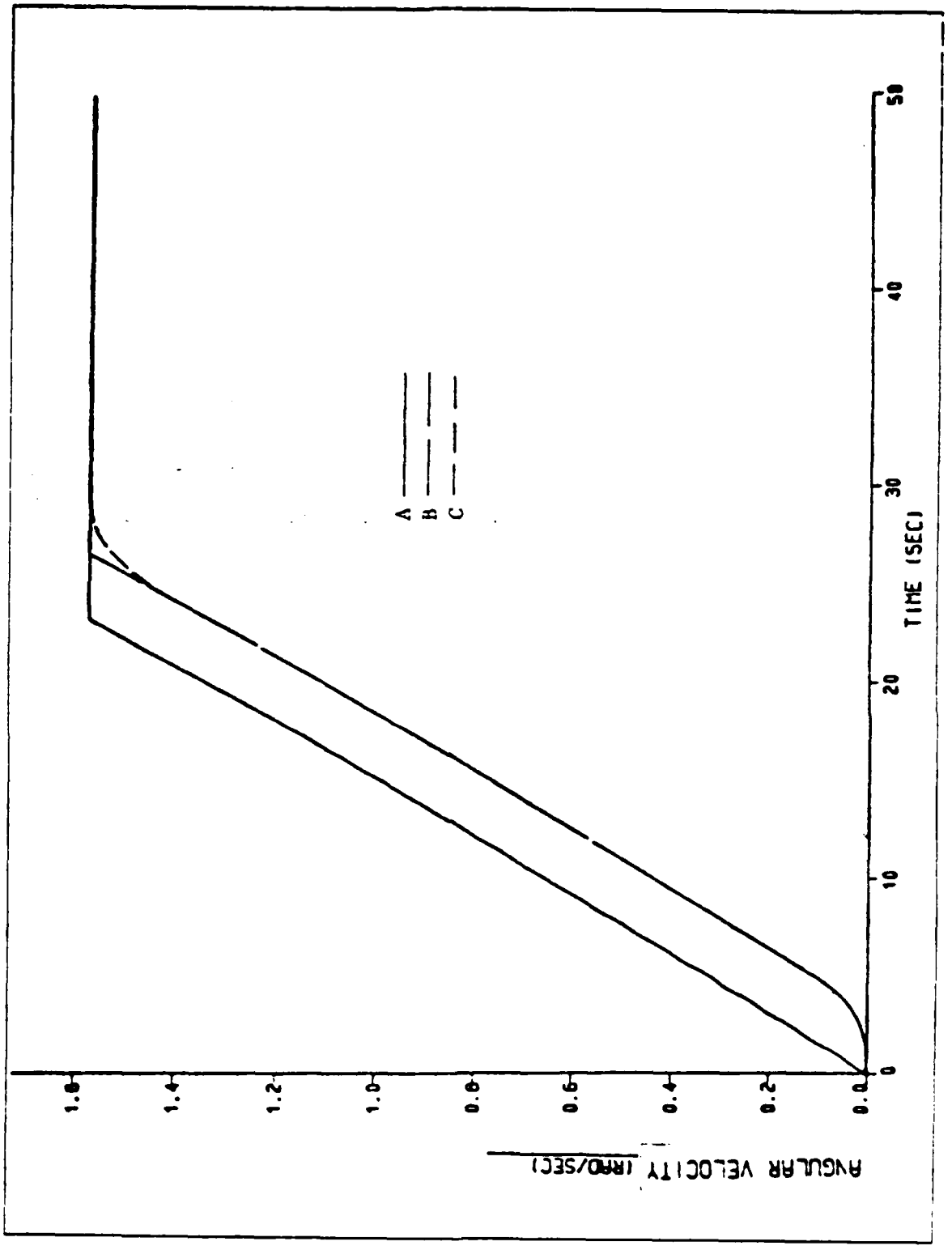

Figure 4.4 Angular velocity vs. time (COM.).

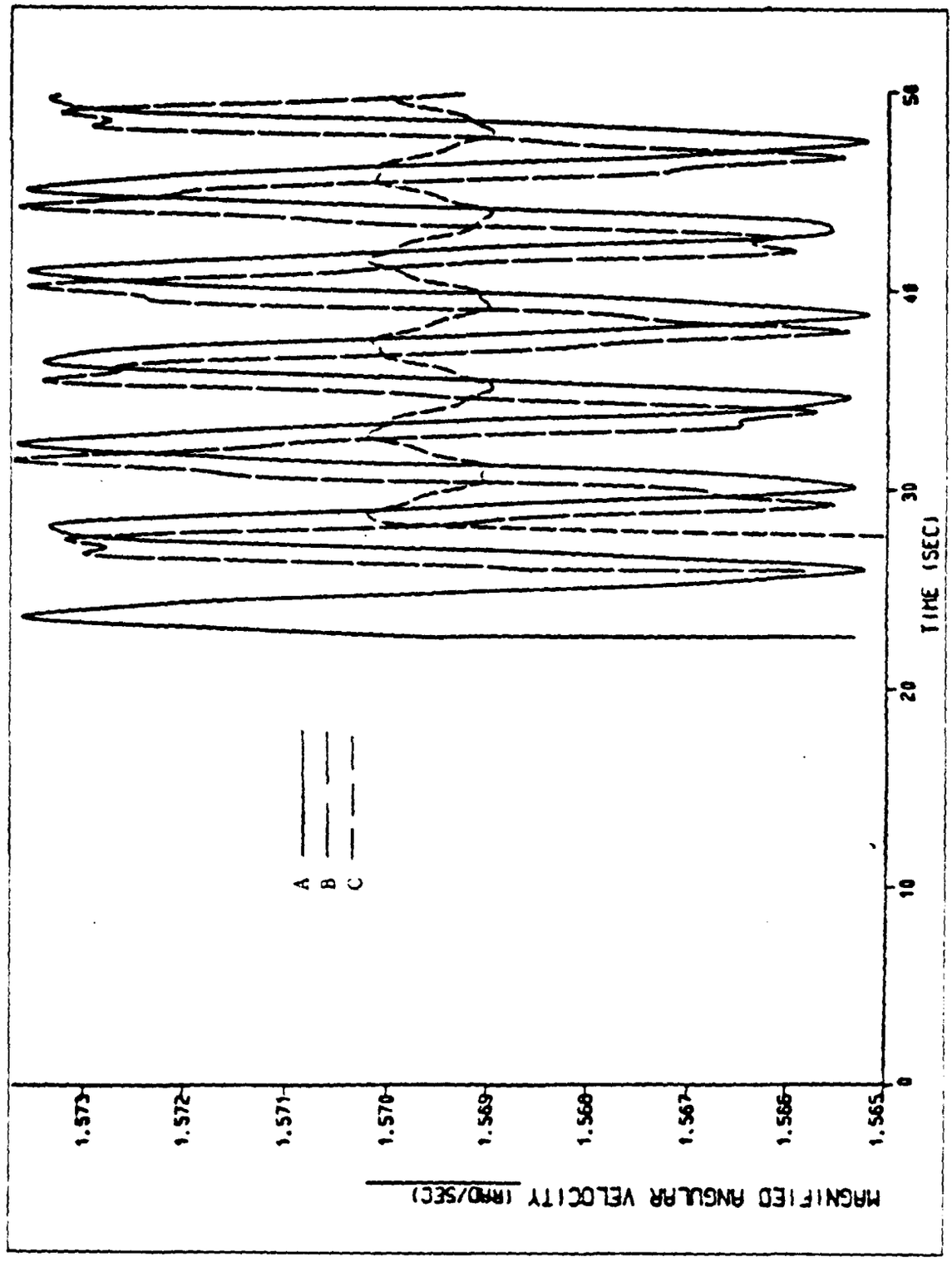

Figure 4.5 Magnified angular velocity vs. time (AL.).

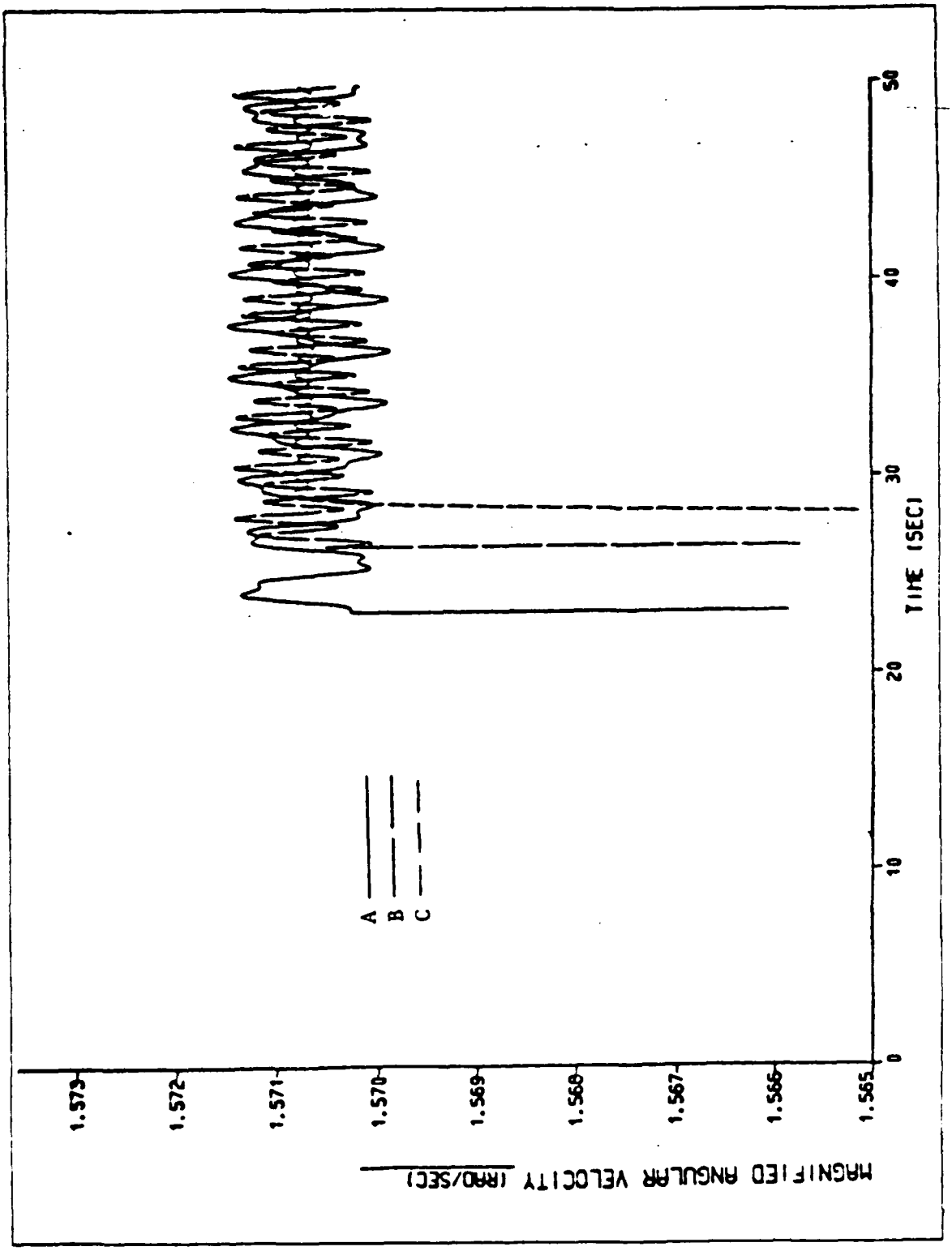

Figure 4.6 Magnified angular velocity vs. time (COM.).

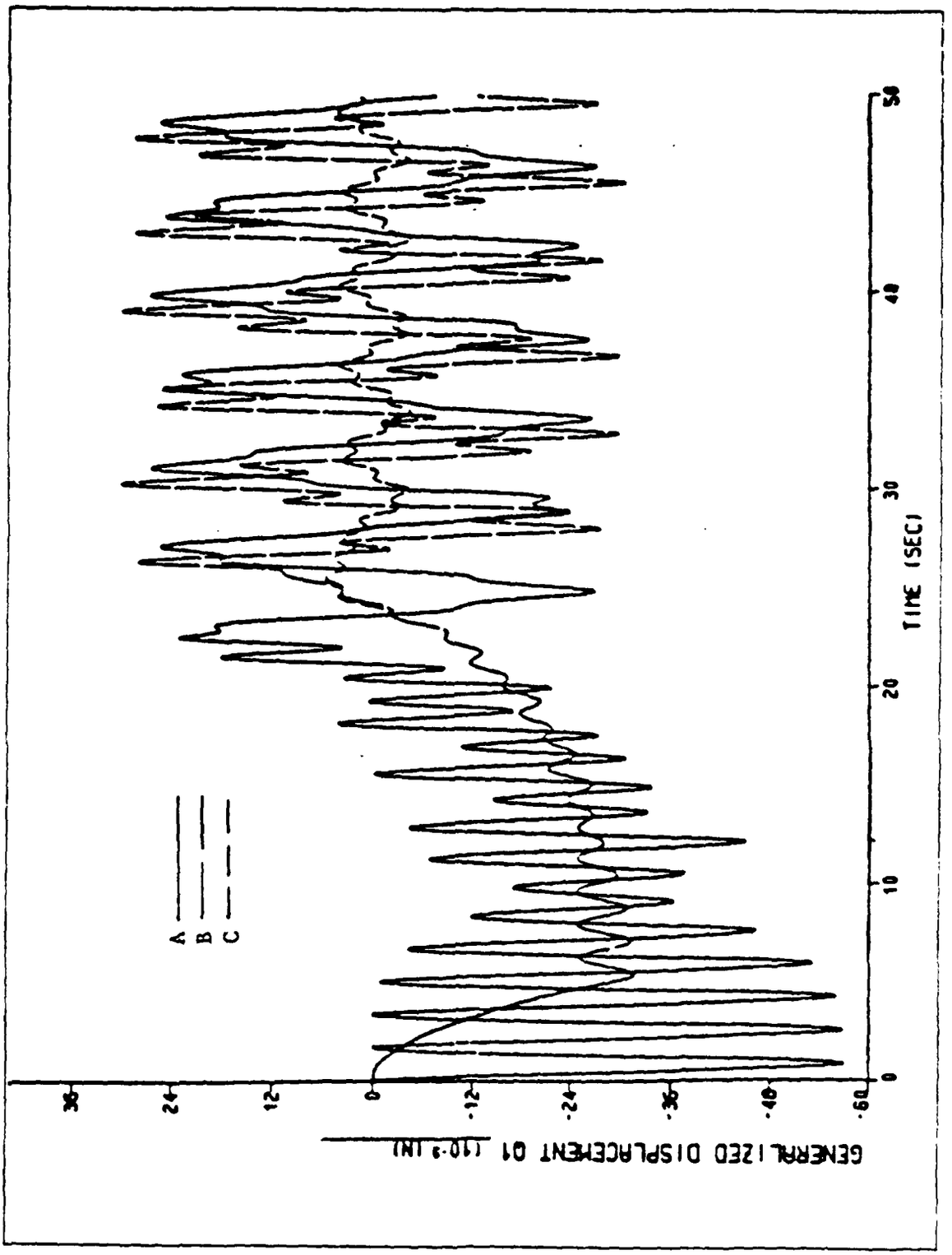

Figure 4.7 First mode generalized displacement vs. time (AL.).

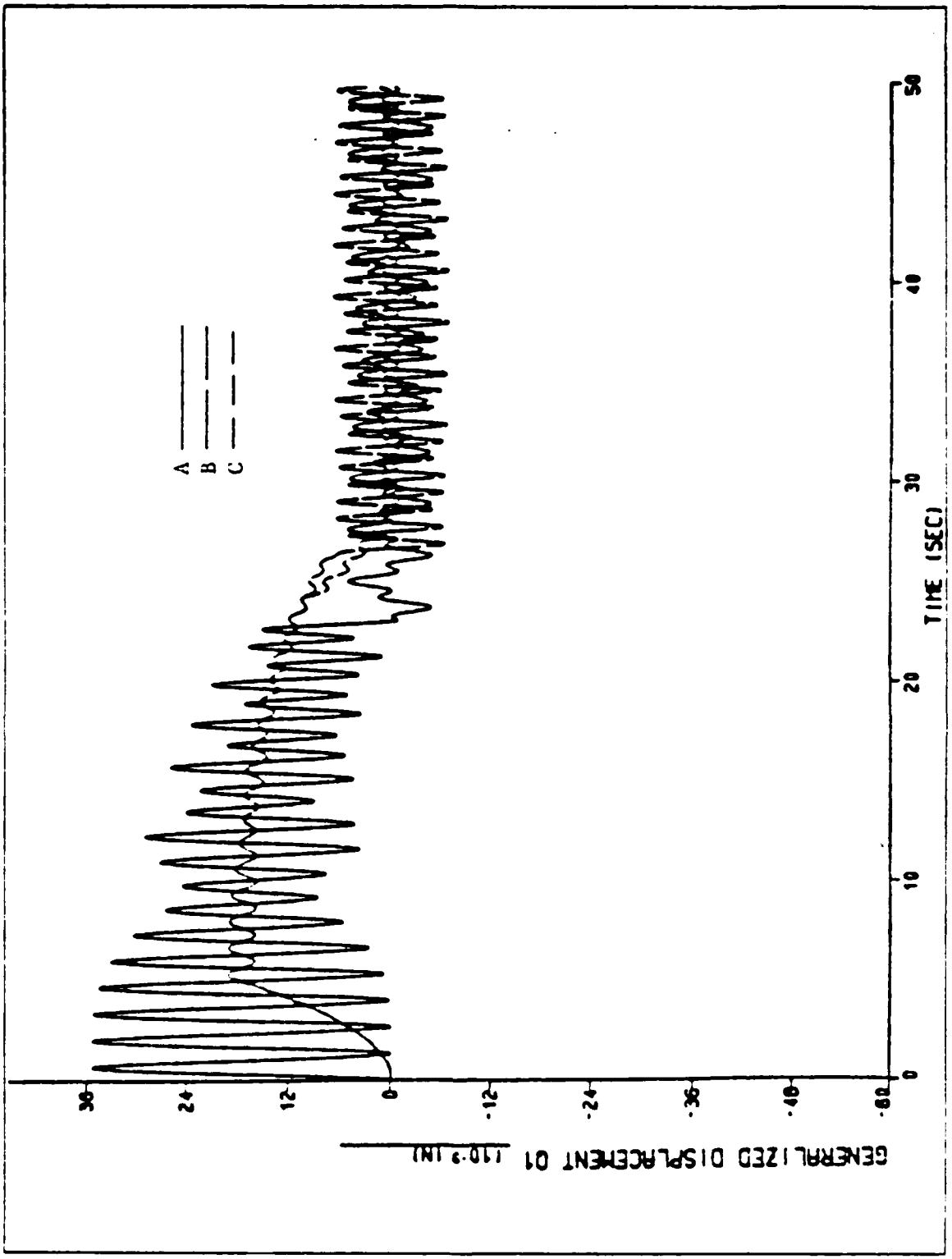

Figure 4.8 First mode generalized displacement vs. time (COM.).

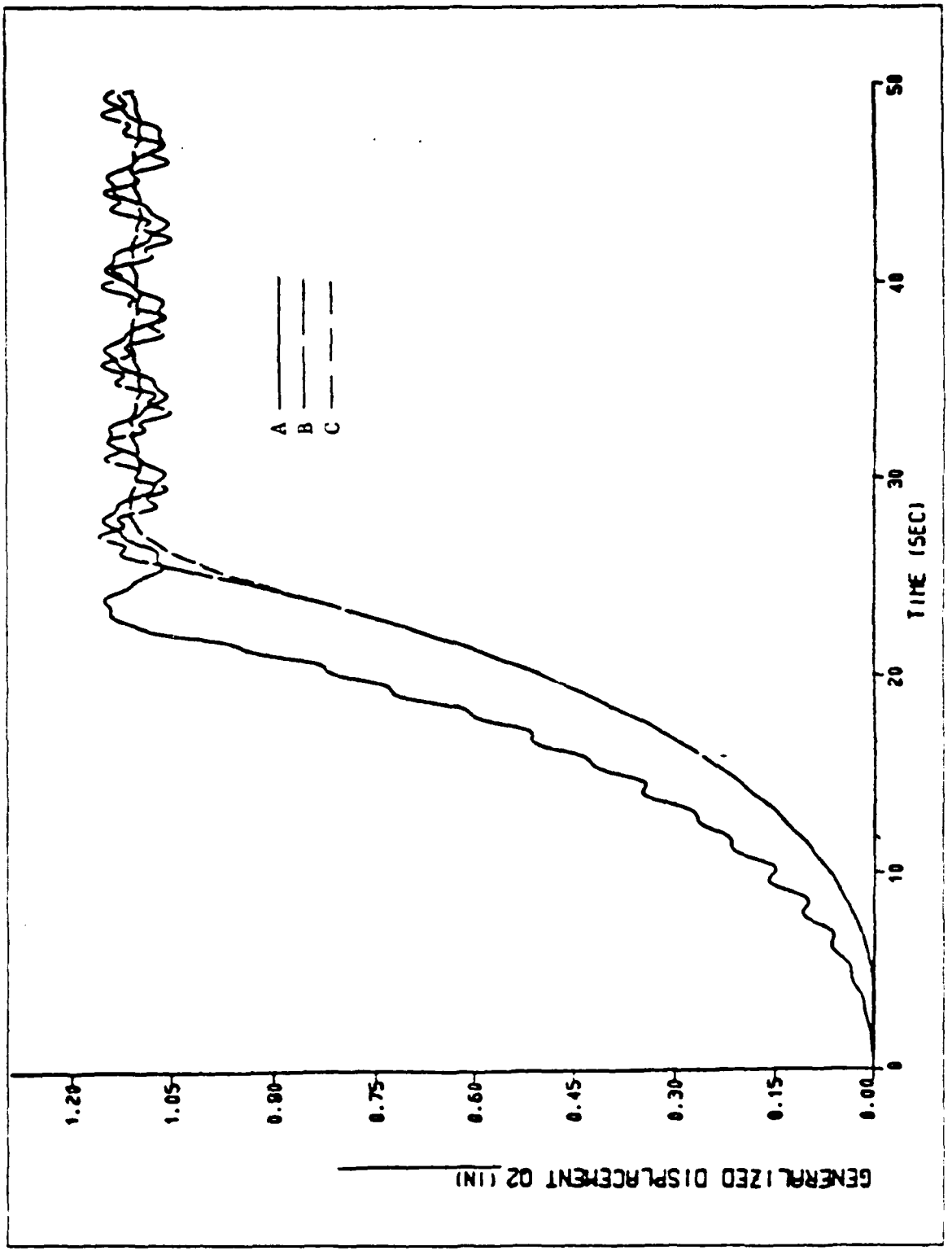

Figure 4.9 Second mode generalized displacement vs. time (AL.).

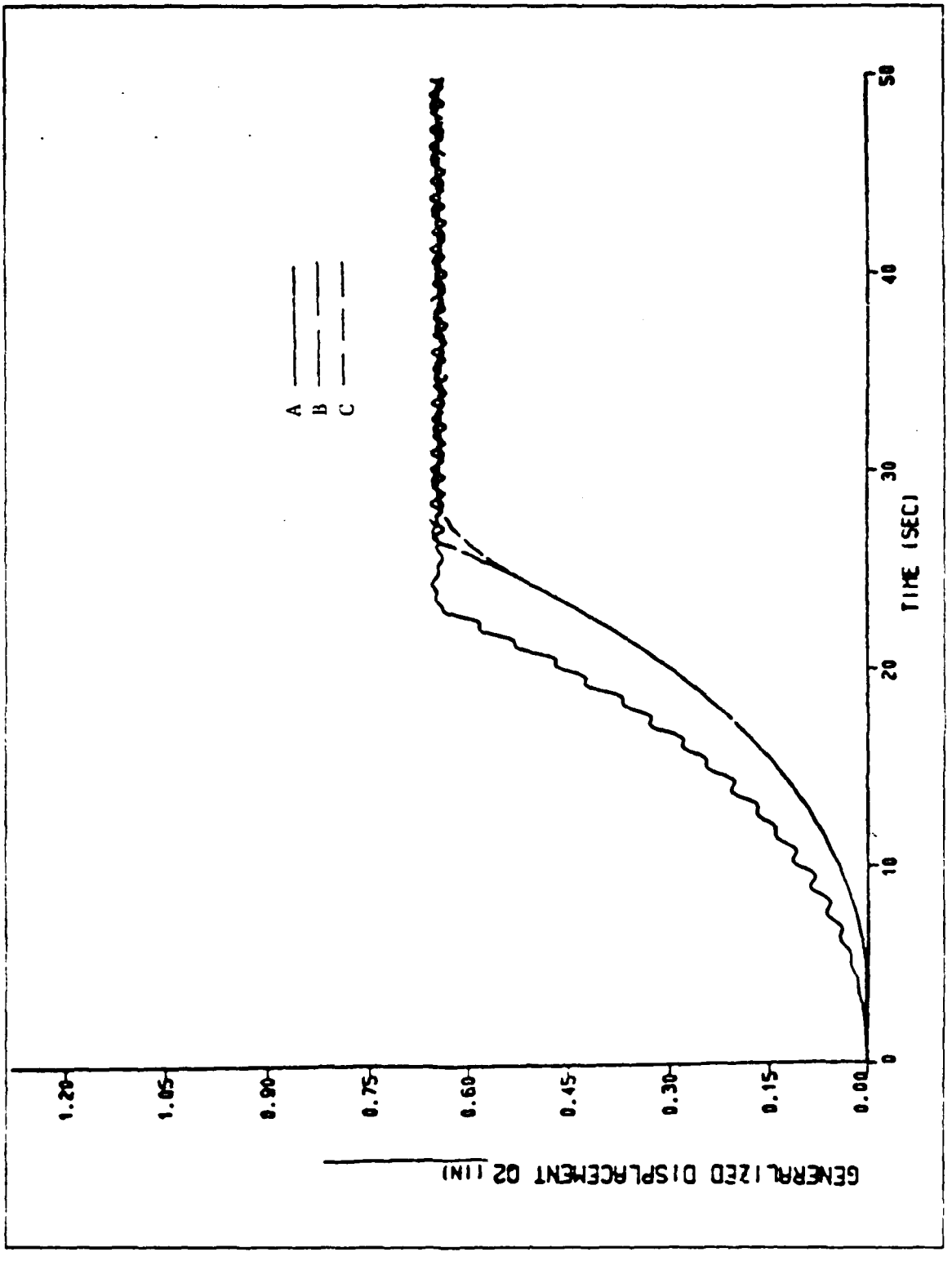

Figure 4.10 Second mode generalized displacement vs. time (COM.).

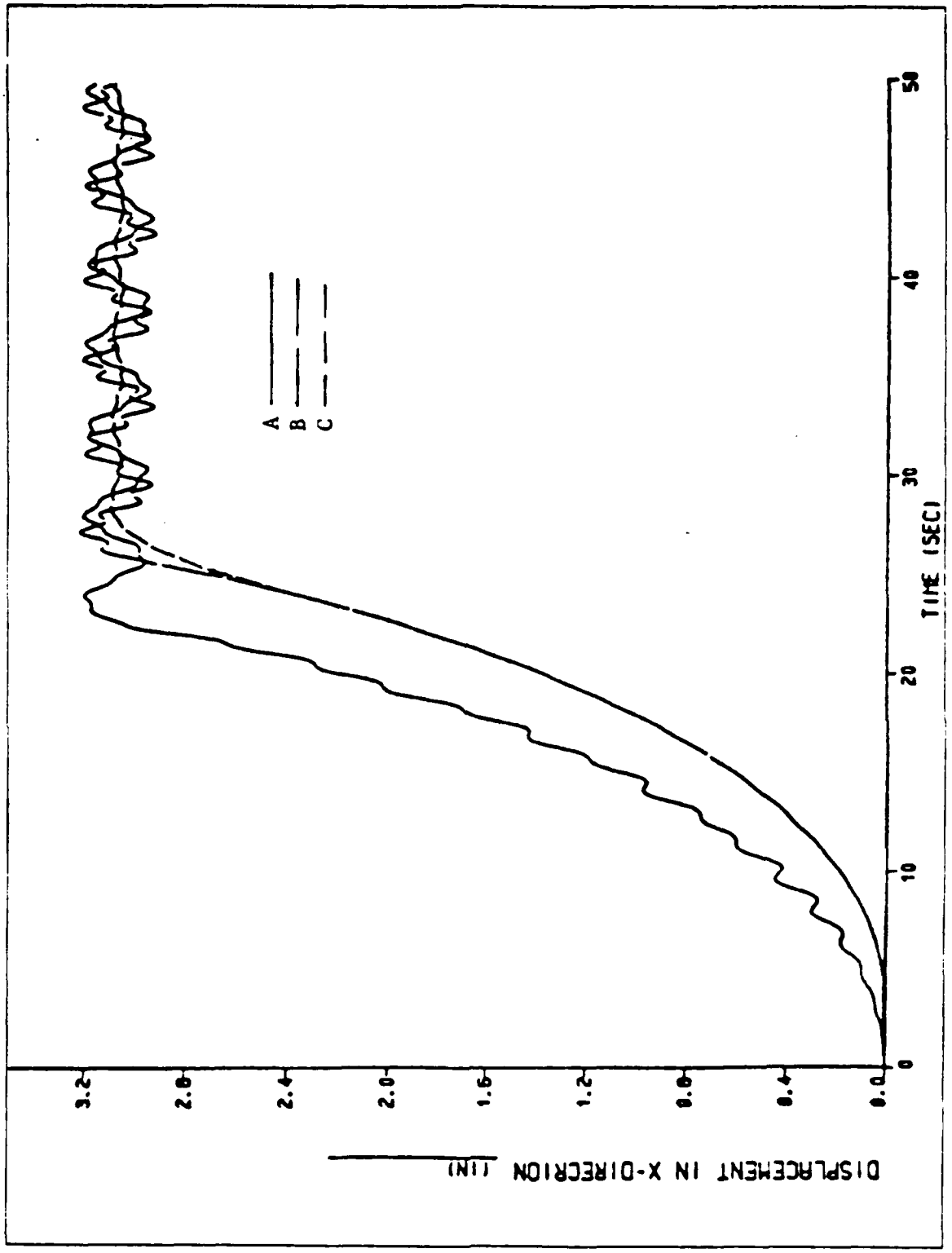

Figure 4.11 Displacement in x-direction vs. time (AL.).

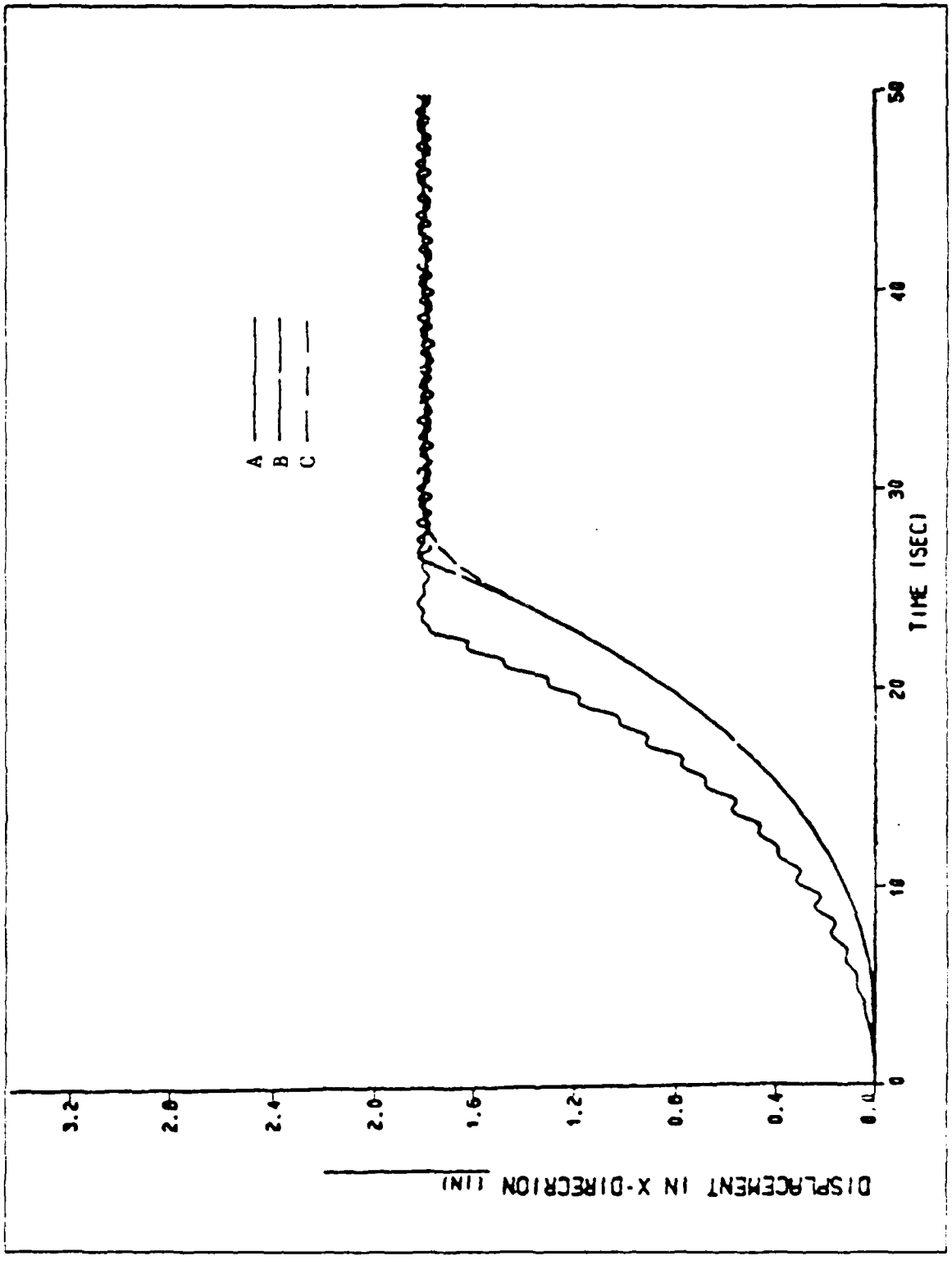

Figure 4.12 Displacement in x-direction vs. time (COM.).

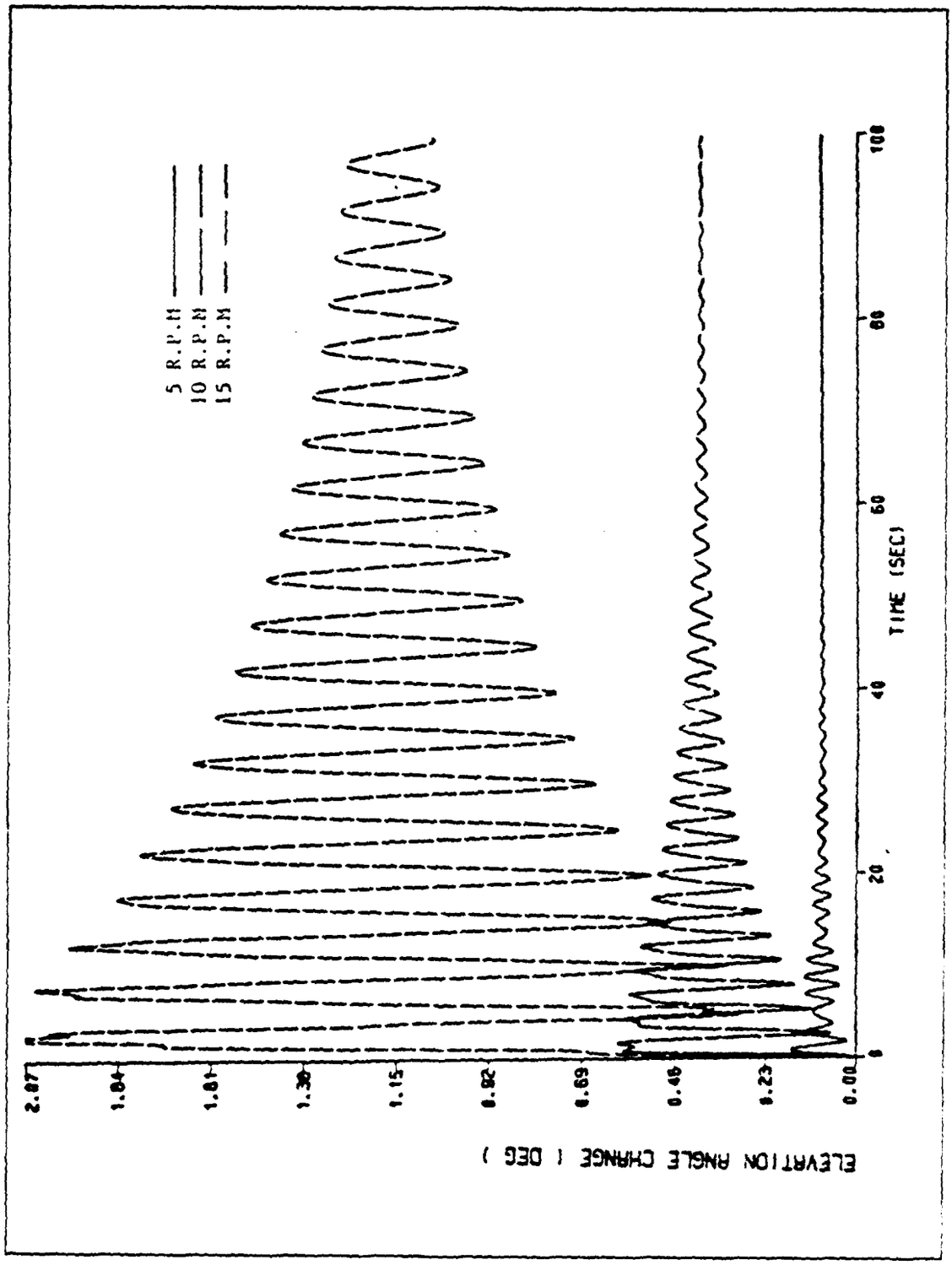

Figure 4.13 Displacement in y-direction vs. time (A.L.).

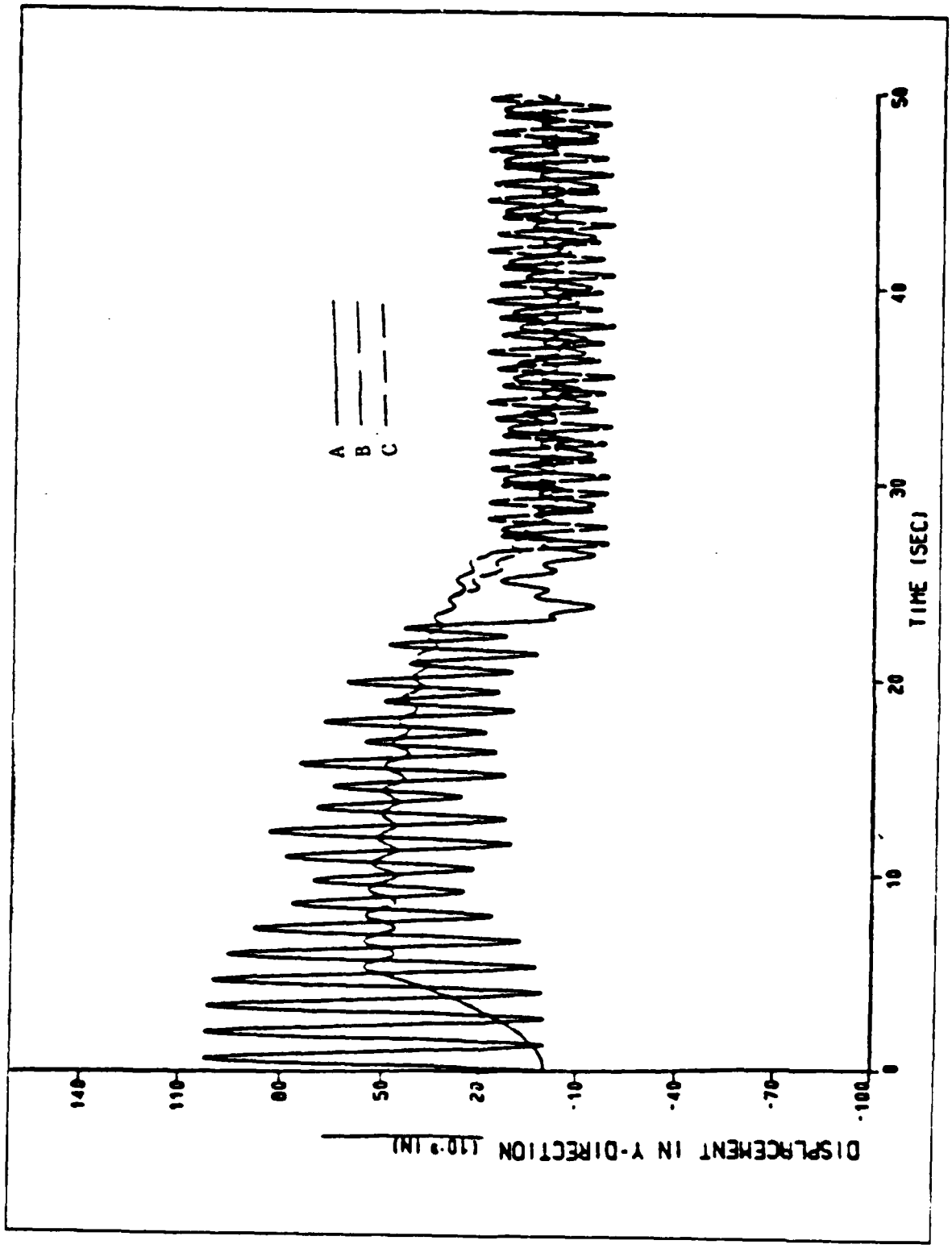

Figure 4.14 Displacement in y-direction vs. time (C.O.M.).

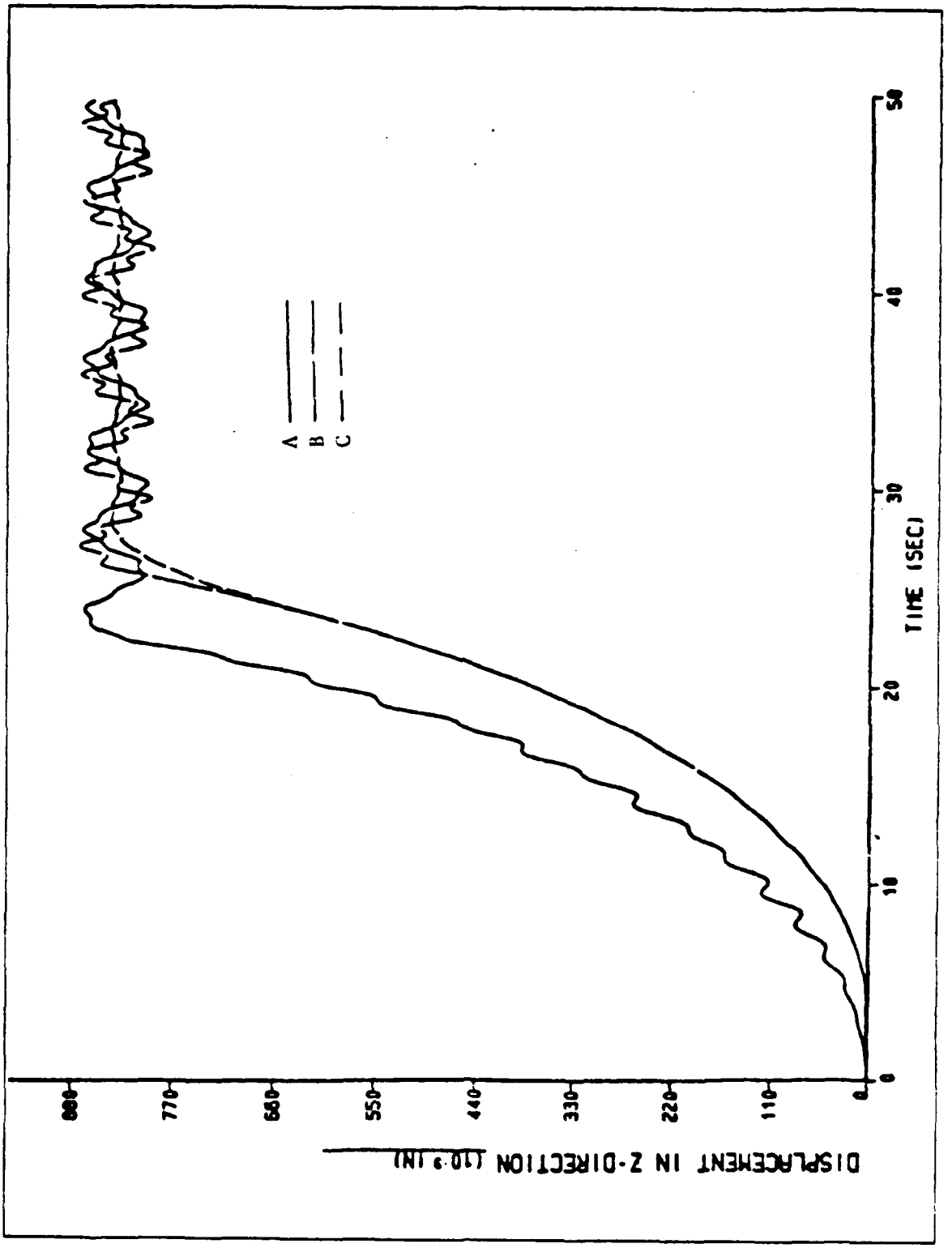

Figure 4.15 Displacement in z-direction vs. time (AL.).

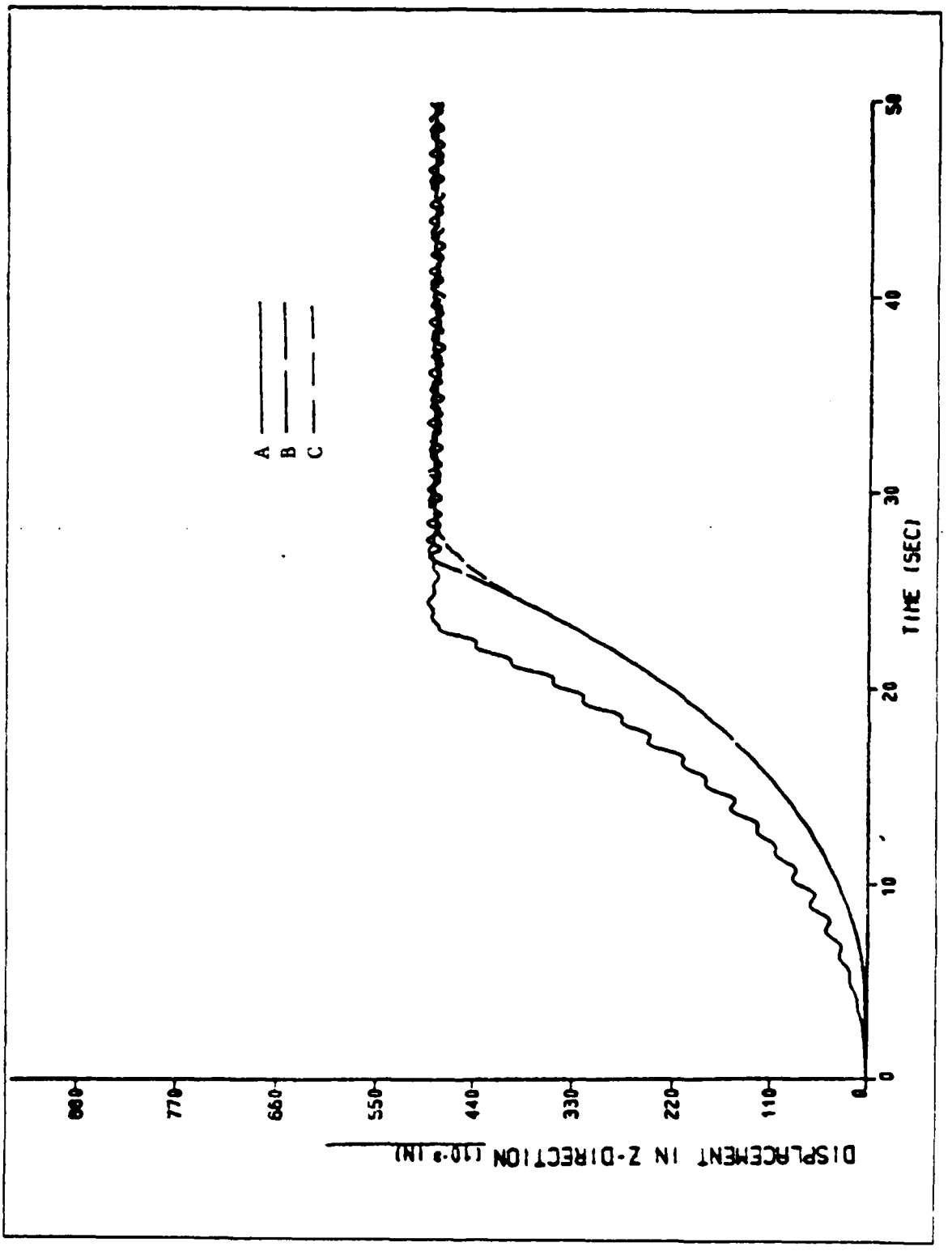

Figure 4.16 Displacement in z-direction vs. time (COM.).

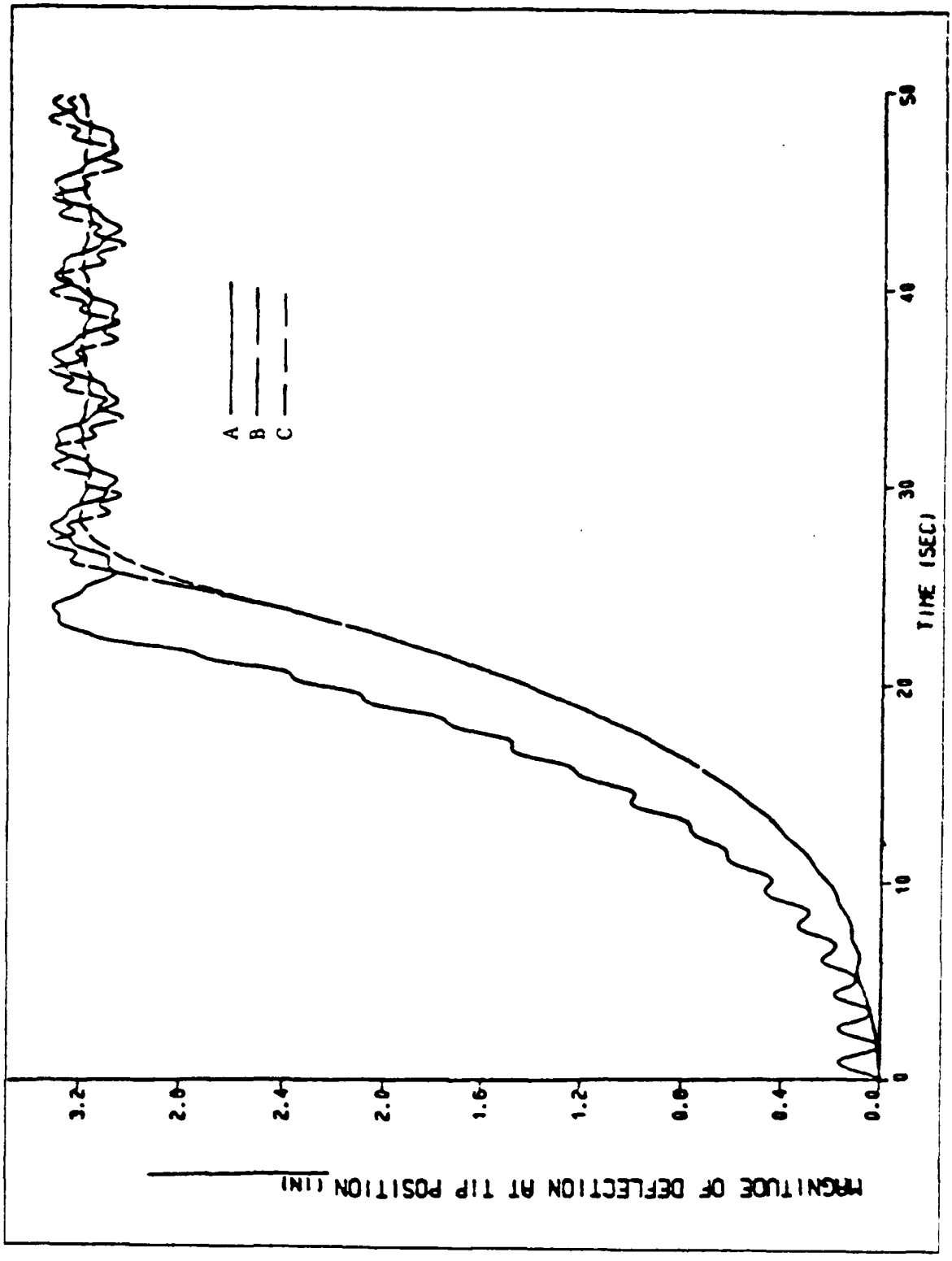

Figure 4.17 Magnitude of deflection at tip position vs. time (AL.).

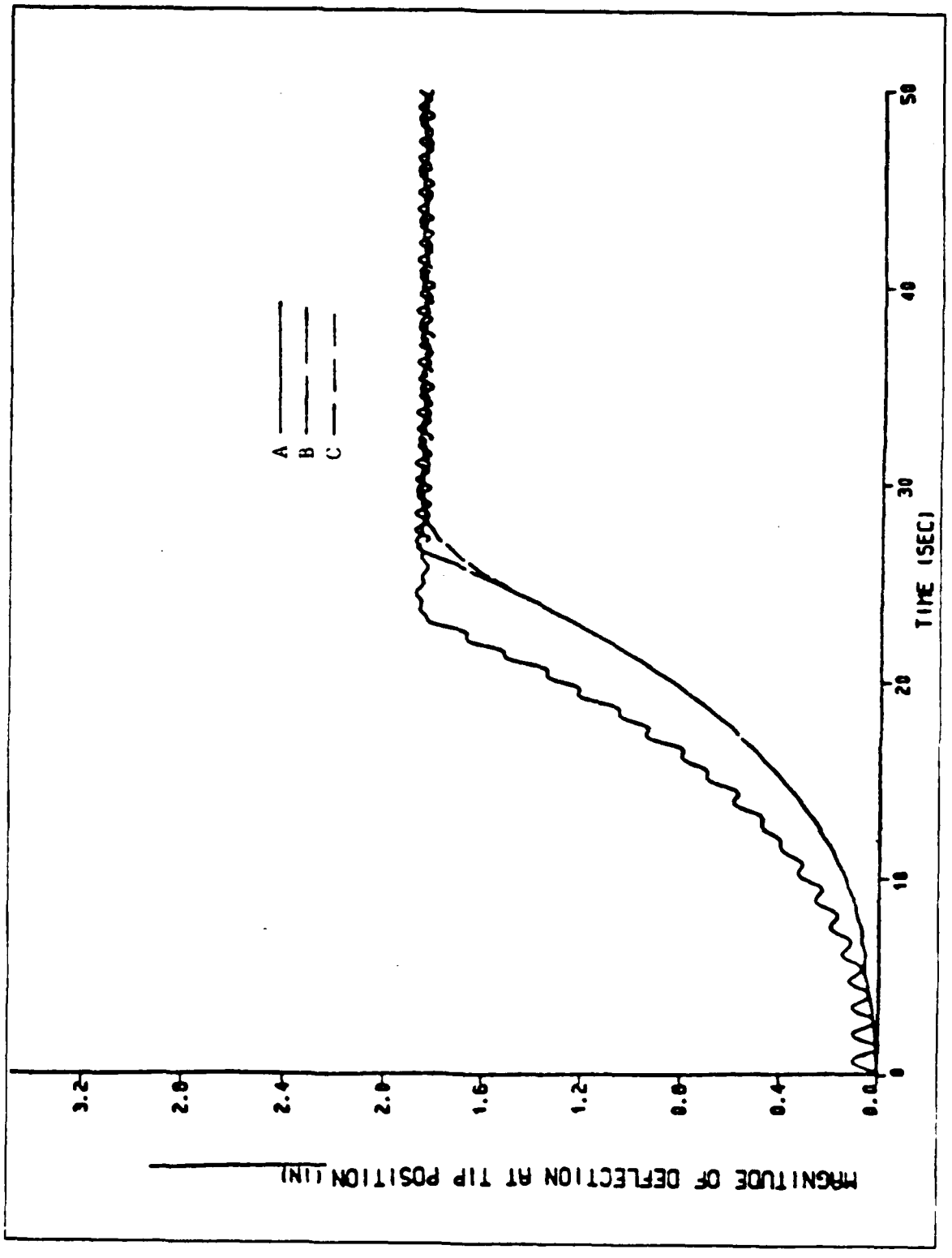

Figure 4.18 Magnitude of deflection at tip position vs. time (COM.).

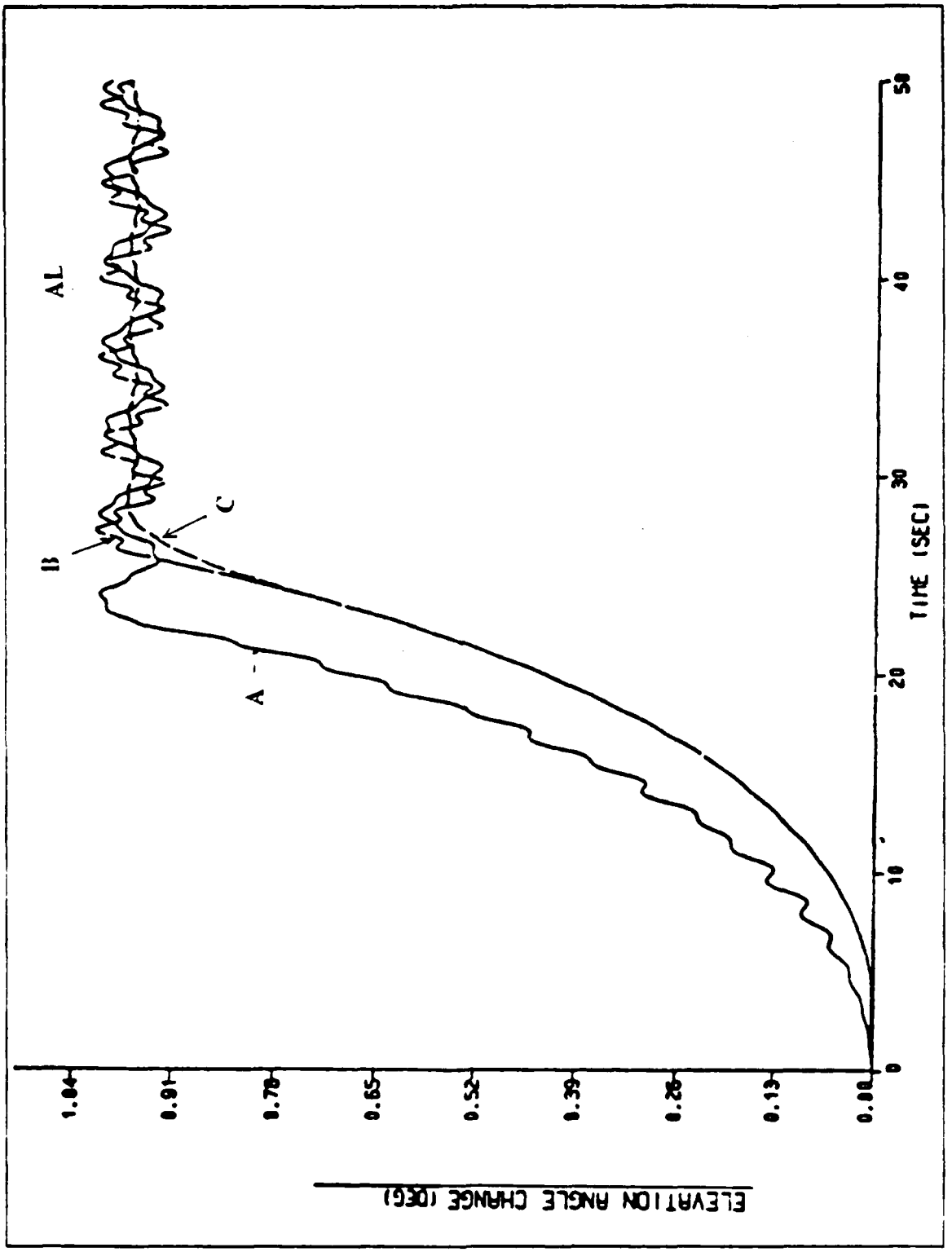

Figure 4.19 Elevation angle change vs. time (AL.).

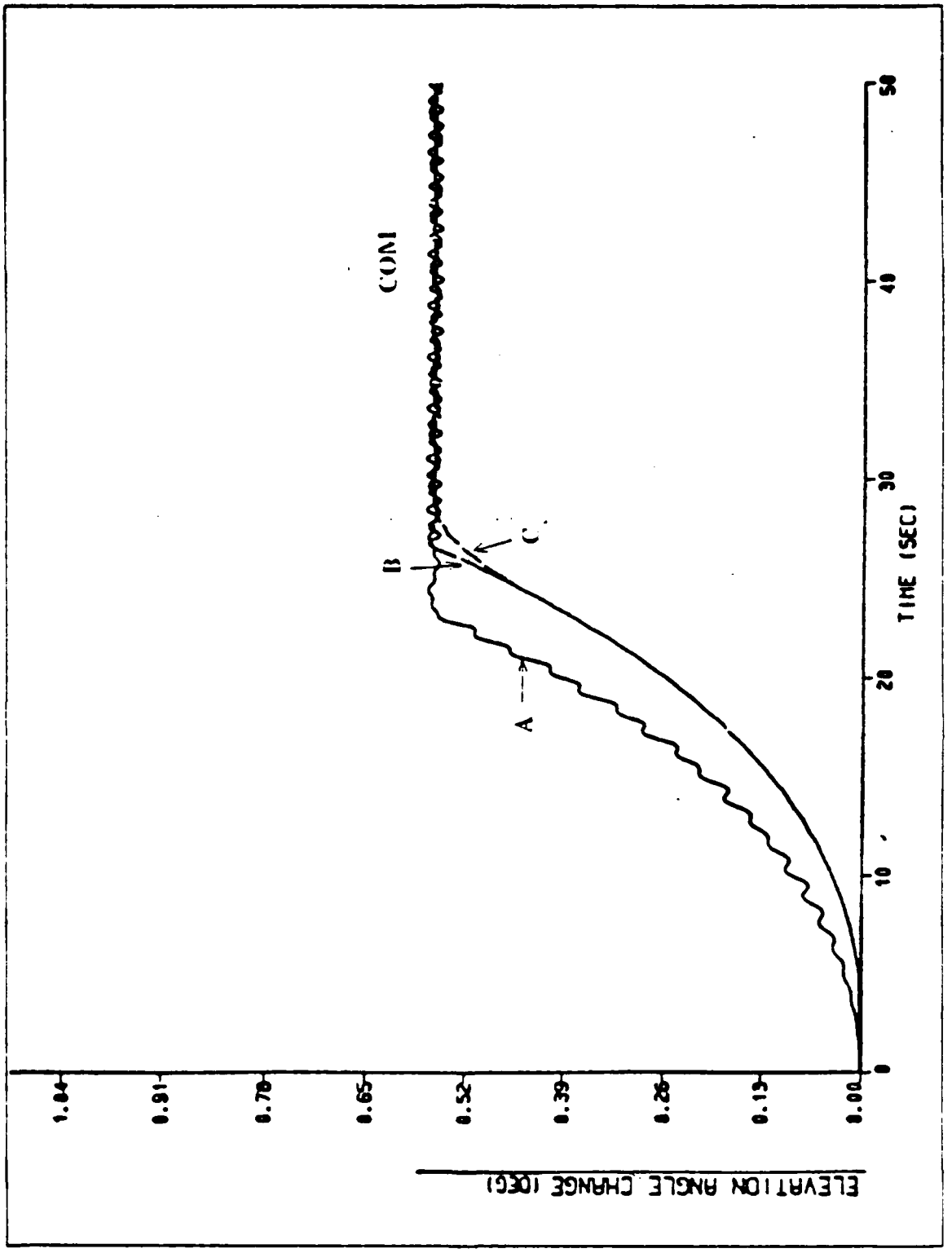

Figure 4.20 Elevation angle change vs. time (COM.).

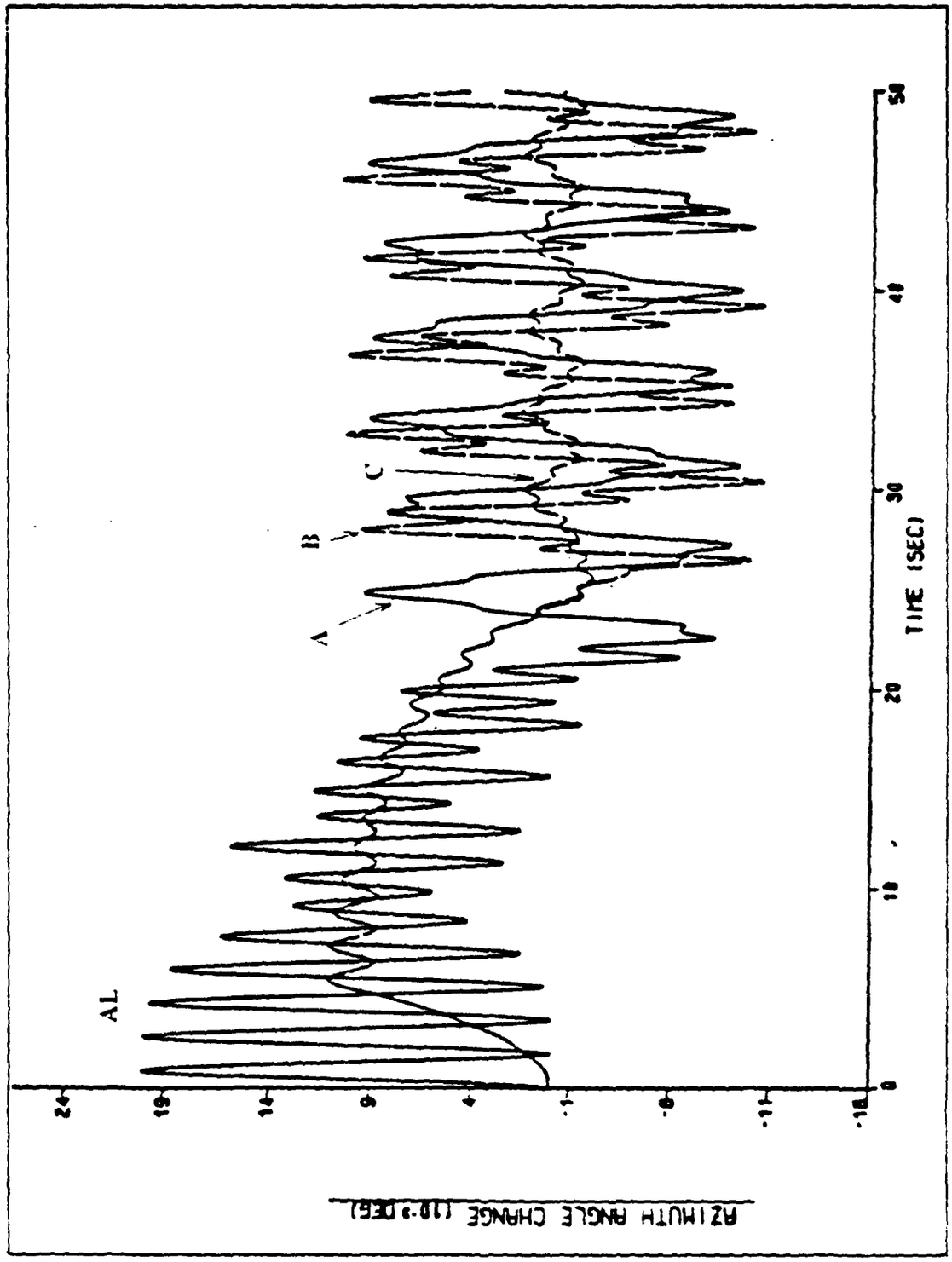

Figure 4.21 Azimuth angle change vs. time (AL.).

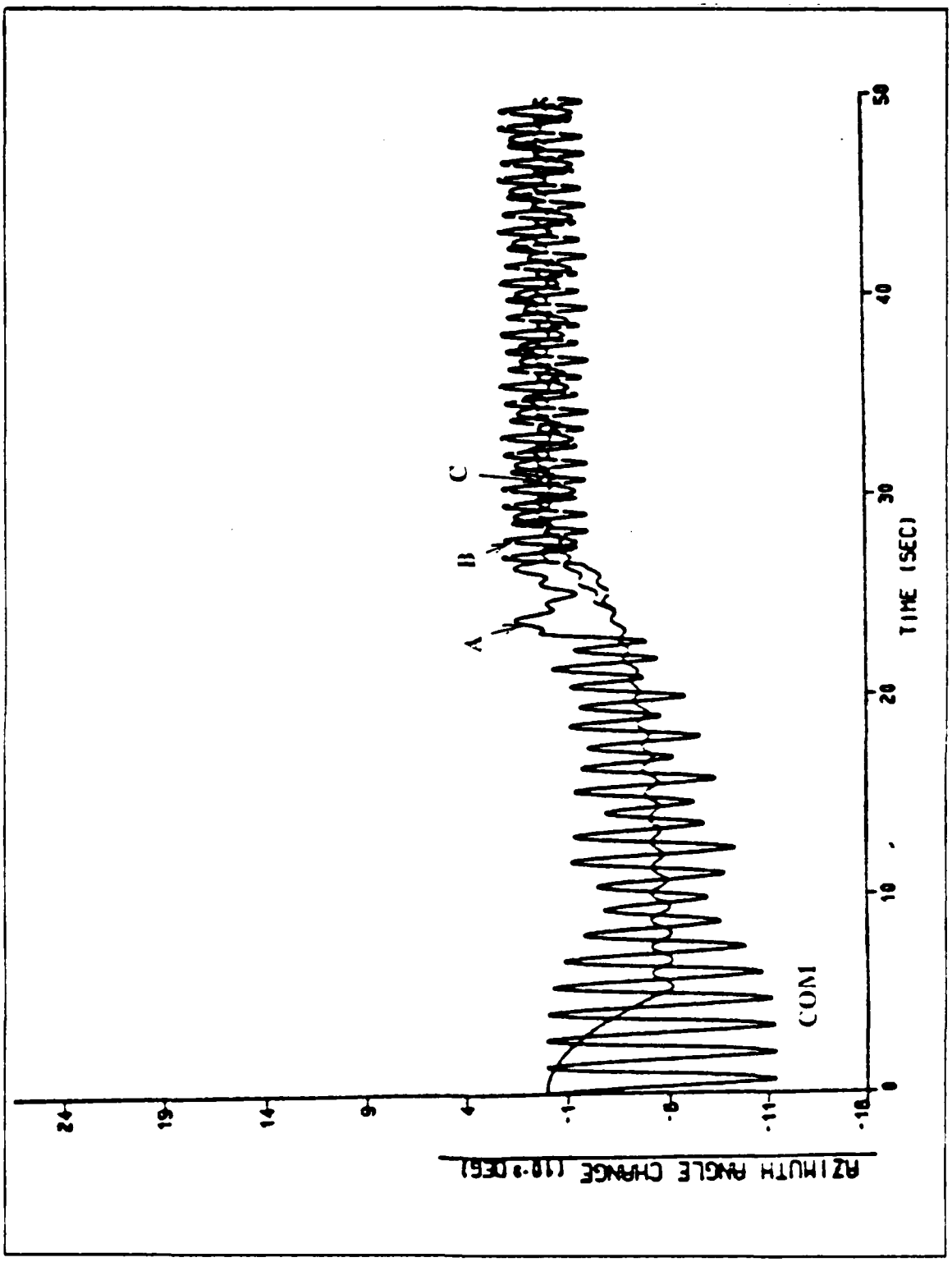

Figure 4.22 Azimuth angle change vs. time (COM.).

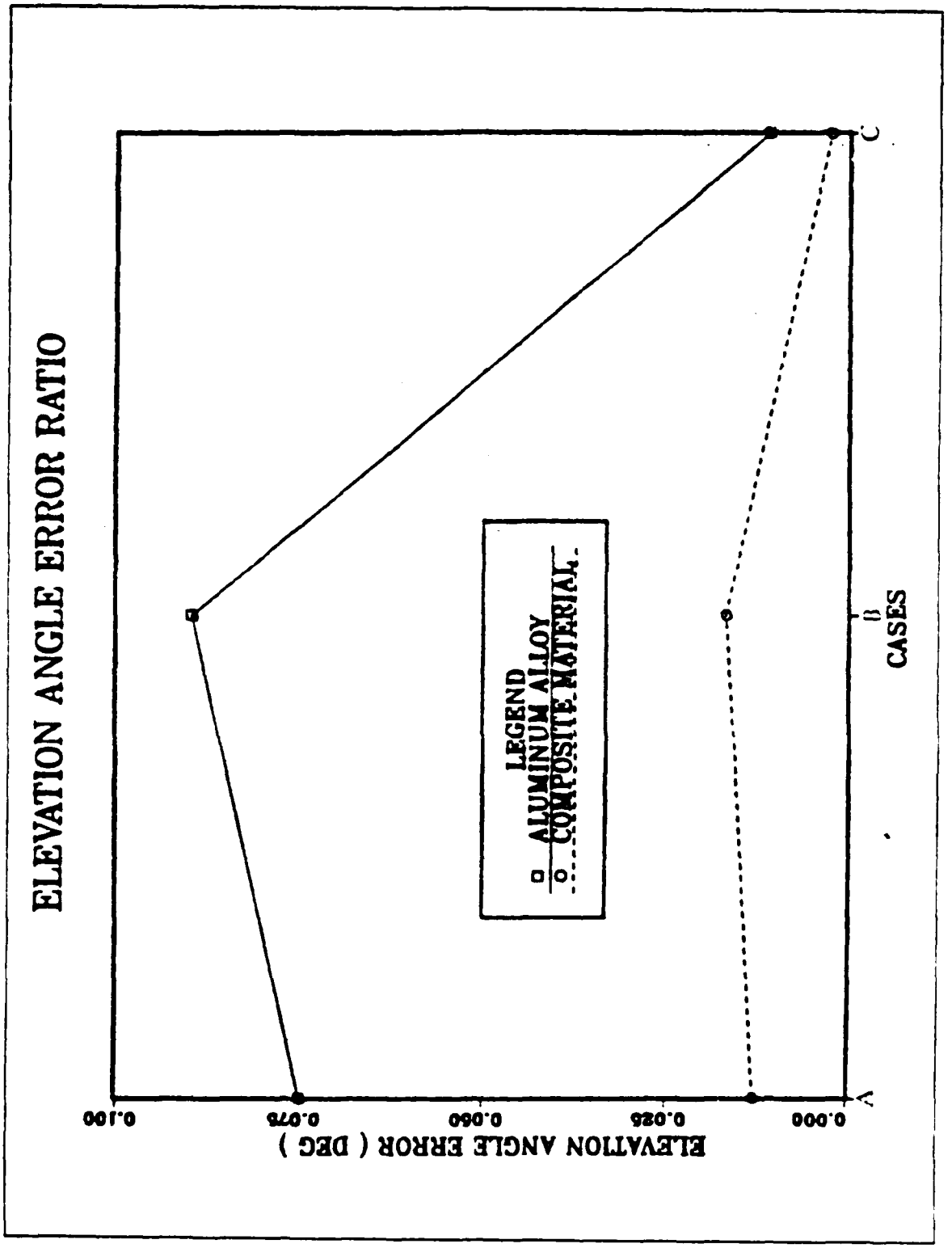

Figure 4.23 Pointing error in elevation angle vs. torque applying procedure.

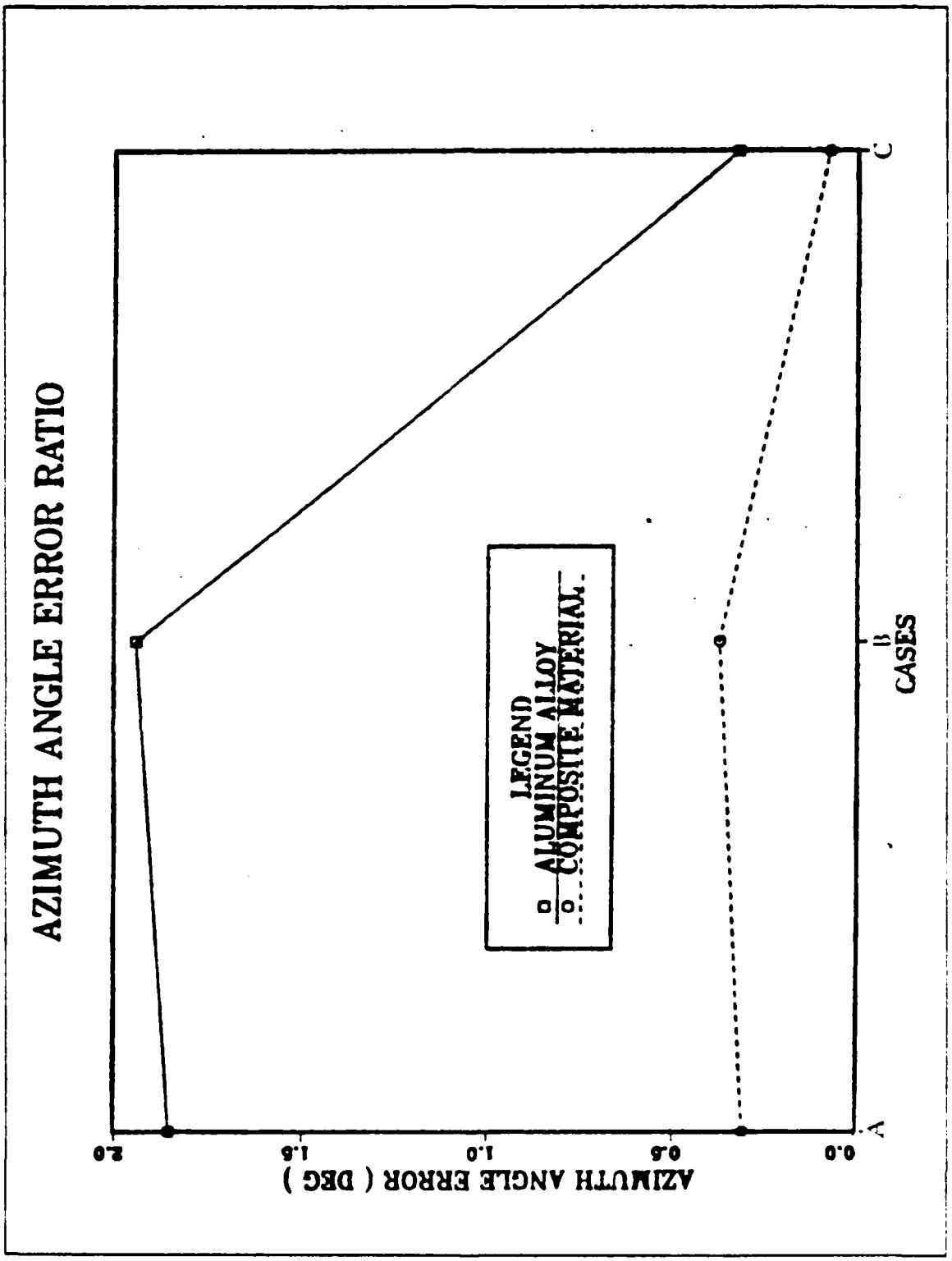

Figure 4.24 Pointing error in azimuth angle vs. torque applying procedure.

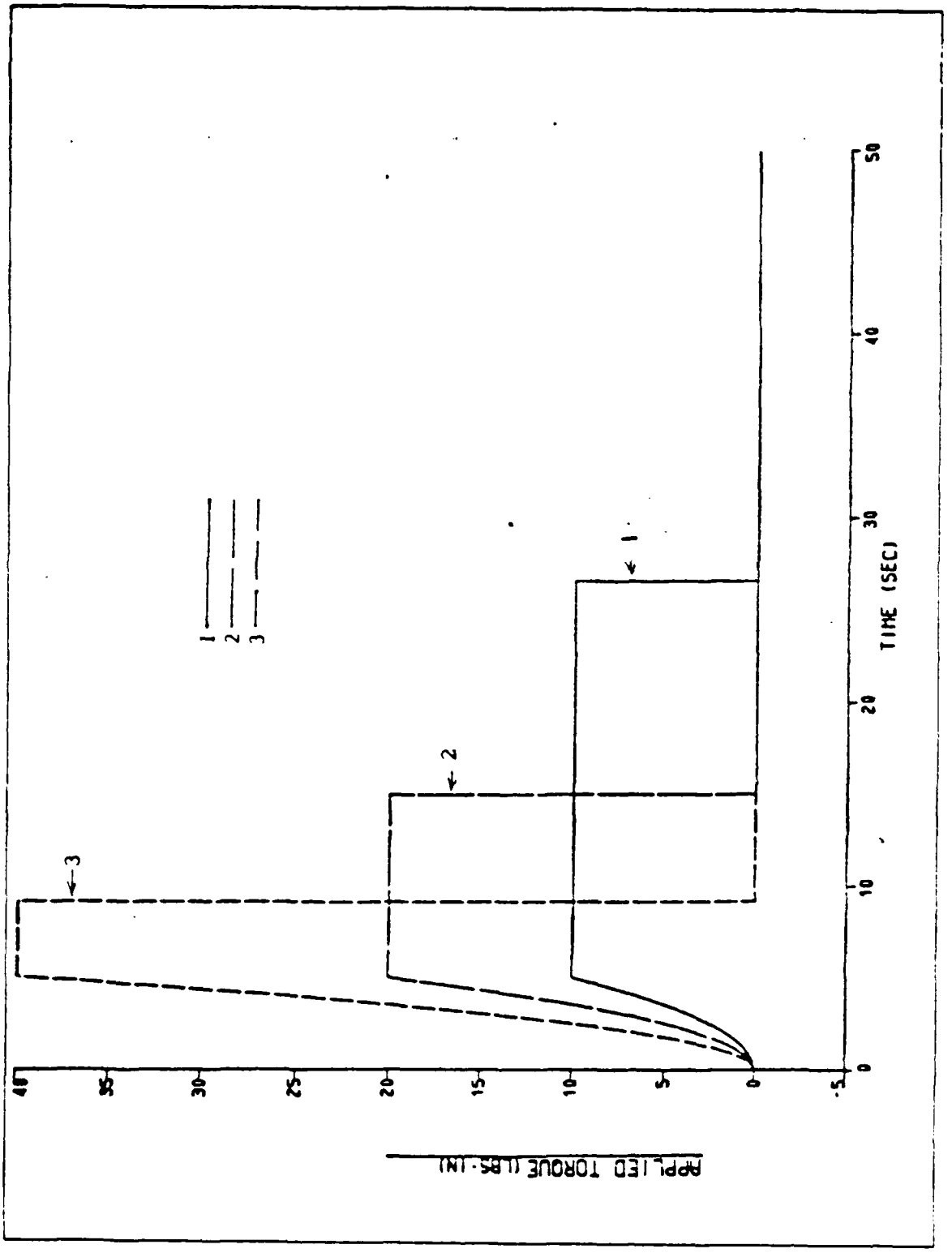

Figure 4.25 Applied torque with changing magnitude vs. time (AL.).

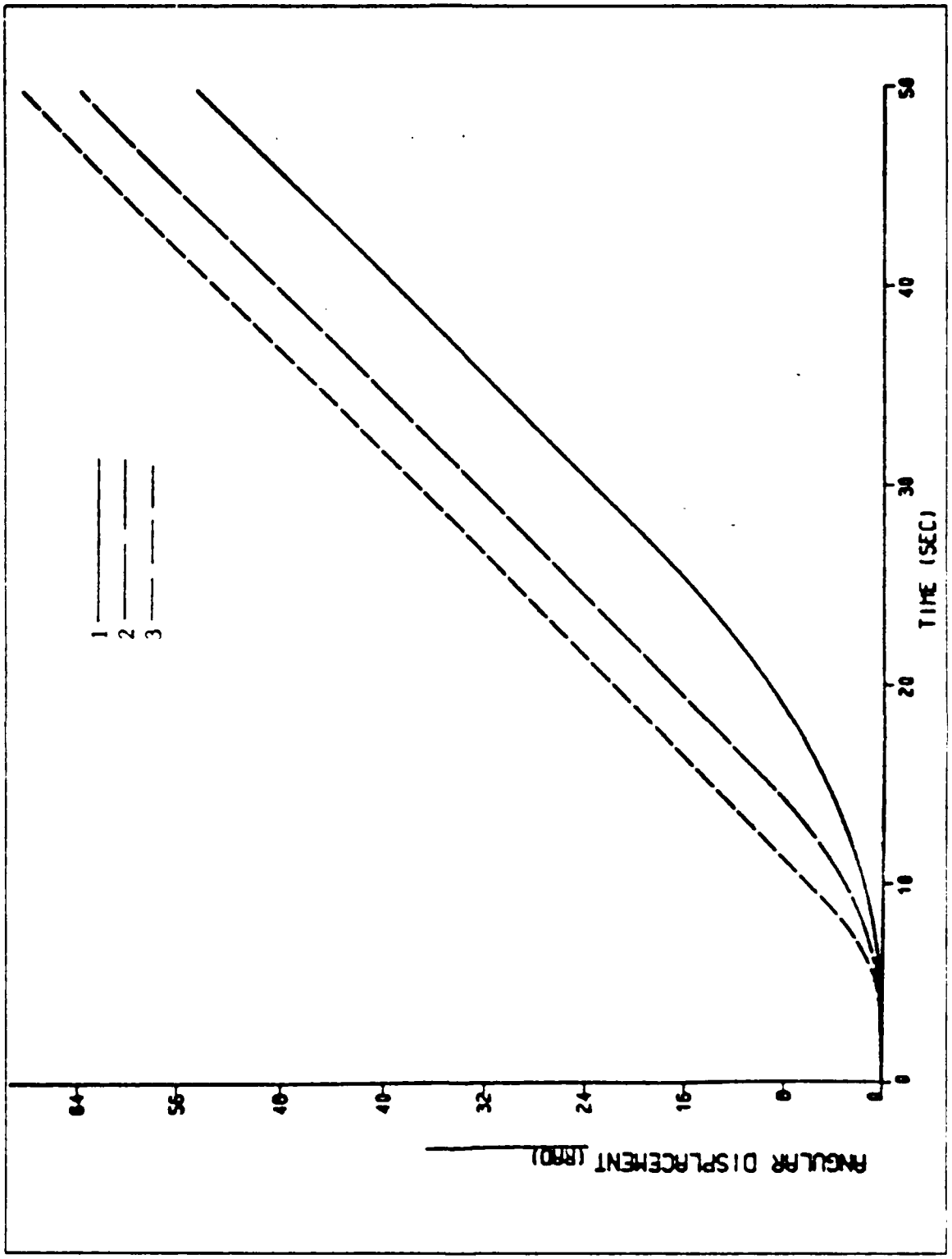

Figure 4.26 Angular displacement vs. time (AL.).

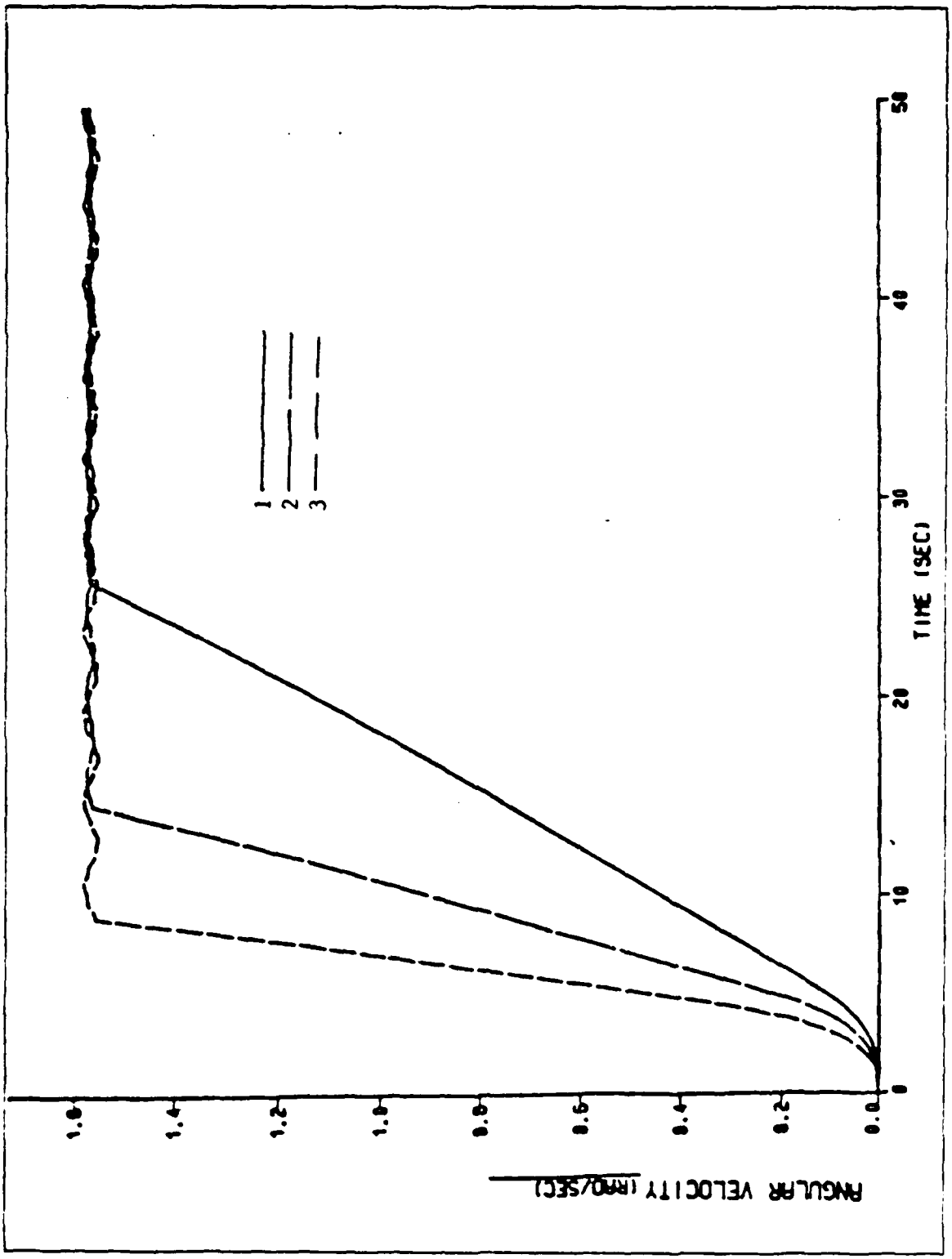

Figure 4.27 Angular velocity vs. time (AL.).

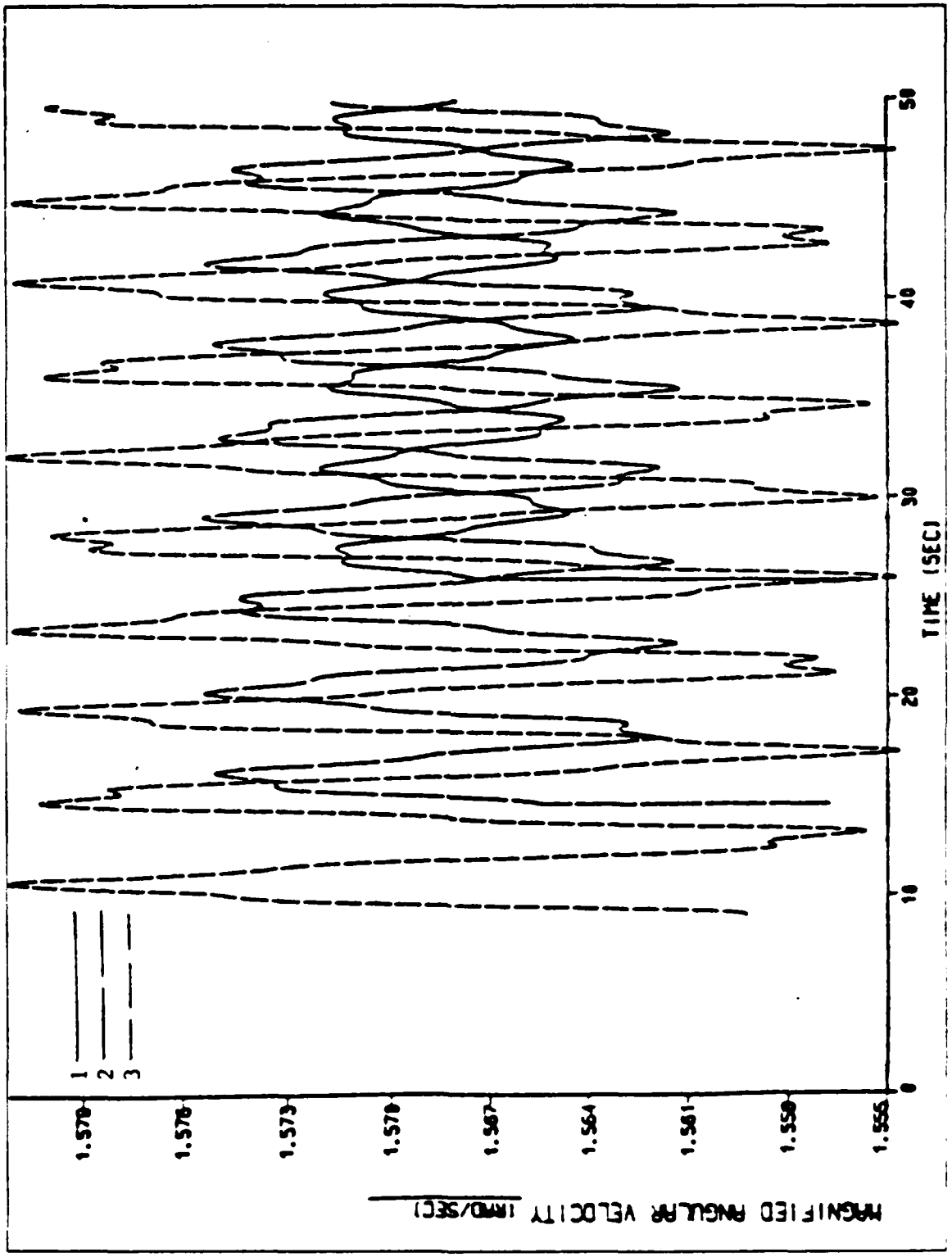

Figure 4.28 Magnified angular velocity vs. time (AL. 1.

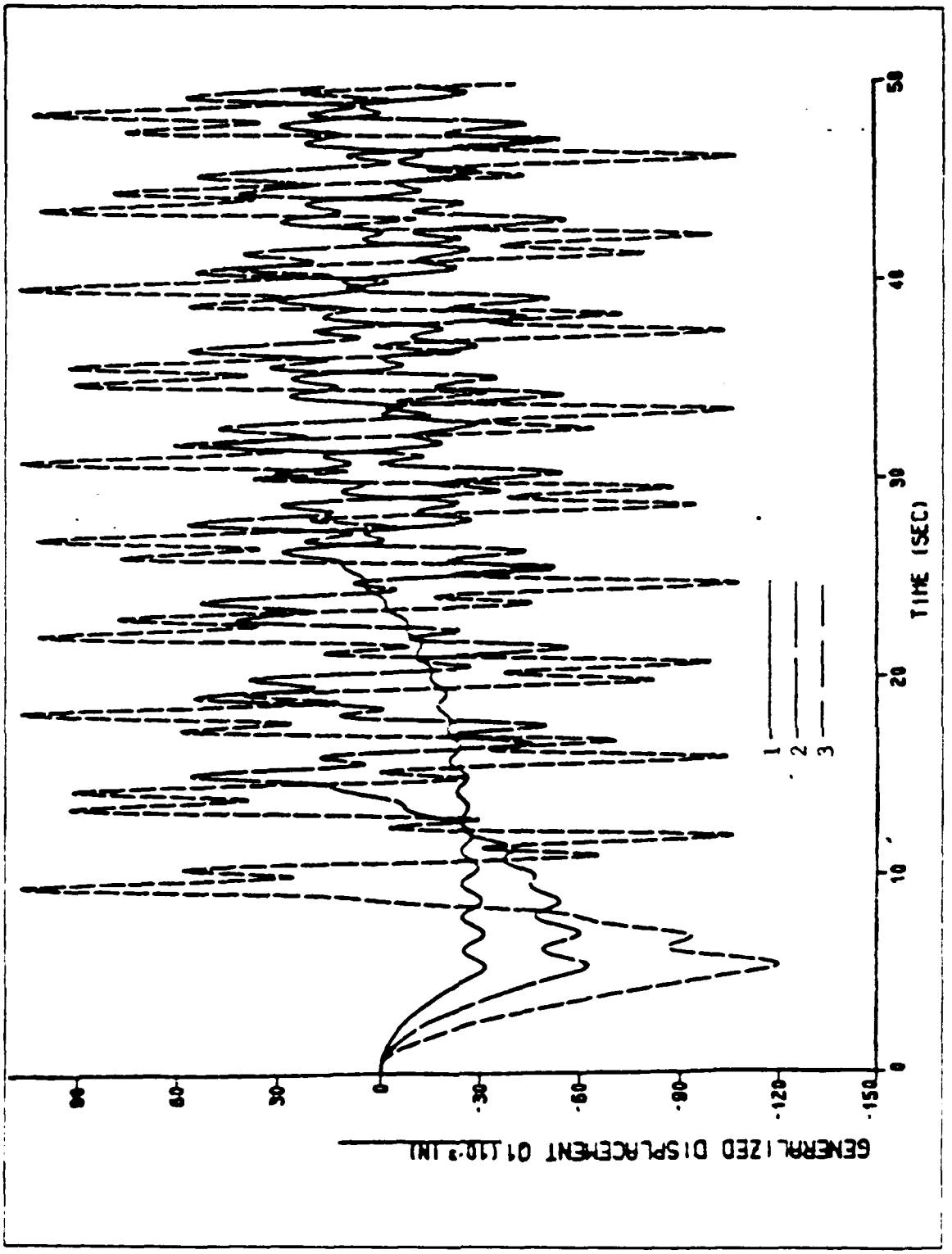

Figure 4.29 First mode generalized displacement vs. time (AL.).

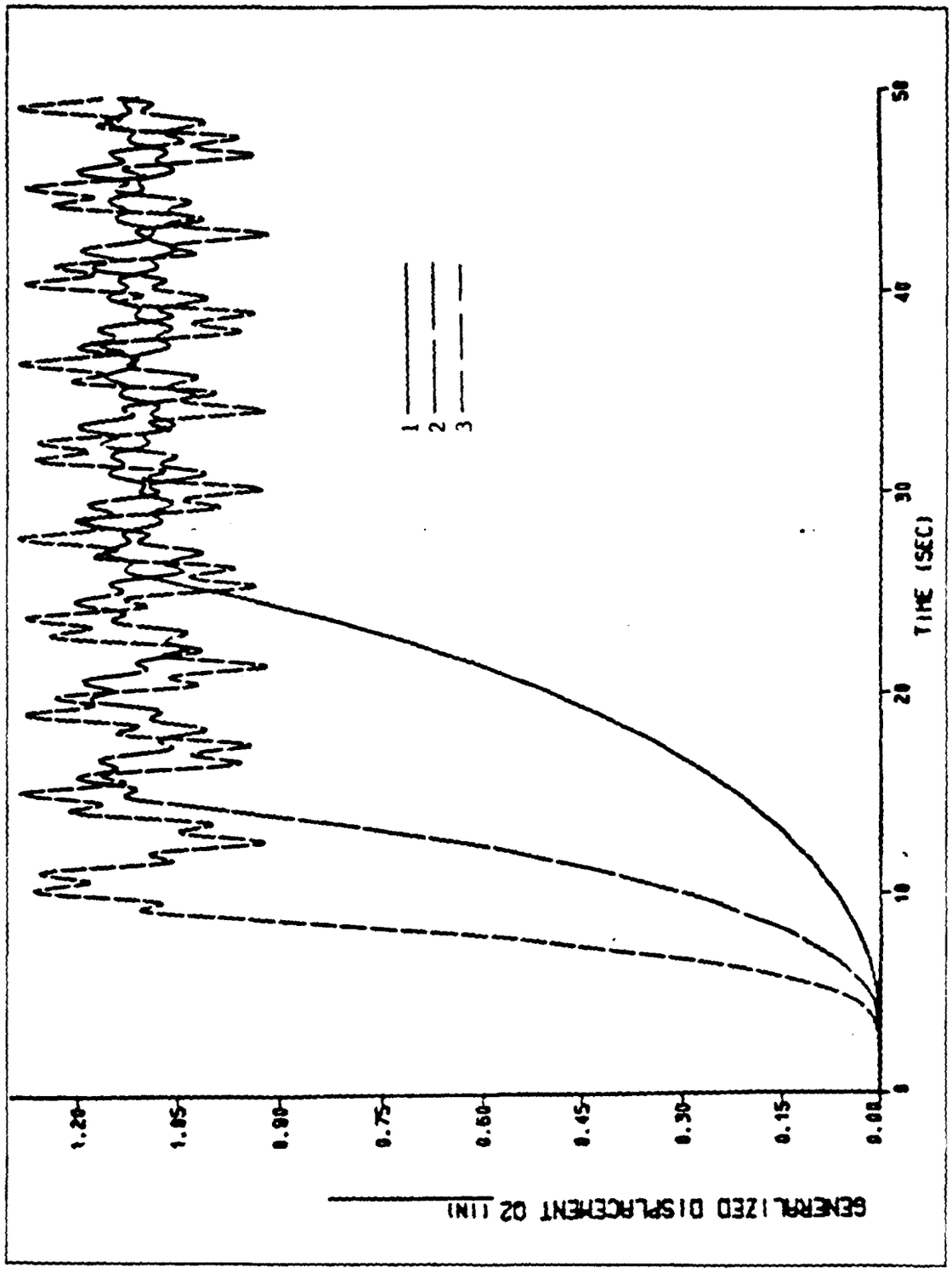

Figure 4.30 Second mode generalized displacement vs. time (AL.).

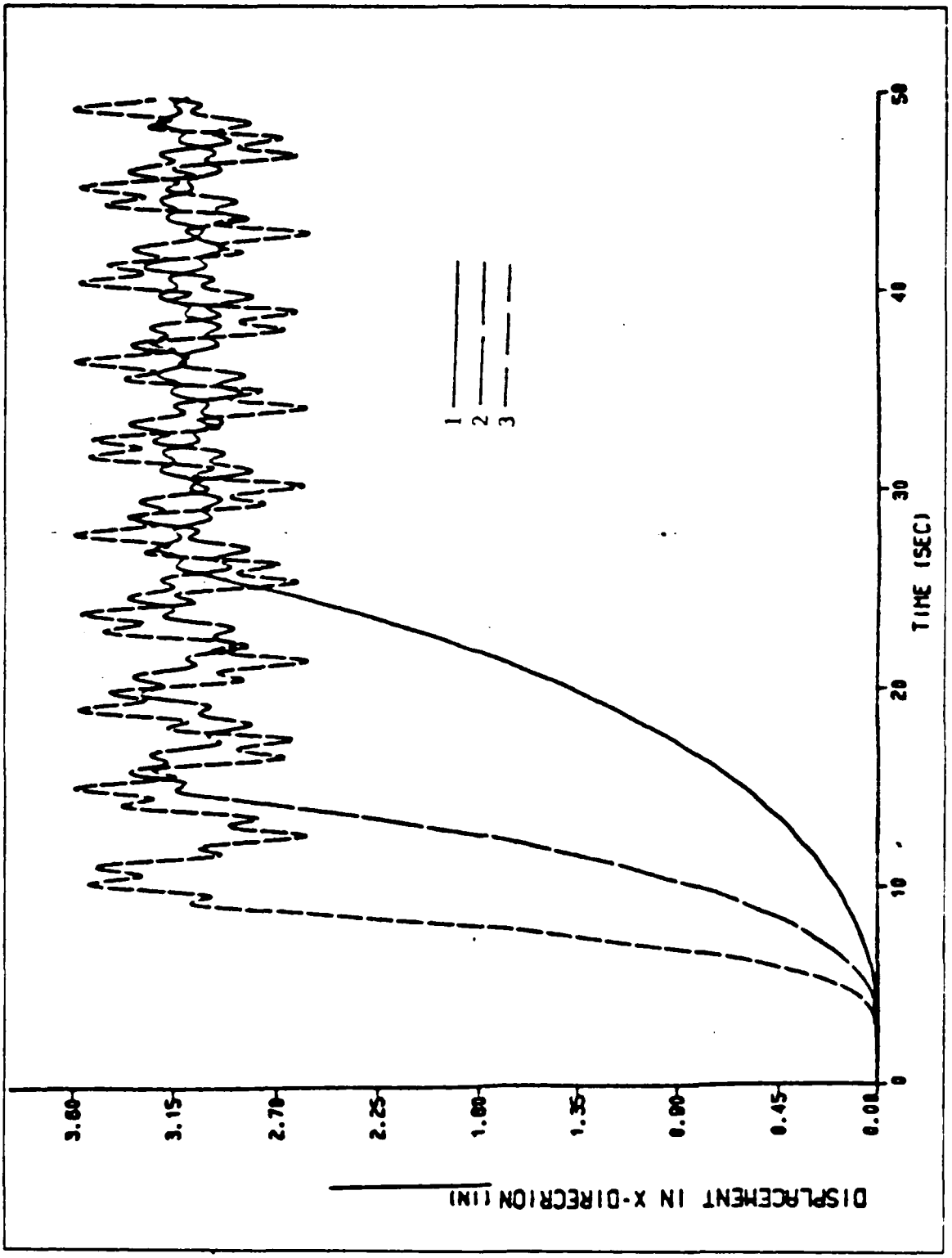

Figure 4.31 Displacement in x-direction vs. time (AL.).

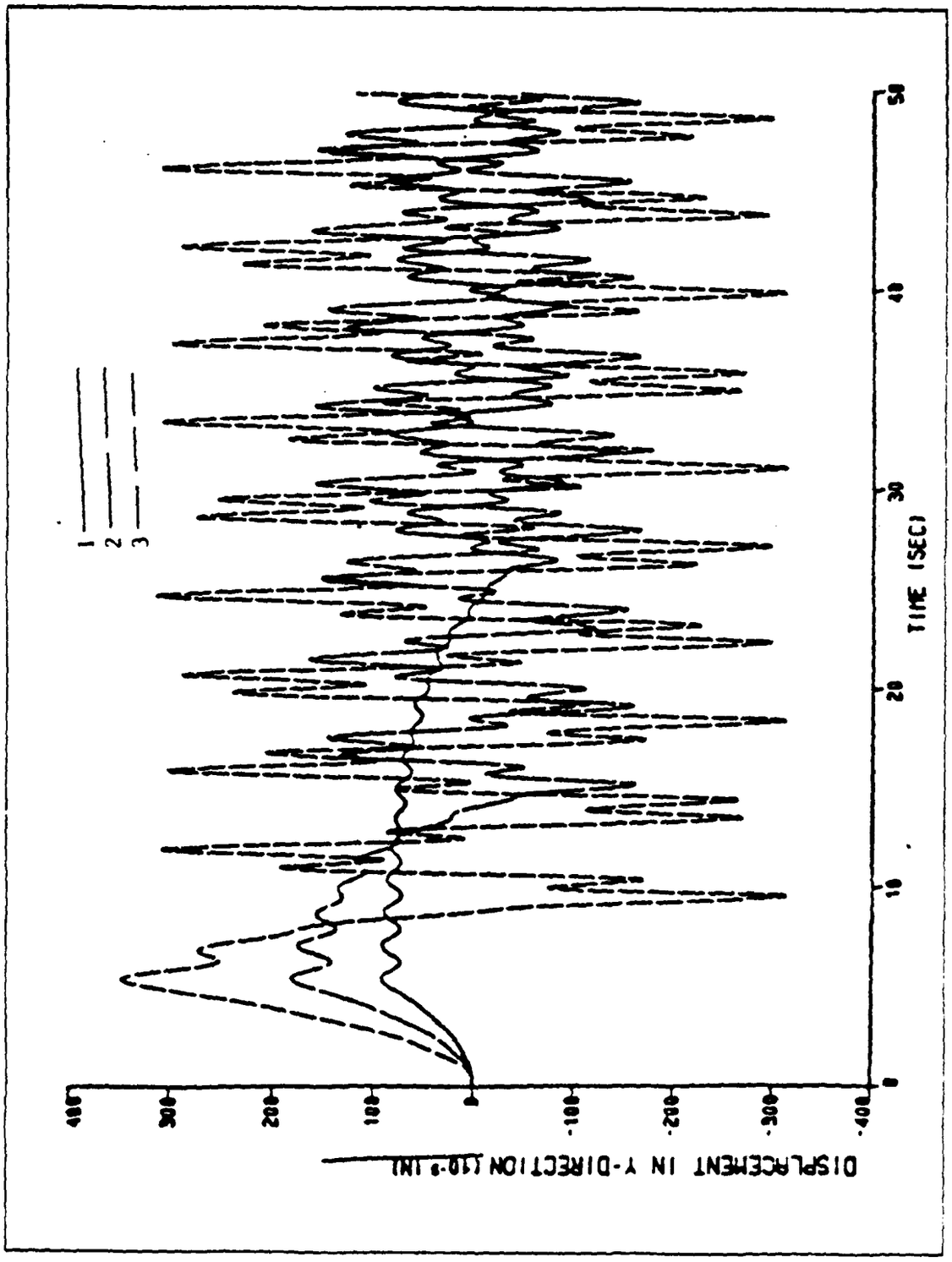

Figure 4.32 Displacement in y-direction vs. time (AL.).

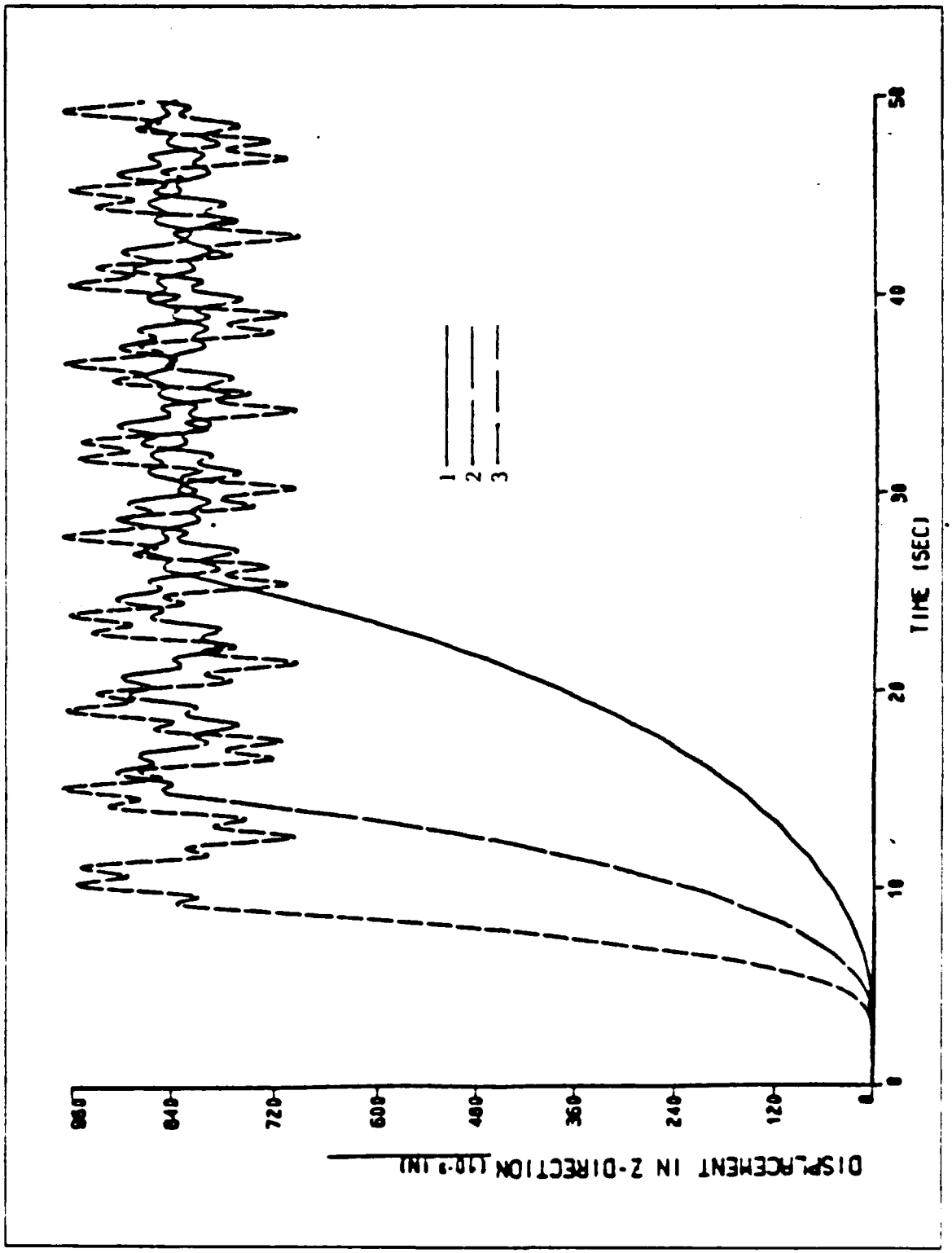

Figure 4.33 Displacement in z-direction vs. time (AL.).

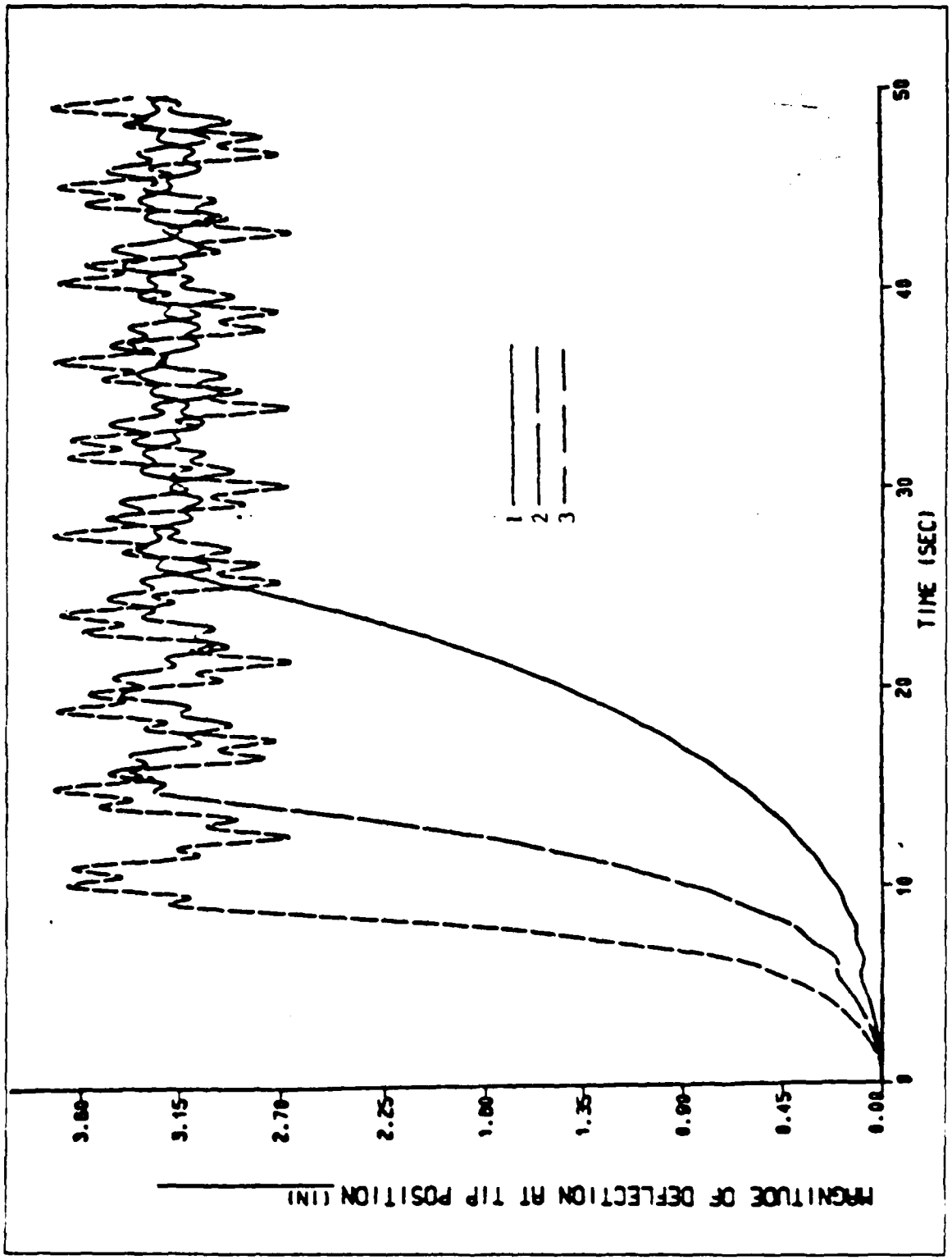

Figure 4.34 Magnitude of deflection at tip position vs. time (AL.).

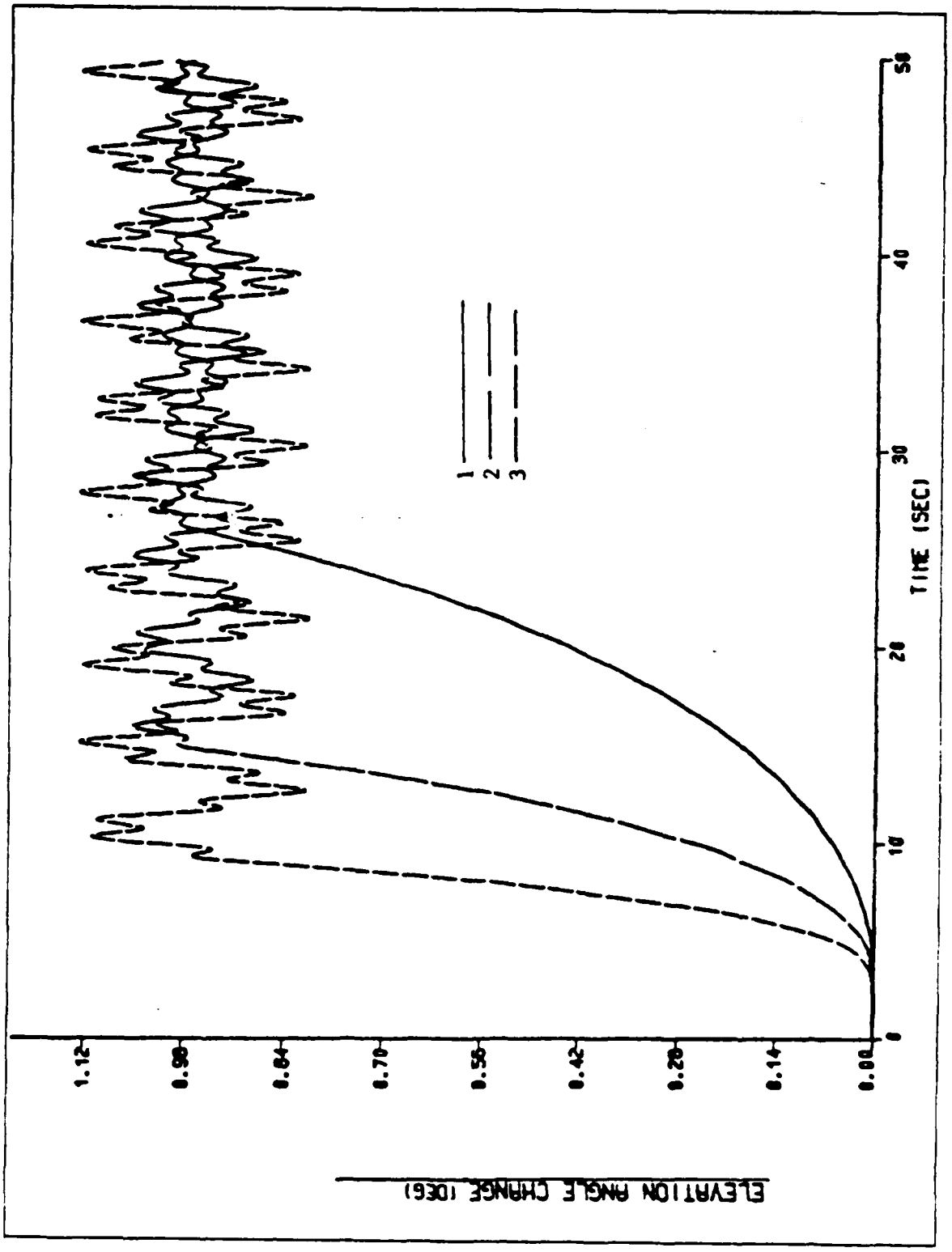

Figure 4.35 Elevation angle change vs. time (AL.).

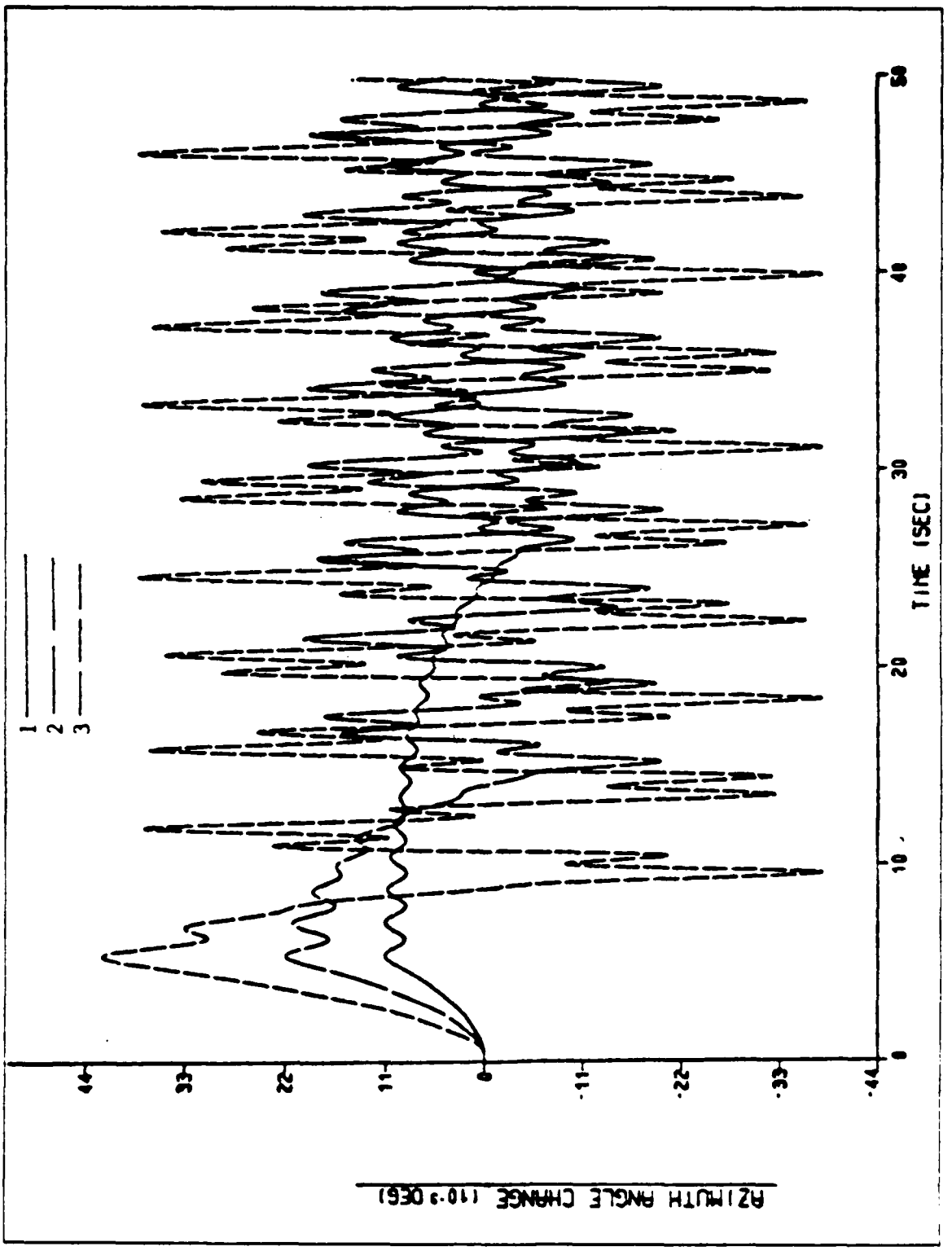

Figure 4.36 Azimuth angle change vs. time (AL.).

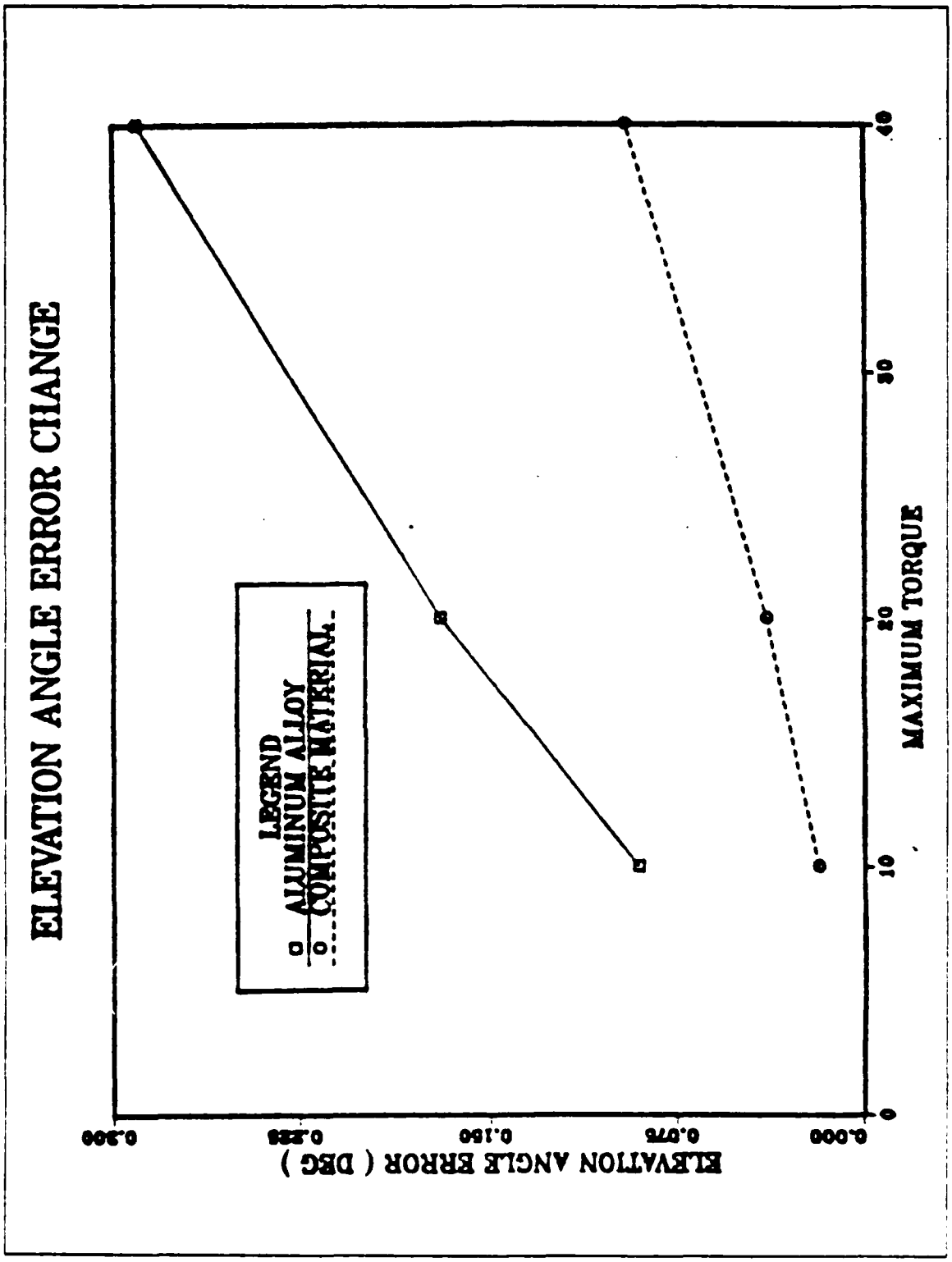

Figure 4.37 Pointing error change in elevation angle vs. magnitude of torque (AL.).

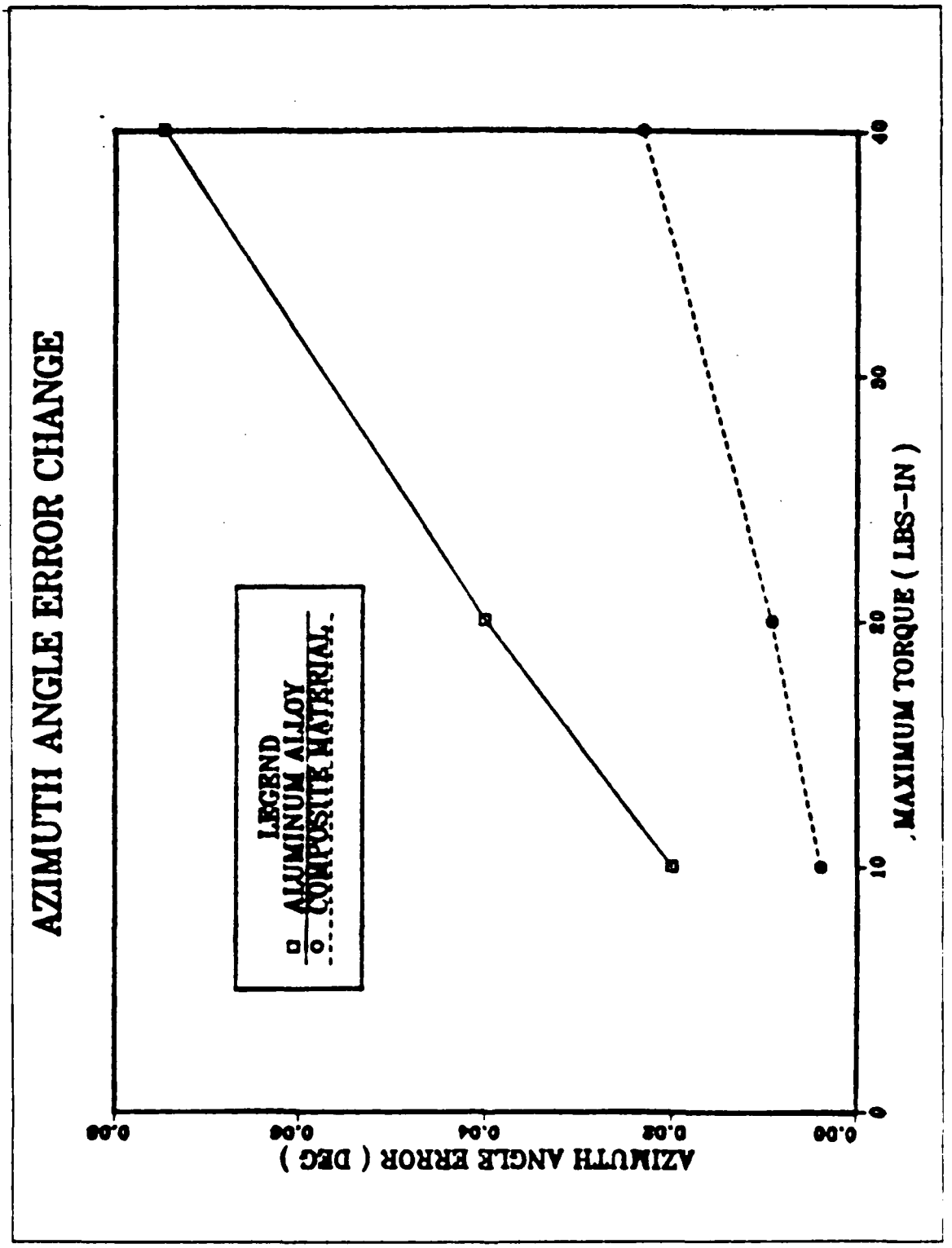

Figure 4.38 Pointing error change in azimuth angle vs. magnitude of torque (AL.).

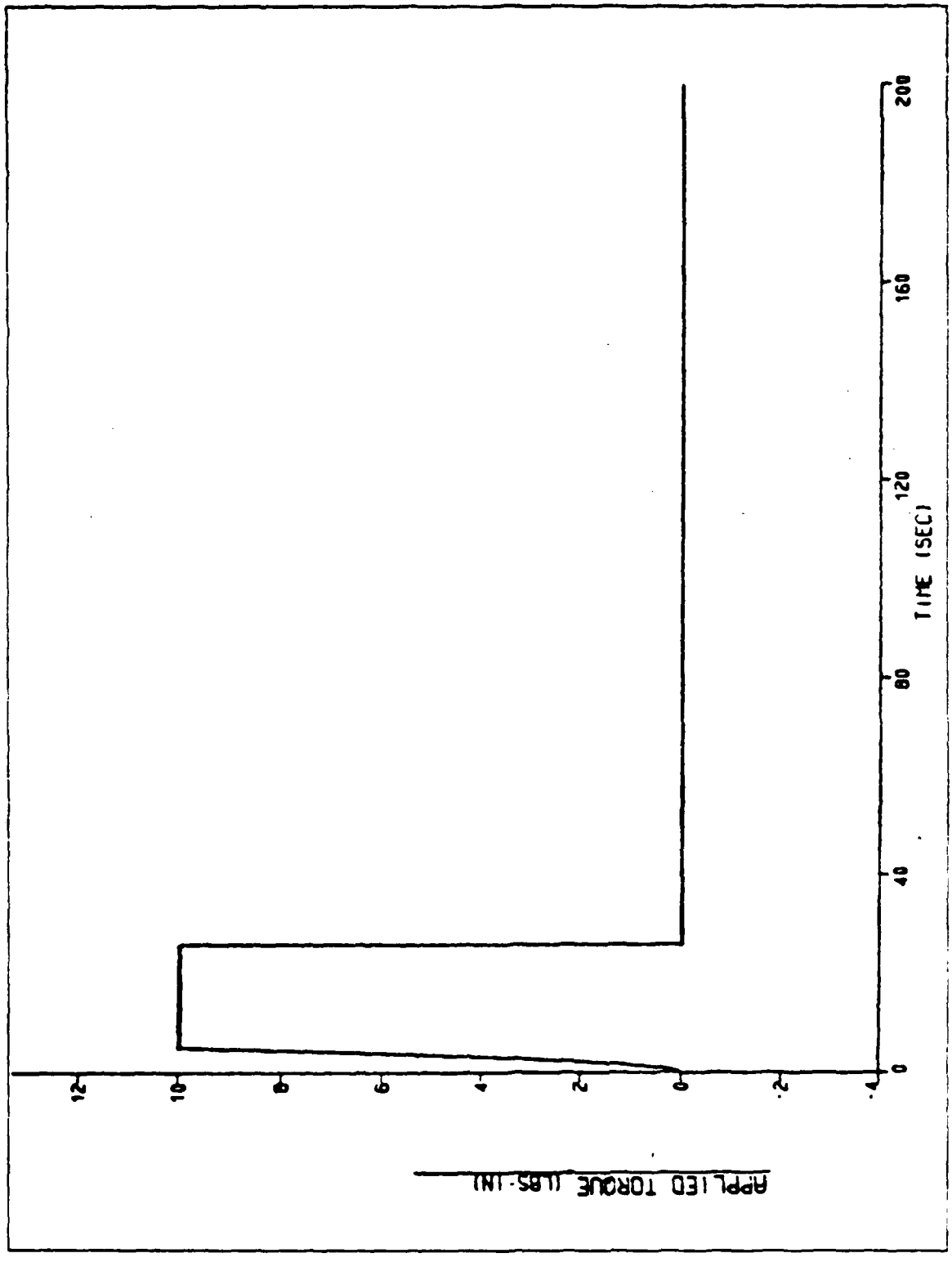

Figure 4.39 Applied torque vs. time with damping (AL.).

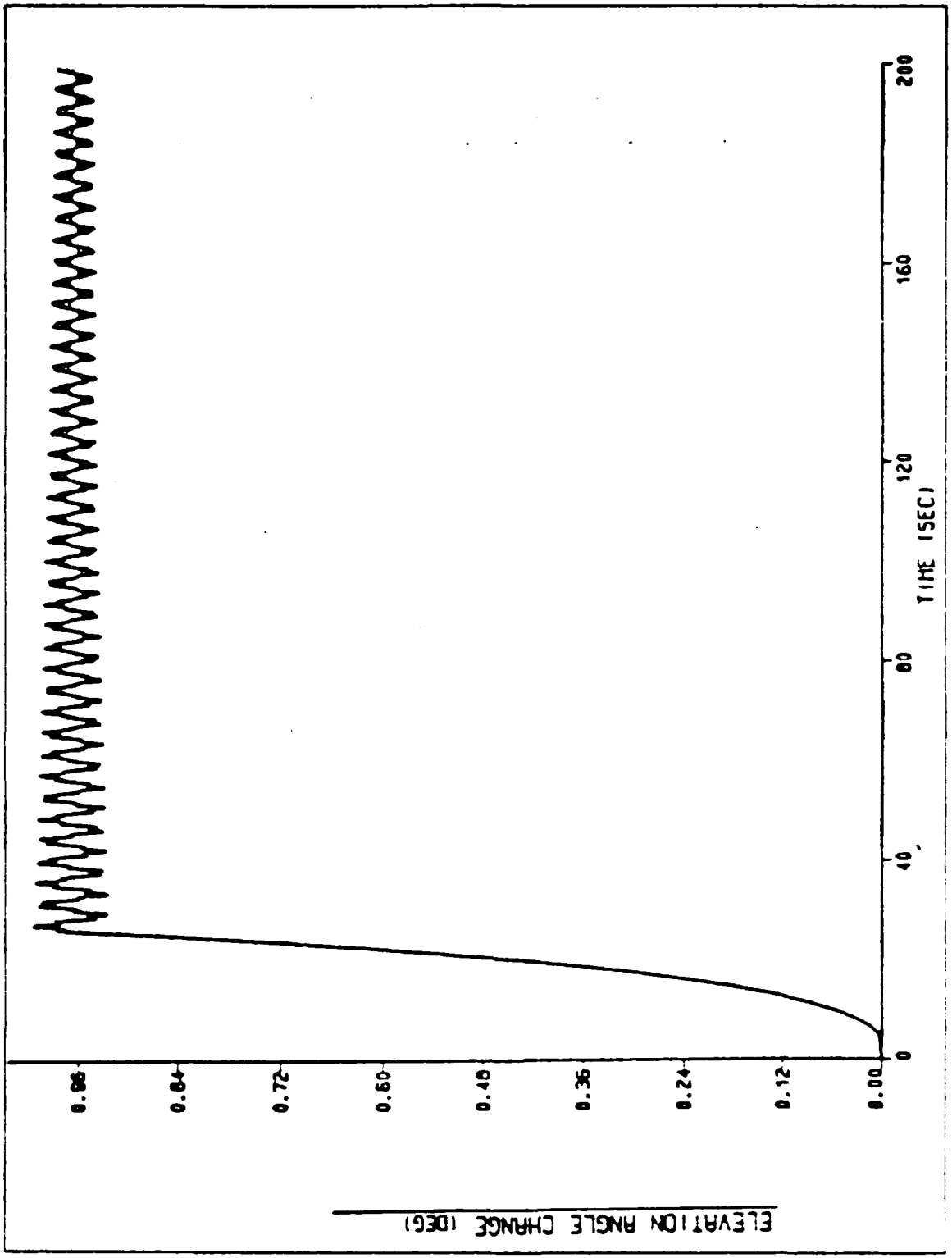

Figure 4.40 Elevation angle change vs. time with damping (λL).

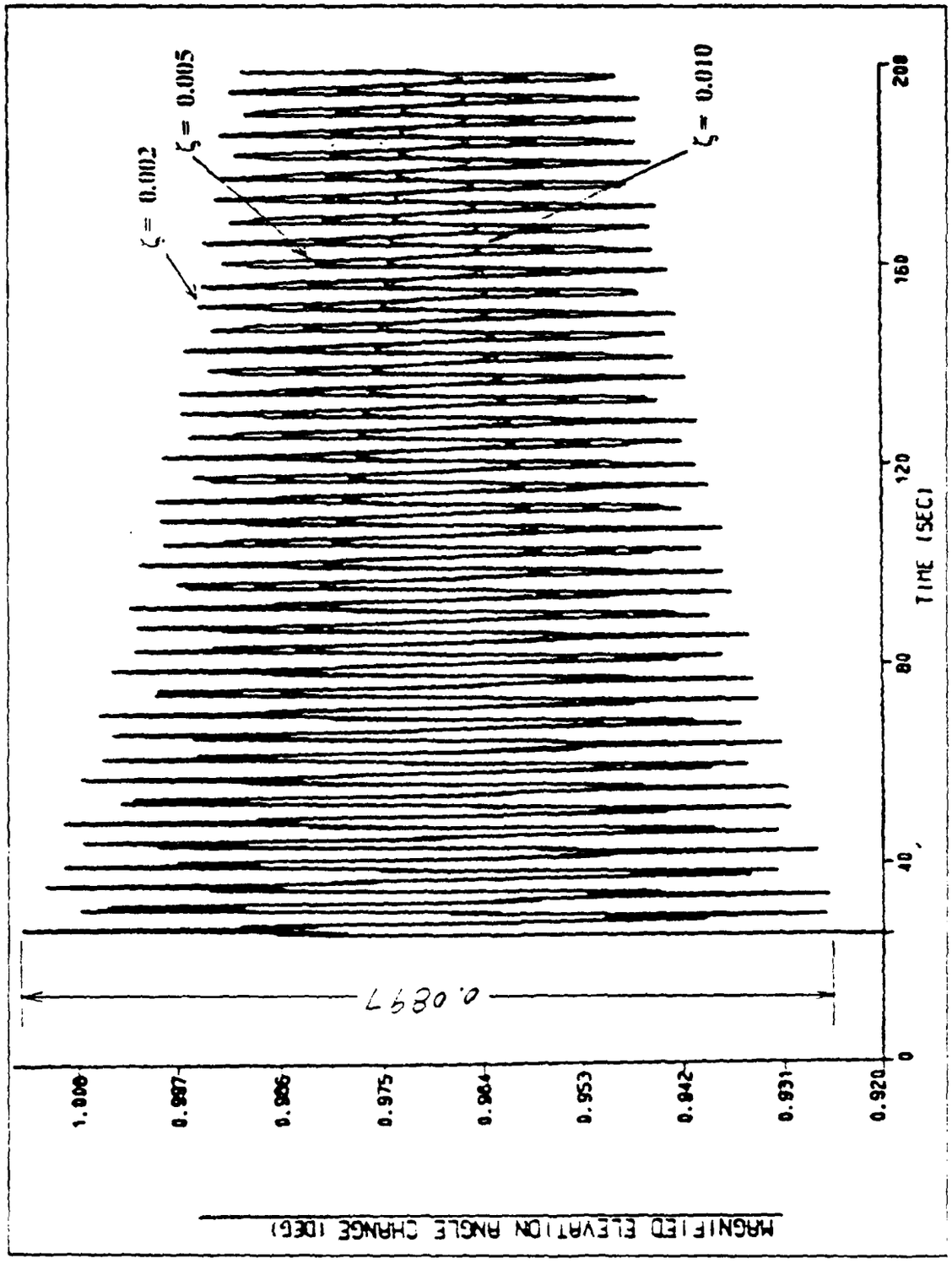

Figure 4.41 Magnified elevation angle vs. time with damping (AL.).

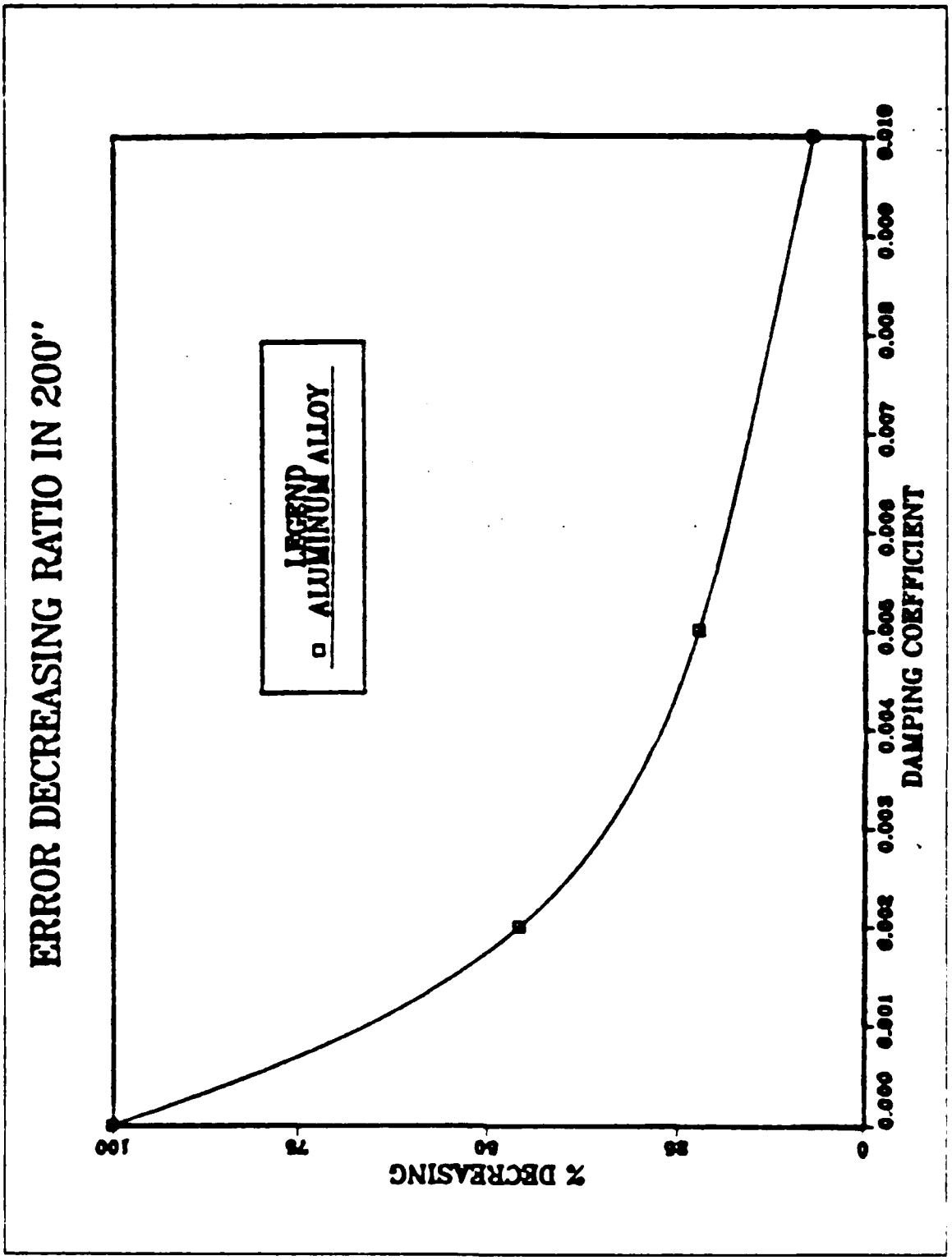

Figure 4.42 Elevation angle error decreasing ratio in 200 sec. vs. damping coefficient.

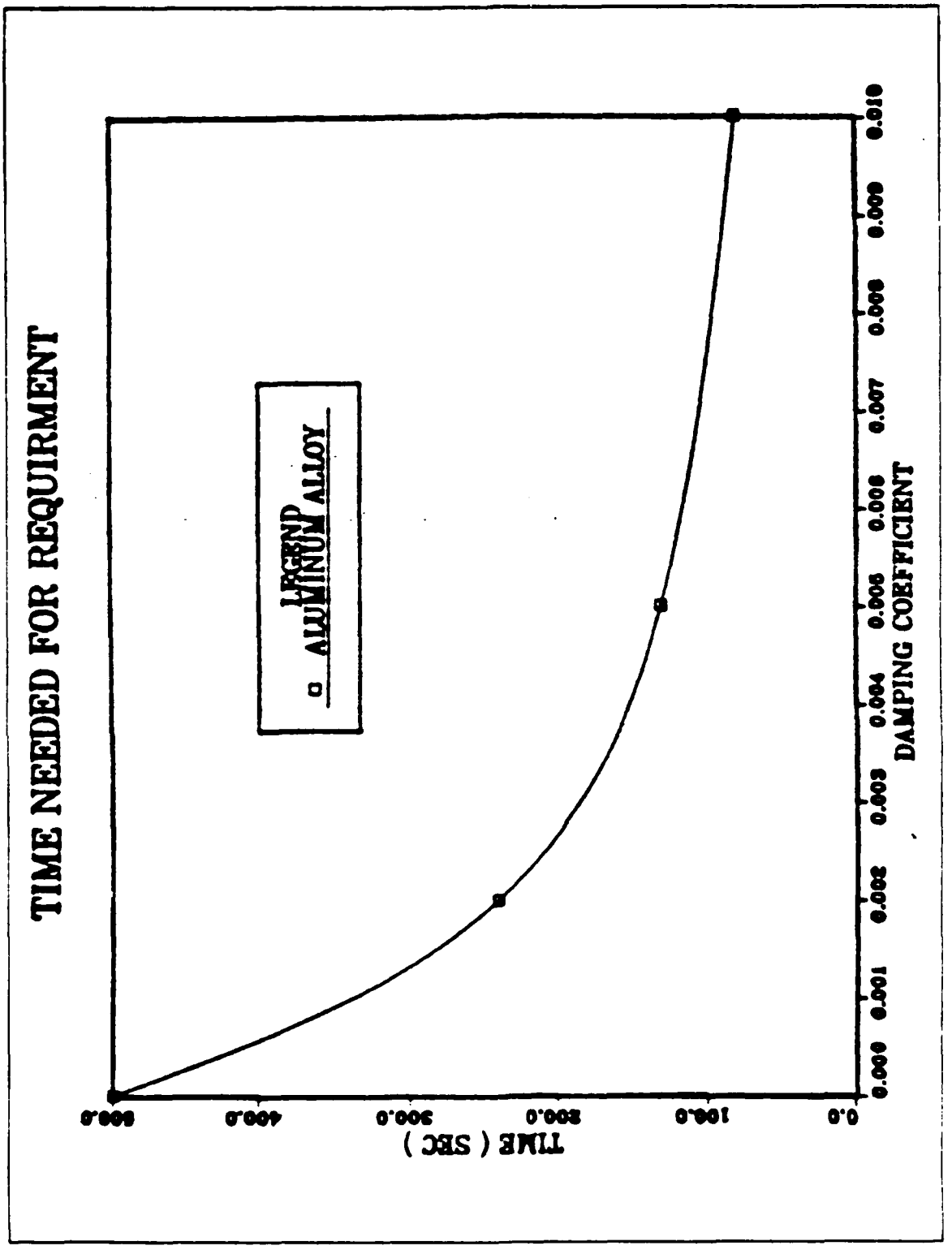

Figure 4.43 Desired time to meet elevation angle error requirement vs. damping coefficient.

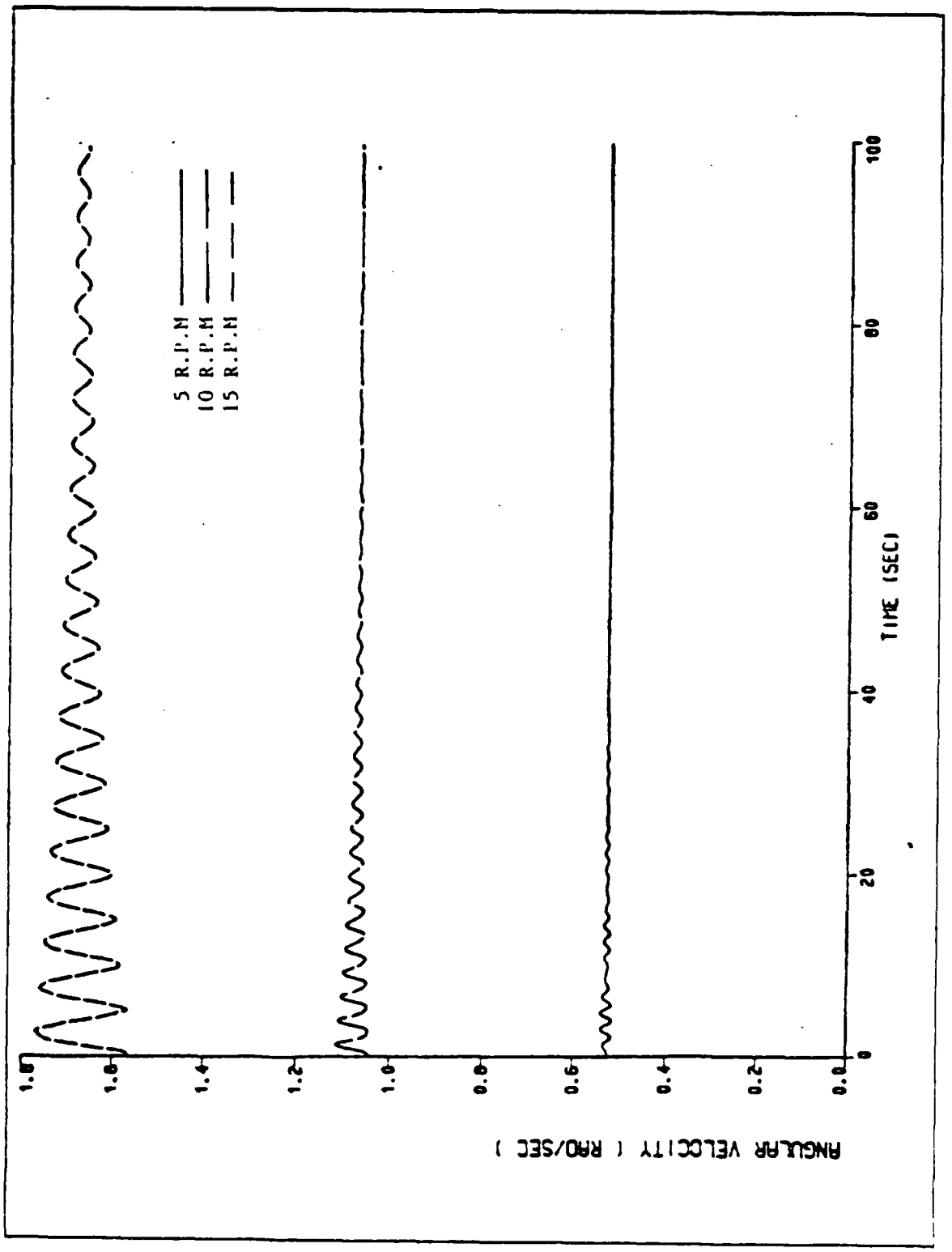

Figure 4.44 Initial angular velocities vs. time with damping (AL.).

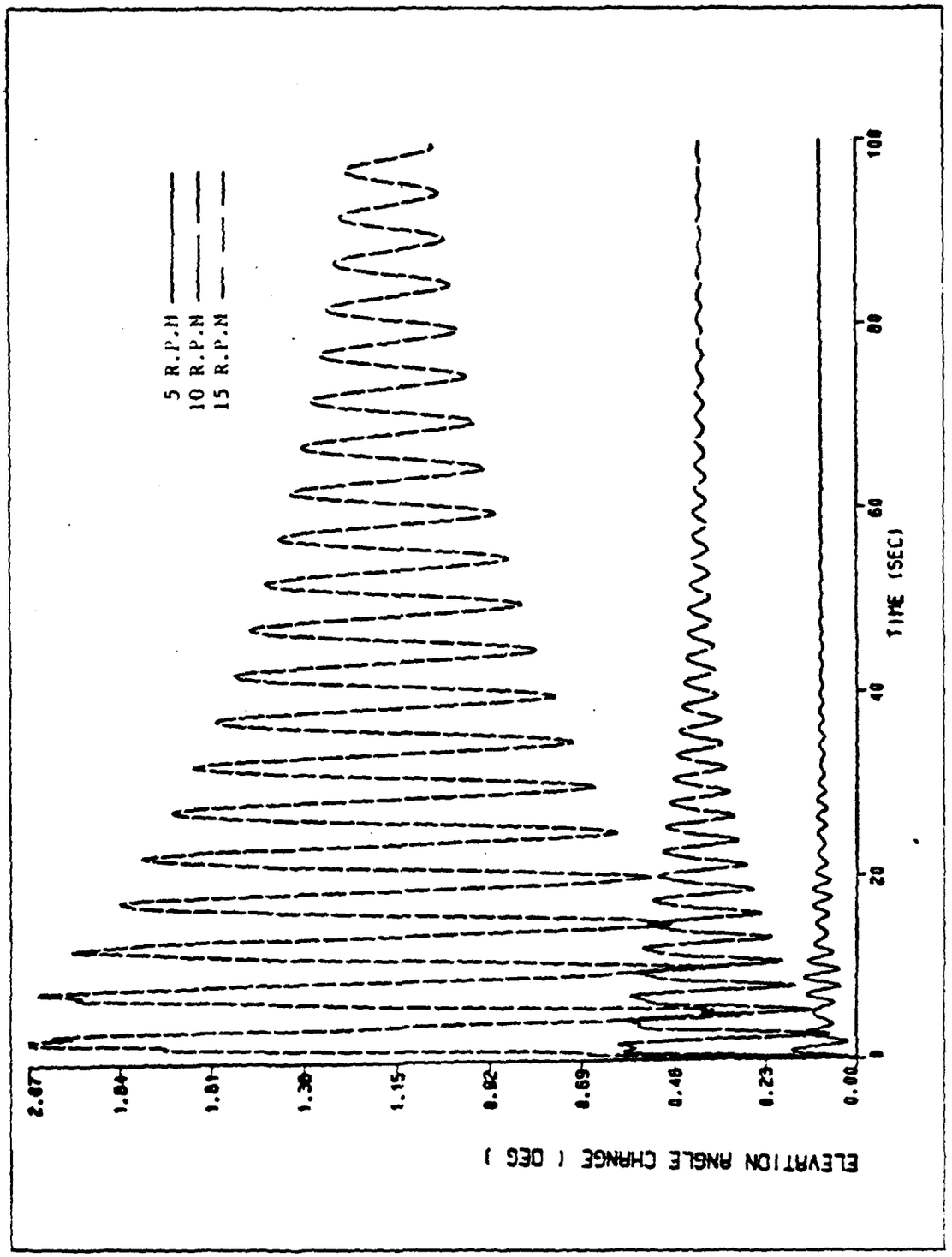

Figure 4.45 Elevation angle change with damping (ζ = 2 %) vs. rotating speed (AL.).

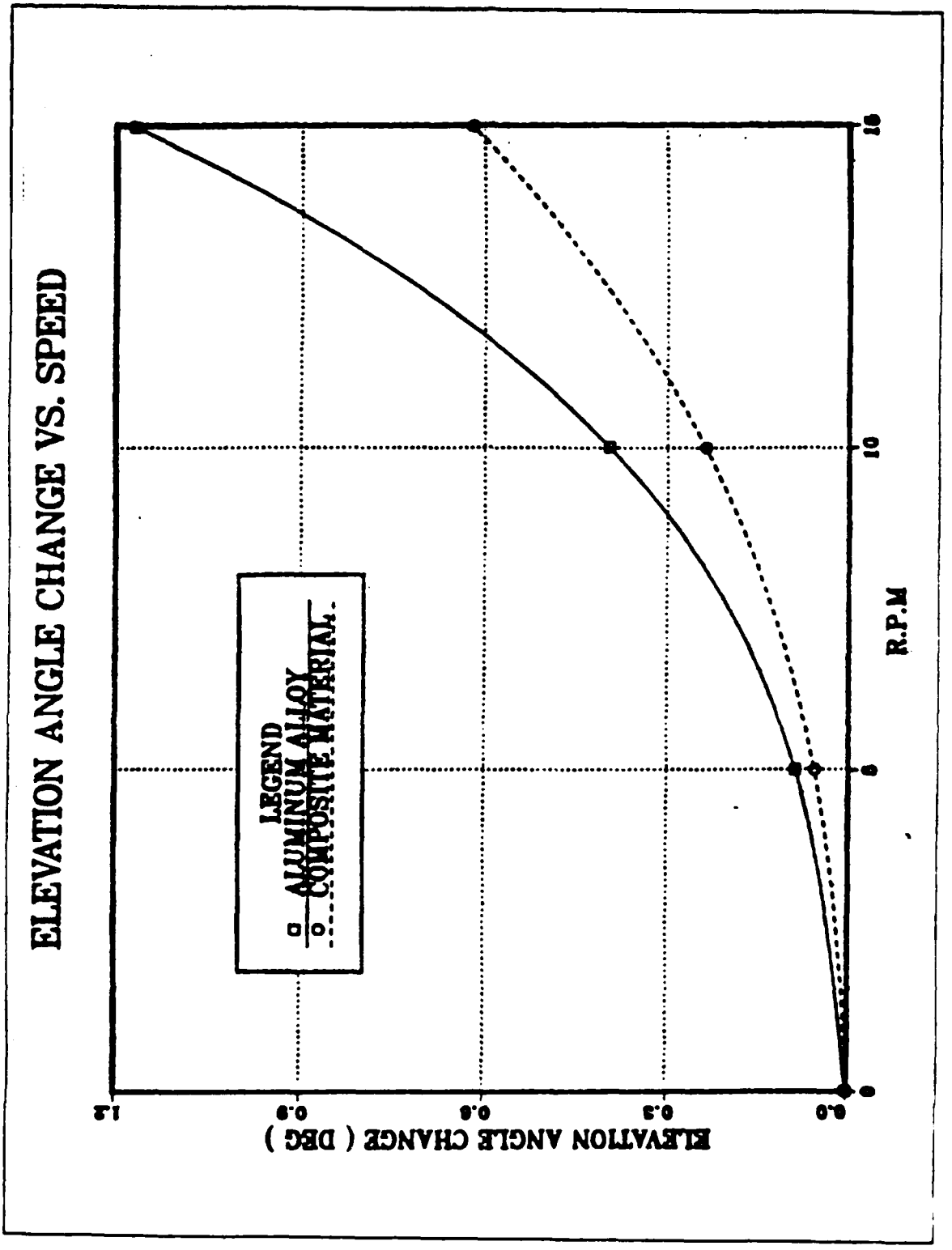

Figure 4.46 Elevation angle change at the equilibrium position vs. rotating speed (AL.).

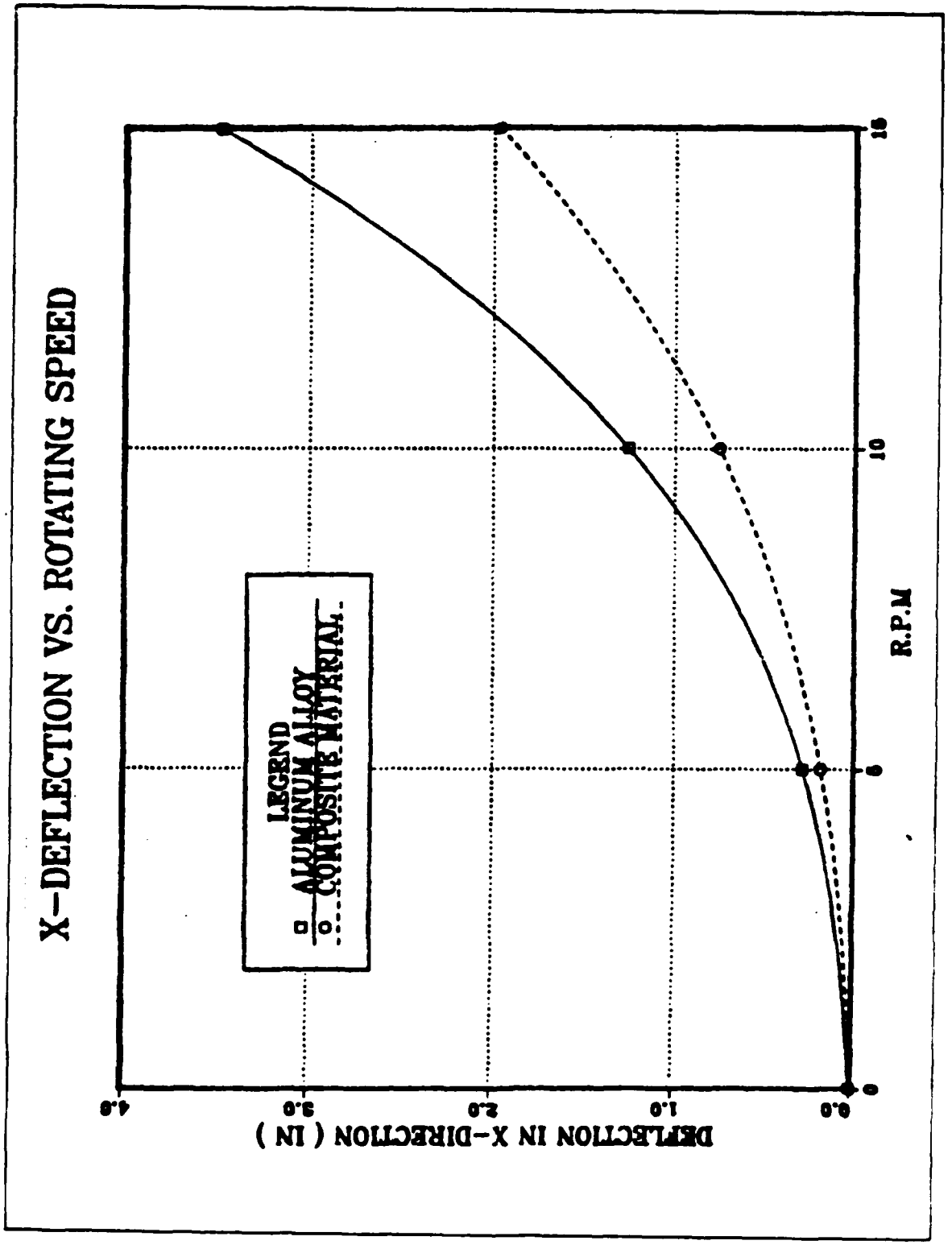

Figure 4.47 Deflection in x-direction vs. rotating speed (AL.).

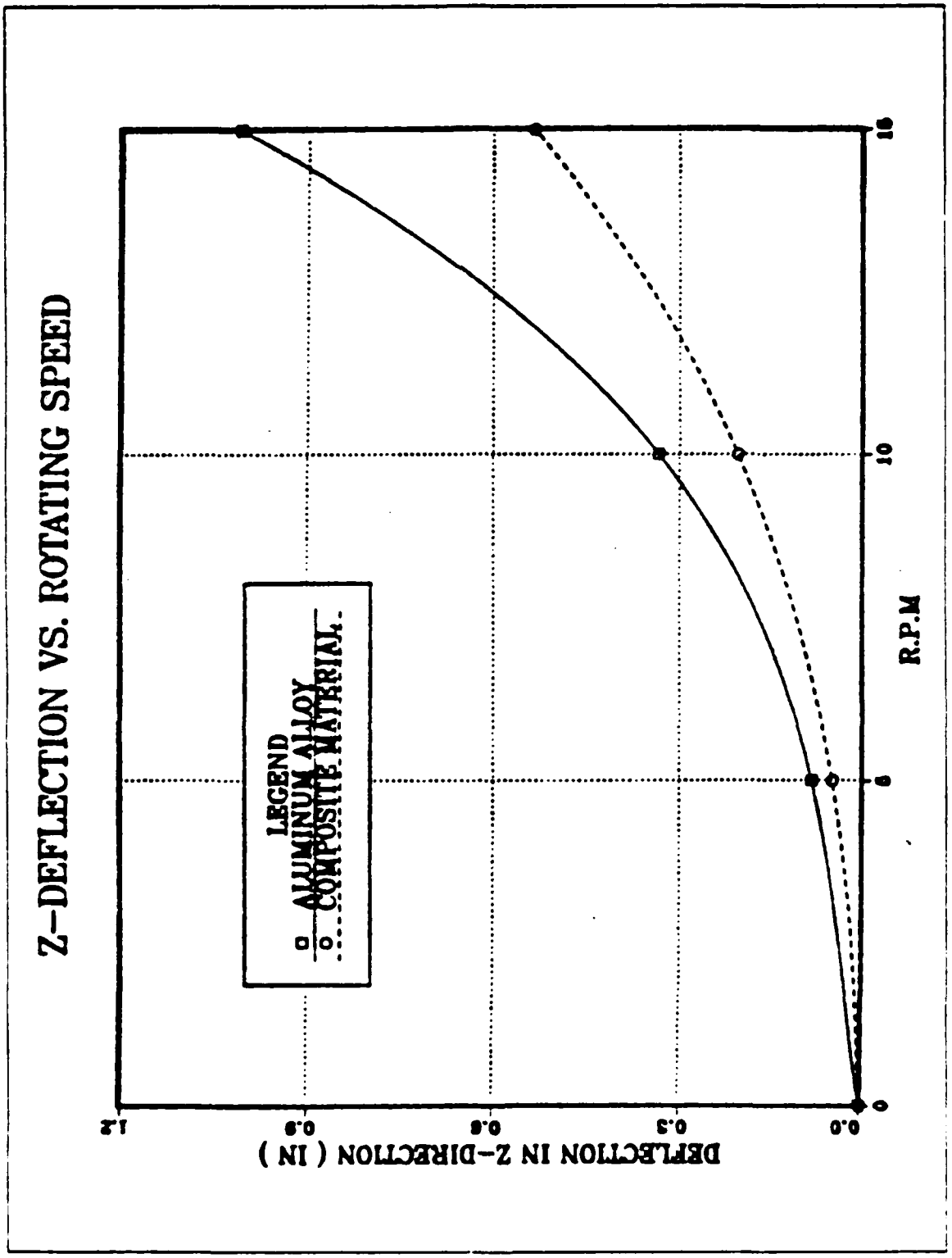

Figure 4.48 Deflection in z-direction vs. rotating speed (AL.).

V. CONCLUSIONS AND RECOMMENDATIONS

A. CONCLUSIONS

The purposes of this research are to investigate the the effects of the flexibility of the LFMR boom on pointing error of the reflector in elevation and azimuth angle and to identify the parameters which are important in pointing error. In this study, the effectiveness of the application of Lagrange's method and mode superposition techniques, computer simulation techniques are also investigated.

The results indicated that the Lagrange's method and mode superposition technique was very effective for this double link boom model analysis. The effects of flexibility of boom was sufficiently expressed with few mode and the boom flexibility was very affective in pointing error. As the material becomes stiffer with light weight, its pointing error becomes smaller. The torque applying and removing procedure is very important to the magnitude of pointing error. If we apply the torque gradually until reaching desired rotating speed and remove slowly with sufficient time, we can reduce the pointing error to much smaller values within requirement. The vibration settling time decreases exponentially as modal damping coefficient increases and the pointing error is linearly dependent on the magnitude of applied torque. The deflection in each direction and elevation angle change in equilibrium condition increase exponentially as the rotating speed increases. Sensitivity of deflection depends on flexibility of the boom.

B. RECOMMENDATIONS

In this research, we regarded the deployable reflector as a concentrated tip mass. In this case, we don't need consideration of the flexibility of the reflector but in actual model the flexibility of the reflector will affect the accuracy of the pointing error, therefore flexibility of the deployable reflector has to be considered for the future work.

As we have seen in the comparison of two material boom, the flexibility of boom was very affective in the pointing error. Stiffer material with light weight will play important role in the reduction of pointing error of the flexible boom.

APPENDIX A
DERIVATIONS OF THE EQUATIONS OF MOTION

In this Appendix, we develop simplified dynamic equations of motion for 2 cases of the boom system with tip mass.

The large motion caused by rotation and the small motion created by elastic deformation will be expressed by generalized coordinates then apply Lagrange's equations to develop the equations of motion. In these analysis, the local rotary inertia and shear deformation of booms are neglected.

From the equations 2.7 and 2.8 Lagrange's equations are

$$\frac{d}{dt}\left[\frac{\partial T}{\partial \dot{\theta}}\right] - \frac{\partial T}{\partial \theta} + \frac{\partial U}{\partial \theta} = \tau \qquad \text{(eqn A.1)}$$

and

$$\frac{d}{dt}\left[\frac{\partial T}{\partial \dot{q}_h}\right] - \frac{\partial T}{\partial q_h} + \frac{\partial U}{\partial q_h} = 0 \qquad \text{(eqn A.2)}$$

$(h = 1, 2, 3, \ldots\ldots, n)$

where

θ :	the generalized coordinates of the large motion
q_h :	the generalized coordinates of the small motion
τ :	applied torque to the system
n :	number of modes (or number of degrees of freedom)

1. SINGLE LINK BOOM SYSTEM IN PLANAR MOTION

a. Geometry of the system

In model analysis, since the extension deformation is negligible, only the bending deformation is considered in the analysis.

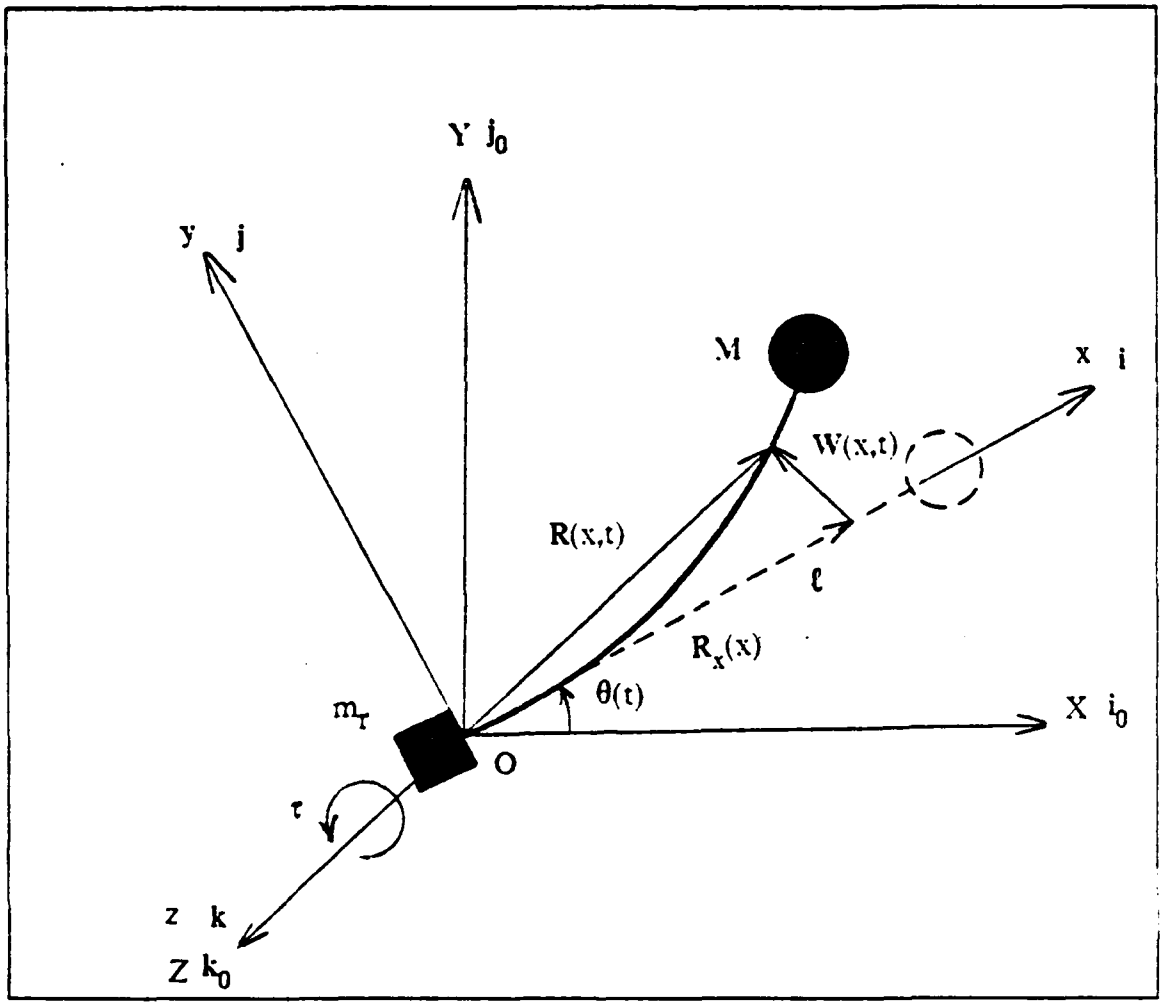

Figure A.1 Parameters of the single link boom system.

M :	tip mass
m_T :	mass of electronics box
ℓ :	length of the link
τ :	applied torque
θ(t) :	angular displacement
$\dot{\theta}$(t) :	angular velocity
R_x(x) :	position vector in local x-direction
W(x,t) :	deformation vector of boom
R(x,t) :	position vector of the point on the boom after deformation
i :	unit vector of local x-direction
j :	unit vector of local y-direction

$\mathbf{k}$: unit vector of local z-direction

$\mathbf{i}_0$: unit vector of global X-direction

$\mathbf{j}_0$: unit vector of global Y-direction

$\mathbf{k}_0$: unit vector of global Z-direction

b. **Position and velocity**

During rotation the boom deforms and the positions of any point in the system can be expressed the vector sum of a vector $\mathbf{R}_x(x)$ from the origin to x and a vector $\mathbf{W}(x,t)$ caused by deformation. Then the position vector $\mathbf{R}(x,t)$ is expressed as

$$\mathbf{R}(x,t) = \mathbf{R}_x(x) + \mathbf{W}(x,t) \qquad \text{(eqn A.3)}$$

where $\mathbf{R}_x(x)$ is only x dependent variable
so

$$\mathbf{R}_x(x) = \mathbf{R}_x(x)\,\mathbf{i}$$

and $\mathbf{W}(x,t)$ is deformation obtained from modal summation method
then

$$\mathbf{W}(x,t) = \sum_i \varphi_i(x)\, q_i(t) \qquad \text{(eqn 2.21)}$$

where

$\varphi_i(x)$ is *i-th* mode shape function
$q_i(t)$ is *i-th* mode generalized coordinates

If we consider the deformation of the boom consists of translation and extension, then equation 2.21 becomes

$$\mathbf{W}(x,t) = \sum_i [\, \varphi_i^x(x)\, q_i(t)\, \mathbf{i} + \varphi_i^y(x)\, q_i(t)\, \mathbf{j}\,] \qquad \text{(eqn A.4)}$$

where

$\varphi_i^x(x)\,\mathbf{i}$ is *i-th* mode shape function in extension

$\varphi_i^y(x)\,\mathbf{j}$ is *i-th* mode shape function in translation

From equation 2.21 and A.4 the position of the point on the boom is

$$\mathbf{R}(x,t) = R_x(x)\,\mathbf{i} + \sum_i [\,\varphi_i^x(x)\,\mathbf{i} + \varphi_i^y(x)\,\mathbf{j}\,]\,q_i(t) \qquad \text{(eqn A.5)}$$

Now the velocities of the point on the boom is necessary to formulate the kinetic energy to apply Lagrange's equation. The velocity is obtained by simply differentiating the equation A.5
then

$$\dot{\mathbf{R}}(x,t) = R_x(x)\,\mathbf{i} + \sum_i [\,\varphi_i(x)\,\mathbf{i} + \varphi_i^y(x)\,\mathbf{j}\,]\,\dot{q}_i(t) \qquad \text{(eqn A.6)}$$

$$+ \sum_i [\,\varphi_i^x(x)\,\dot{\mathbf{i}} + \varphi_i^y(x)\,\dot{\mathbf{j}}\,]\,q_i(t)$$

$$= [R_x + \sum_i \varphi_i^x(x)\,q_i(t)\,]\,\dot{\mathbf{i}} + \sum_i \varphi_i^y(x)\,q_i(t)\,\dot{\mathbf{j}}$$

$$+ \sum_i [\,\varphi_i^x(x)\,\dot{q}_i(t)\,\mathbf{i} + \varphi_i^y(x)\dot{q}_i(t)\,\mathbf{j}\,]$$

But time derivative of unit vector i and j are

$$\dot{\mathbf{i}} = \dot{\theta}\,\mathbf{k} \times \mathbf{i} = \dot{\theta}\,\mathbf{j}$$
$$\dot{\mathbf{j}} = \dot{\theta}\,\mathbf{k} \times \mathbf{j} = -\dot{\theta}\,\mathbf{i}$$
$$\dot{\mathbf{k}} = \dot{\theta}\,\mathbf{k} \times \mathbf{k} = 0$$

substitute these quantities to the equation A.6 and simplify
then

$$\dot{\mathbf{R}}(x,t) = \{\,R_x + \sum_i \varphi_i^x(x)\,q_i(t)\,\}\,\dot{\theta}\,\mathbf{j} - \dot{\theta}\sum_i \varphi_i^y(x)\,q_i(t)\,\mathbf{i} \qquad \text{(eqn A.7)}$$

$$+ \sum_i \varphi_i^x(x)\,\dot{q}_i(t)\,\mathbf{i} - \sum_i \varphi_i^y(x)\,\dot{q}_i(t)\,\mathbf{j}$$

$$= [\,\sum_i \varphi_i^x(x)\,\dot{q}_i(t) - \dot{\theta}\sum_i \varphi_i^y(x)\,q_i(t)\,]\,\mathbf{i}$$

$$+ [\, R_x(x)\,\dot{\theta} + \dot{\theta} \sum_i \varphi_i^x(x)\, q_i(t) + \sum_i \varphi_i^y(x)\, \dot{q}_i(t)\,]\, j$$

c. kinetic energy and potential energy

Recall the equation A.7 and drop the all terms concerning $\varphi_i^x(x)$ and express $\varphi_i^y(x)$ simply $\varphi_i(x)$
then equation A.7 reduces to

$$\dot{R}(x,t) = R_x\,\dot{\theta}\, j - \dot{\theta} \sum_i \varphi_i(x)\, q_i(t)\, i + \sum_i \varphi_i^y(x)\, \dot{q}_i(t)\,]\, j \qquad \text{(eqn A.8)}$$

$$= -\dot{\theta} \sum_i \varphi_i(x) q_i(t)\, i + [\, R_x(x)\,\dot{\theta} + \sum_i \varphi_i(x)\, \dot{q}_i(t)\,]\, j$$

From the equation 2.17, the kinetic energy of the whole system is

$$T = T_{bm} + T_{lm} + T_{rf} \qquad \text{(eqn A.9)}$$

$$= \frac{1}{2} \int_0^{\ell} \dot{R}(x,t) \bullet \dot{R}(x,t)\, dm$$

$$+ \frac{1}{2} M\, \dot{R}(\ell,t) \bullet \dot{R}(\ell,t)$$

$$+ \frac{1}{2} I_{r_{zz}}\, \dot{\theta}^2$$

but

$$\dot{R}(x,t) \bullet \dot{R}(x,t) = [\, -\dot{\theta} \sum_i \varphi_i(x)\, q_i(t)\,]^2 + [\, R_x(x)\,\dot{\theta} + \sum_i \varphi(x)\, q_i(t)\,]^2 \qquad \text{(eqn A.10)}$$

$$= \dot{\theta}^2 [\, \sum_i \varphi_i(x)\, q_i(t)\,]^2 + [\, R_x(x)\,\dot{\theta}\,]^2$$

$$+ 2\, R_x(x)\,\dot{\theta} \sum_i \varphi_i(x)\, q_i(t) - [\, \sum_i \varphi_i(x)\, \dot{q}_i(t)\,]^2$$

and

AD-A181 488 DYNAMIC ANALYSIS OF THE FLEXIBLE BOOM IN THE W-ROSS SATELLITE(U) NAVAL POSTGRADUATE SCHOOL MONTEREY CA C S KANG MAR 87 2/2

UNCLASSIFIED F/G 22/1 NL

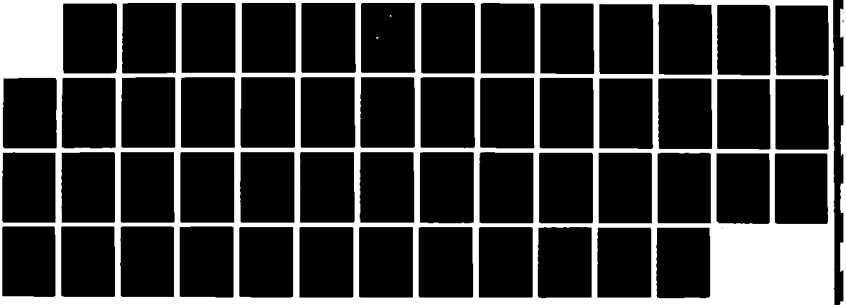

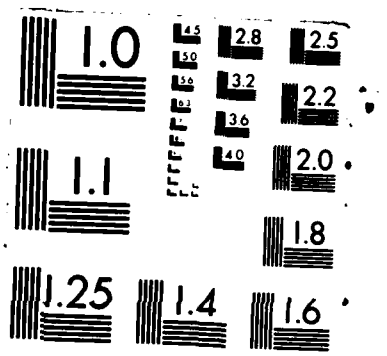
1.0
1.1
1.25
1.4
1.6
1.8
2.0
2.2
2.5
2.8
3.2
3.6
4.0
4.5
5.0
5.6

$$\left[\sum_i \varphi_i(x)\, q_i(t)\right]^2 = \sum_i \varphi_i^2(x)\, q_i^2(t) + 2\sum_{i\neq j} \varphi_i(x)\, \varphi_j(x)\, q_i(t) q_j(t)$$

$$\left[\sum_i \varphi_i(x)\, \dot{q}_i(t)\right]^2 = \sum_i \varphi_i^2(x)\, \dot{q}_i^2(t) + 2\sum_{i\neq j} \varphi_i(x)\, \varphi_j(x)\, q_i(t) \dot{q}_j(t)$$

$$(\text{for } i \neq j \neq 0)$$

Substituting into equation A.10

then

$$\dot{\mathbf{R}}(x,t)\bullet\dot{\mathbf{R}}(x,t) = \dot{\theta}^2 \left[\sum_i \varphi_i^2(x)\, q_i^2(t) + 2\sum_{i\neq j} \varphi_i(x)\, \varphi_j(x)\, q_i(t)\, q_j(t) + R_x^2(x)\, \dot{\theta}^2\right] + 2\, R_x(x)\, \dot{\theta} \sum_i \varphi_i(x)\, q_i(t) + \sum_i \varphi_i^2(x)\, \dot{q}_i^2(t) + 2\sum_{i\neq j} \varphi_i(x)\, \varphi_j(x)\, q_i(t)\, \dot{q}_j(t) \qquad \text{(eqn A.11)}$$

$$(\text{for } i \neq j)$$

Now equation A.9 can be rewritten as

$$T = \frac{1}{2}\dot{\theta}^2 \sum_i q_i^2(t) \left[\int_0^{\ell} \varphi_i^2(x)\, dm + M\, \varphi_i^2(\ell)\right] \qquad \text{(eqn A.12)}$$

$$+ \dot{\theta}^2 \sum_{i\neq j} q_i(t)\, q_j(t) \left[\int_0^{\ell} \varphi_i(x)\, \varphi_j(x)\, dm + M\, \varphi_i(\ell)\, \varphi_j(\ell)\right]$$

$$+ \frac{1}{2} \sum_i \dot{q}_i^2(t) \left[\int_0^{\ell} \varphi_i^2(x)\, dm + M\, \varphi_i^2(\ell)\right]$$

$$+ \sum_{i\neq j} \dot{q}_i(t)\, \dot{q}_j(t) \left[\int_0^{\ell} \varphi_i(x)\, \varphi_j(x)\, dm + M\, \varphi_i(\ell)\, \varphi_j(\ell)\right]$$

$$+ \frac{1}{2}\dot{\theta}^2 \left[\int_0^{\ell} R_x^2(x)\, dm + M\, R_x^2(\ell)\right]$$

$$+ \dot{\theta} \sum_i \dot{q}_i(t) \left[\int_0^{\ell} R_x(x)\, \varphi_i(x)\, dm + M\, R_x(\ell)\, \varphi_i(\ell)\right]$$

$$+ \frac{1}{2} I_{r_{zz}} \dot{\theta}^2 \qquad (\text{for } i \neq j)$$

From orthogonality relationship

$$\int_0^{\ell} \varphi_i(x)\, \varphi_j(x)\, dm + M\, \varphi_i(x)\, \varphi_j(\ell) = 0 \qquad (\text{for } i \neq j) \qquad \text{(eqn A.13)}$$

$$= M_i \qquad (\text{for } i = j)$$

where M_i is the *i-th* mode generalized mass, then the kinetic energy of the system can be simplified as follows

$$T = \frac{1}{2} \dot{\theta}^2 \sum_i q_i^2(t)\, M_i + \frac{1}{2} \sum_i \dot{q}_i^2(t)\, M_i \qquad \text{(eqn A.14)}$$

$$+ \frac{1}{2} I_{r_{zz}} \dot{\theta}^2$$

$$+ \frac{1}{2} \dot{\theta}^2 \left[\int_0^{\ell} R_x(x)\, dm + M\, R_x^2(\ell) \right]$$

$$+ \dot{\theta} \sum_i \dot{q}_i(t) \left[\int_0^{\ell} R_x(x)\, \varphi(x)\, dm + M\, R_x(\ell)\, \varphi(\ell) \right]$$

From the equation 2.25, potential energy is

$$U = \frac{1}{2} \sum_i \omega_i^2\, M_i\, q_i^2(t) \qquad \text{(eqn A.15)}$$

d. **Lagrange's equations**

Substitute equations A.14 and A.15 into equations 2.19 and 2.20 to apply Lagangie's equation,

then

$$\frac{\partial T}{\partial \theta} = 0$$

$$\frac{\partial T}{\partial \theta} = \dot{\theta} \sum_i q_i^2(t)\, M_i + \dot{\theta} \left[\int_0^{\ell} R_x^2(x)\, dm + M\, R_x^2(\ell) \right]$$

$$+ \sum_i \dot{q}_i(t) \left[\int_0^{\ell} R_x(x)\, \varphi_i(x)\, dm + M\, R_x(\ell)\, \varphi_i(\ell) \right]$$

$$+ I_{r_{zz}}\, \dot{\theta}$$

$$= \dot{\theta} \left[\sum_i q_i^2(t)\, M_i + \int_0^{\ell} R_x^2(x)\, dm + M\, R_x(\ell) + I_{r_{zz}} \right]$$

$$+ \sum_i \dot{q}_i(t) \left[\int_0^{\ell} R_x(x)\, \varphi_i(x)\, dm + M\, R_x(\ell)\, \varphi_i(\ell) \right]$$

$$\frac{d}{dt} \left[\frac{\partial T}{\partial \dot{\theta}} \right] = \ddot{\theta} \left[\sum_i q_i^2(t)\, M_i + \int_0^{\ell} R_x^2(x)\, dm + M\, R_x^2(\ell) + I_{r_{zz}} \right]$$

$$+ 2\, \dot{\theta} \sum_i \dot{q}_i(t)\, q_i(t)\, M_i$$

$$+ \sum_i \ddot{q}_i(t) \left[\int_0^{\ell} R_x(x)\, \varphi_i(x)\, dm + M\, R_x(\ell)\, \varphi_i(\ell) \right]$$

$$\frac{\partial U}{\partial \theta} = \frac{\partial U}{\partial \dot{\theta}} = \frac{d}{dt} \left[\frac{\partial U}{\partial \dot{\theta}} \right] = 0$$

$$\frac{\partial T}{\partial q_h} = \theta^2\, q_h(t)\, M_h$$

$$\frac{\partial T}{\partial \dot{q}_h} = \dot{q}_h(t)\, M_h + \dot{\theta} \left[\int_0^{\ell} R_x(x)\, \varphi_i(x)\, dm + M\, R_x(\ell)\, \varphi(\ell) \right]$$

$$\frac{d}{dt} \left[\frac{\partial T}{\partial \dot{q}_h} \right] = \ddot{q}_h(t)\, M_h + \ddot{\theta} \left[\int_0^{\ell} R_x(x)\, \varphi_i(x)\, dm + M\, R_x(\ell)\, \varphi_i(\ell) \right]$$

$$\frac{\partial U}{\partial q_h} = \omega^2{}_h \, M_h \, q_h(t)$$

$$\frac{\partial U}{\partial \dot{q}_h} = \frac{d}{dt}\left[\frac{\partial U}{\partial \dot{q}_h} \right] = 0$$

From all these quantities, equation A.1 becomes

$$\ddot{\theta} \left[\sum_i q_i^2(t) \, M_i + \int_0^{\ell} R_x^2(x) dm + M \, R_x^2(\ell) + I_{r_{zz}} \right] \qquad \text{(eqn A.16)}$$

$$+ 2 \dot{\theta} \sum_i \dot{q}_i(t) \, q_i(t) \, M_i + \sum_i \ddot{q}_i(t) \left[\int_0^{\ell} R_x(x) \, \varphi_i(x) \, dm + M \, R_x(\ell) \, \varphi(\ell) \right] = \tau$$

and equation A.2 becomes

$$\ddot{\theta} \left[\int_0^{\ell} R_x(x) \, \varphi_h(x) \, dm + M \, R_x(\ell) \, \varphi_h(\ell) \right] + \ddot{q}_h(t) \, M_h \qquad \text{(eqn A.17)}$$

$$- \dot{\theta}^2 \, q_h(t) \, M_h + \omega_h^2 \, M_h \, q_h(t) = - 2 \zeta \, \omega_h \, M_h \, \dot{q}_h(t)$$

$$(h = 1, 2, 3, \ldots\ldots, n)$$

In the equation A.16 and A.17, if we select n numbers degree of freedom of the system, that is, if we select n numbers of mode shape, we could have $n+1$ numbers of equations.

2. DOUBLE LINK BOOM SYSTEM IN PLANAR MOTION

a. Geometry of the system

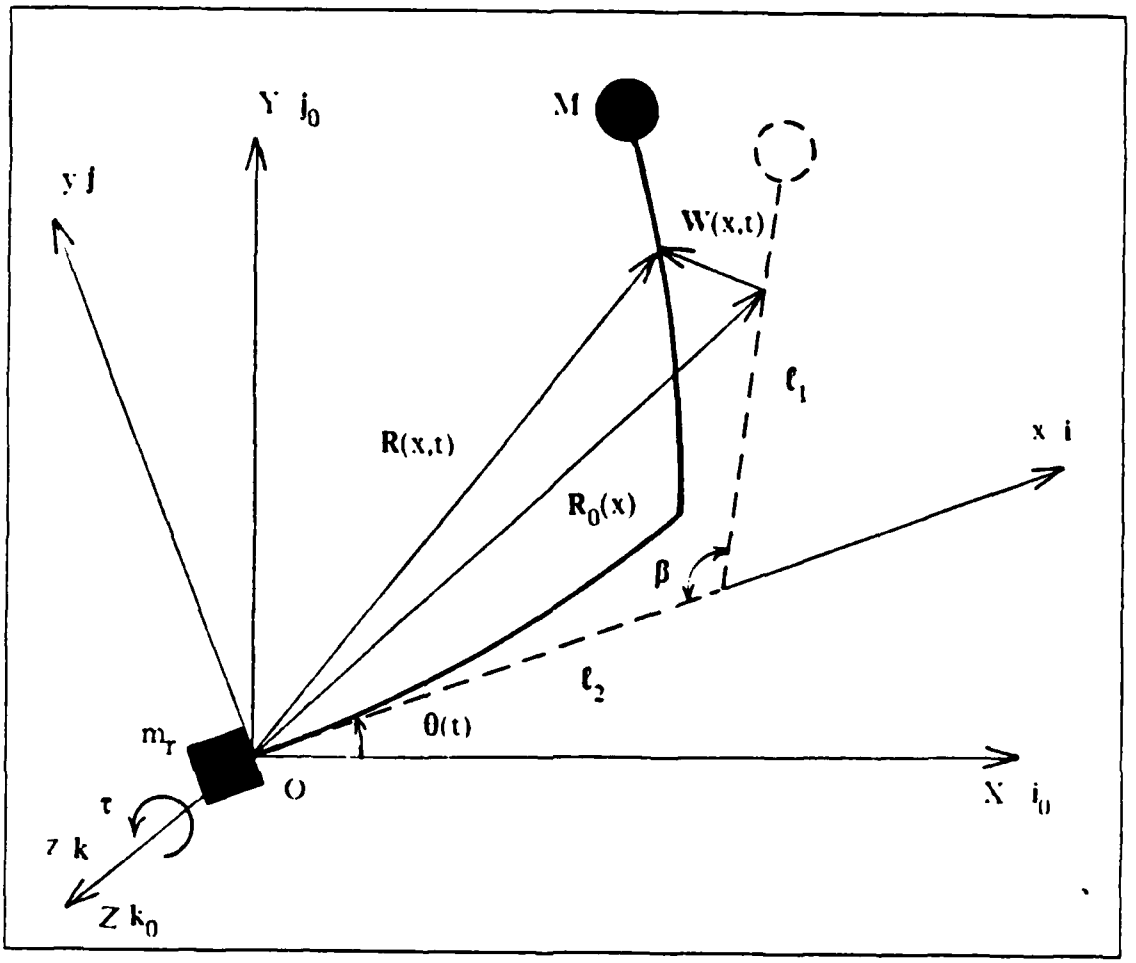

Figure A.2 Parameters of the double link boom system in planar motion.

M :	tip mass
m_T :	mass of electronics box
ℓ_1 :	length of lower boom
ℓ_2 :	length of upper boom
β :	angle between two links
τ :	applied torque
$\theta(t)$:	angular displacement
$\dot{\theta}(t)$:	angular velocity
$R_0(x)$:	position vector of the point on the boom in the local x-direction

$\mathbf{R}(x,t)$: position vector of the point on the boom after deformation

$\mathbf{W}(x,t)$: deformation vector of boom

$\mathbf{i}$: unit vector of local x-direction

$\mathbf{j}$: unit vector of local y-direction

$\mathbf{k}$: unit vector of local z-direction

$\mathbf{i}_0$: unit vector of global X-direction

$\mathbf{j}_0$: unit vector of global Y-direction

$\mathbf{k}_0$: unit vector of global Z-direction

b. **position and velocity**

In this double link system, we have to consider the extension deformation as well as the bending deformation.

The position vector of a point on the boom was expressed as a sum of $\mathbf{R}_x(x)$ and $\mathbf{W}(x,t)$.

Then

$$\mathbf{R}(x,t) = \mathbf{R}_0(x) + \mathbf{W}(x,t) \qquad \text{(eqn 2.9)}$$

where

$$\begin{aligned} \mathbf{R}_0(x) &= \mathbf{R}_x(x) + \mathbf{R}_y(x) \qquad \text{(eqn A.18)} \\ &= R_x(x)\,\mathbf{i} + R_y(x)\,\mathbf{j} \end{aligned}$$

From equation A.4 and A.18 the position vector of the point on the boom is

$$\mathbf{R}(x,t) = R_x(x)\,\mathbf{i} + R_y(x)\,\mathbf{j} + \sum_i [\,\varphi_i(x)\,\mathbf{i} + \varphi_i^y(x)\,\mathbf{j}\,]\,q_i(t) \qquad \text{(eqn A.19)}$$

Now by differentiating the equation A.19, we obtain the velocity of the point on the boom.

$$\begin{aligned} \dot{\mathbf{R}}(x,t) = {} & R_x(x)\,\dot{\mathbf{i}} + R_y(x)\,\dot{\mathbf{j}} + \sum_i [\,\varphi_i(x)\,\mathbf{i} + \varphi_i^y(x)\,\mathbf{j}\,]\,\dot{q}_i(t) \qquad \text{(eqn A.20)} \\ & + \sum_i [\,\varphi_i^x(x)\,\dot{\mathbf{i}} + \varphi_i^y(x)\,\dot{\mathbf{j}}\,]\,q_i(t) \end{aligned}$$

Substitute the time derivative of unit vector to the equation A.20 and simplify then

$$\dot{\mathbf{R}}(x,t) = [\, -\dot{\theta}\{ R_y(x) + \sum_i \varphi_i^y(x)\, q_i(t) \} + \sum_i \varphi_i^x(x)\, \dot{q}_i(t) \,]\, \mathbf{i} \qquad \text{(eqn A.21)}$$

$$+ [\, R_x(x)\, \dot{\theta} + \dot{\theta} \sum_i \varphi_i^x(x)\, q_i(t) + \sum_i \varphi_i^y(x)\, \dot{q}_i(t) \,]\, \mathbf{j}$$

c. **Kinetic energy and potential energy**

From the equation A.21

$$\dot{\mathbf{R}}(x,t) = [\, -\dot{\theta}\{ R_y(x) + \sum_i \varphi_i^y(x)\, q_i(t) \} + \sum_i \varphi_i^x(x)\, \dot{q}_i(t) \,]\, \mathbf{i} \qquad \text{(eqn A.22)}$$

$$+ [\, R_x(x)\, \dot{\theta} + \dot{\theta} \sum_i \varphi_i^x(x)\, q_i(t) + \sum_i \varphi_i^y(x)\, \dot{q}_i(t) \,]\, \mathbf{j}$$

The dot product of $\dot{\mathbf{R}}(x,t)$ is

$$\dot{\mathbf{R}}(x,t) \bullet \dot{\mathbf{R}}(x,t) = [\, -\dot{\theta}\{ R_y(x) + \sum_i \varphi_i^y(x)\, q_i(t) \} \qquad \text{(eqn A.23)}$$

$$+ \sum_i \varphi_i^x(x)\, \dot{q}_i(t) \,]^2 + [\, R_x(x)\, \dot{\theta} + \dot{\theta} \sum_i \varphi_i^x(x)\, q_i(t) + \sum_i \varphi_i^y(x)\, \dot{q}_i(t) \,]^2$$

$$= \dot{\theta}^2 \sum_i [\, R_y^2(x) + 2\, R_y(x) \sum_i \varphi_i^y(x)\, q_i(t) + \{ \sum_i \varphi_i^y(x)\, q_i(t) \}^2 \,]$$

$$- 2\dot{\theta} [\, \{ R_y(x) + \sum_i \varphi_i^y(x)\, q_i(t) \} \sum_i \varphi_i^x(x)\, q_i(t) \,] + [\, \sum_i \varphi_i^x(x)\, \dot{q}_i(t) \,]^2$$

$$+ \dot{\theta}^2 [\, R_x^2(x) + 2\, R_x(x) \sum_i \varphi_i^x(x)\, q_i(t) + \{ \sum_i \varphi_i^x(x)\, q_i(t) \}^2 \,]$$

$$+ 2\dot{\theta} [\, \{ R_x(x) + \sum_i \varphi_i^x(x)\, q_i(t) \} \sum_i \varphi_i(x)\, \dot{q}_i(t) \,] + [\, \sum_i \varphi_i^y(x)\, \dot{q}_i(t) \,]^2$$

$$= \dot{\theta}^2 [\, \{ R_x^2(x) + R_y^2(x) \} + 2 \sum_i q_i(t) \{ R_x(x)\, \varphi_i^x(x) + R_y(x)\, \varphi_i^y(x) \}$$

$$+ \{ \sum_i \varphi_i^x(x)\, q_i(t) \}^2 + \{ \sum_i \varphi_i^y(x)\, q_i(t) \}^2 \,]$$

$$+ 2\dot{\theta} \sum_i q_i(t)\,\dot{q}_i(t) [\{ R_x(x) + \varphi_i^x(x) \}\, \varphi_i^y(x) - \{ R_y(x) + \varphi_i^y(x) \}\, \varphi_i^x(x)]$$

$$+ [\{ \sum_i \varphi_i^x(x)\, q_i(t) \}^2 + \{ \sum_i \varphi_i^y(x)\, q_i(t) \}^2]$$

From the geometry of the system

$$R_x^2(x) + R_y^2(x) = R_0^2(x) \qquad \text{(eqn A.24)}$$

$$R_x^2(\ell) + R_y^2(\ell) = R_0^2(\ell)$$

Substituting equation A.24 into equation A.23 and apply the equation A.9 then kinetic energy is

$$T = \frac{1}{2}\dot{\theta}^2 [\int_0^\ell R_0^2(x)\, dm + M\, R_0^2(\ell) + \int_0^\ell \{ (\sum_i \varphi_i^x(x)\, q_i(t))^2 \qquad \text{(eqn A.25)}$$

$$+ (\sum_i \varphi_i^y(x)\, q_i(t))^2 \}\, dm + M \{ (\sum_i \varphi_i^x(\ell)\, q_i(t))^2$$

$$+ (\sum_i \varphi_i^y(\ell)\, q_i(t))^2 \}$$

$$+ 2 \sum_i q_i(t) \{ \int_0^\ell (R_x(x)\, \varphi_i^x(x) + R_y(x)\, \varphi_i^y(x))\, dm$$

$$+ M (R_x(\ell)\, \varphi_i^x(\ell) + R_y(\ell)\, \varphi_i^y(\ell) \}]$$

$$+ \frac{1}{2} [\int_0^\ell \{ (\sum_i \varphi_i^x(x)\, \dot{q}_i(t))^2 + (\sum_i \varphi_i^y(x)\, \dot{q}_i(t))^2 \}\, dm$$

$$+ M \{ (\sum_i \varphi_i^x(\ell)\, \dot{q}_i(t))^2 + (\sum_i \varphi_i^y(\ell)\, \dot{q}_i(t))^2) \}]$$

$$+ \dot{\theta} \sum_i \dot{q}_i(t) [\int_0^\ell \{ R_x(x)\, \varphi_i^y(x) - R_y(x)\, \varphi_i^x(x) \}\, dm$$

$$+ M \{ R_x(\ell)\, \varphi_i^y(\ell) - R_y(\ell)\, \varphi_i^x(\ell) \}$$

$$+ \sum_j q_j(t) \{ \int_0^\ell (\varphi_j^x(x)\, \varphi_j^y(x) - \varphi_j^y(x)\, \varphi_i^x(\ell)\, dm$$

$$+ M (\varphi_j^x(\ell) \varphi_i^y(\ell) - \varphi_j^y(\ell) \varphi_i^x(\ell)) \}]$$

$$+ \frac{1}{2} I_{r_{zz}} \dot{\theta}^2$$

Now let's apply the orthogonality relationship

$$\int_0^\ell \{ \varphi_i^x(x) \varphi_j^x(x) + \varphi_i^y(x) \varphi_j^y(x) \} \, dm \qquad \text{(eqn A.26)}$$

$$+ M \{ \varphi_i^x(\ell) \varphi_j^x(\ell) + \varphi_i^y(\ell) \varphi_j^y(\ell) \} = 0 \quad (\text{for } i \neq j)$$

$$= M_i \quad (\text{for } i = j)$$

to the equation A.26 then

$$T = \frac{1}{2} \dot{\theta}^2 [\int_0^\ell R_0^2(x) \, dm + M R_0^2(\ell) + \sum_i q_i^2(t) M_i \qquad \text{(eqn A.27)}$$

$$+ 2 \sum_i q_i(t) \{ \int_0^\ell (R_x(x) \varphi_i^x(x) + R_y(x) \varphi_i^y(x)) \, dm$$

$$+ 2 M (R_x(\ell) \varphi_i^x(\ell) + R_y(\ell) \varphi_i^y(\ell)) \} + I_{r_{zz}}]$$

$$+ \frac{1}{2} \sum_i \dot{q}_i^2(t) M_i$$

$$+ \dot{\theta} \sum_i \dot{q}_i(t) [\int_0^\ell \{ R_x(x) \varphi_i^y(x) - R_y(x) \varphi_i^x(x) \} \, dm$$

$$+ M \{ R_x(\ell) \varphi_i^y(\ell) - R_y(\ell) \varphi_i^x(\ell) \}$$

$$+ \sum_j q_j(t) \{ \int_0^\ell (\varphi_j^x(x) \varphi_j^y(x) - \varphi_j^y(x) \varphi_i^x(\ell)) \, dm$$

$$+ M (\varphi_j^x(\ell) \varphi_i^y(\ell) - \varphi_j^y(\ell) \varphi_i^x(\ell)) \}]$$

From the equation 2.25, potential energy is

$$U = \frac{1}{2} \sum_i \omega_i^2 M_i q_i^2(t) \qquad \text{(eqn A.15)}$$

d. **Lagrange's equation**

Apply Lagrange's equations A.1 and A.2

then

$$\frac{\partial T}{\partial \theta} = 0$$

$$\frac{\partial T}{\partial \dot{\theta}} = \dot{\theta} \left[\int_0^{\ell} R_0^2(x)\, dm + M R_0^2(\ell) + \sum_i q_i^2(t) M_i \right.$$

$$+ 2 \sum_i q_i(t) \left\{ \int_0^{\ell} \left(R_x(x) \varphi_i^x(x) + R_y(x) \varphi_i^y(x) \right) dm \right.$$

$$\left. \left. + 2 M \left(R_x(\ell) \varphi_i^x(\ell) + R_y(\ell) \varphi_i^y(\ell) \right) \right\} + I_{r_{zz}} \right]$$

$$+ \sum_i \dot{q}_i(t) \left[\int_0^{\ell} \left\{ R_x(x) \varphi_i^y(x) - R_y(x) \varphi_i^x(x) \right\} dm \right.$$

$$+ M \left\{ R_x(\ell) \varphi_i^y(\ell) - R_y(\ell) \varphi_i^x(\ell) \right\}$$

$$+ \sum_j q_j(t) \left\{ \int_0^{\ell} \left(\varphi_j^x(x) \varphi_j^y(x) - \varphi_j^y(x) \varphi_i^x(\ell) \right) dm \right.$$

$$\left. \left. + M \left(\varphi_j^x(\ell) \varphi_i^y(\ell) - \varphi_j^y(\ell) \varphi_i^x(\ell) \right) \right\} \right]$$

$$\frac{d}{dt} \left[\frac{\partial T}{\partial \dot{\theta}} \right] = \ddot{\theta} \left[\int_0^{\ell} R_0^2(x)\, dm + M R_0^2(\ell) + \sum_i q_i^2(t) M_i \right.$$

$$+ 2 \sum_i q_i(t) \left\{ \int_0^{\ell} \left(R_x(x) \varphi_i^x(x) + R_y(x) \varphi_i^y(x) \right) dm \right.$$

$$\left. \left. + 2 M \left(R_x(\ell) \varphi_i^x(\ell) + R_y(\ell) \varphi_i^y(\ell) \right) \right\} + I_{r_{zz}} \right]$$

$$+ 2 \dot{\theta} \sum_i \dot{q}_i(t) q_i(t) M_i$$

$$+ 2 \dot{\theta} \sum_i \dot{q}_i \left\{ \int_0^{\ell} \left(R_x(x) \varphi_i^x(x) + R_y(x) \varphi_i^y(x) \right) dm \right.$$

$$+ \sum_i \ddot{q}_i(t) \left[\int_0^{\ell} \{ R_x(x)\, \varphi_i^{y}(x) - R_y(x)\, \varphi_i^{x}(x) \}\, dm \right.$$

$$+ M \{ R_x(\ell)\, \varphi_i^{y}(\ell) - R_y(\ell)\, \varphi_i^{x}(\ell) \}$$

$$+ \sum_j q_j(t) \{ \int_0^{\ell} (\varphi_j^{x}(x)\, \varphi_j^{y}(x) - \varphi_j^{y}(x)\, \varphi_i^{x}(\ell))\, dm$$

$$\left. + M (\varphi_j^{x}(\ell)\, \varphi_i^{y}(\ell) - \varphi_j^{y}(\ell)\, \varphi_i^{x}(\ell)) \} \right]$$

$$\frac{\partial U}{\partial \theta} = \frac{\partial U}{\partial \dot{\theta}} = \frac{d}{dt} \left[\frac{\partial U}{\partial \dot{\theta}} \right] = 0$$

$$\frac{\partial T}{\partial q_h} = \dot{\theta}^2 \left[q_h(t)\, M_h + \{ \int_0^{\ell} (R_x(x)\, \varphi_i^{x}(x) + R_y(x)\, \varphi_i^{y}(x))\, dm \right.$$

$$+ M \{ R_x(\ell)\, \varphi_i^{x}(\ell) + R_y(\ell)\, \varphi_i^{y}(\ell)) \} + I_{r_{zz}} \right]$$

$$+ \dot{\theta} \sum_j \dot{q}_i(t) \left[\int_0^{\ell} (\varphi_h^{x}(x)\, \varphi_i^{y}(x) - \varphi_h^{y}(x)\, \varphi_i^{x}(x)\, dm \right.$$

$$\left. + M (\varphi_h^{x}(\ell)\, \varphi_i^{y}(\ell) - \varphi_h^{y}(\ell)\, \varphi_i^{x}(\ell) \} \right]$$

$$\frac{\partial T}{\partial \dot{q}_h} = \dot{\theta} \left[\int_0^{\ell} \{ R_x(x)\, \varphi_h^{y}(x) + R_y(x)\, \varphi_h^{x}(x))\, dm \right.$$

$$+ M (R_x(\ell)\, \varphi_h^{y}(\ell) - R_y(\ell)\, \varphi_h^{x}(\ell) \}$$

$$+ \sum_j q_j(t) \{ \int_0^{\ell} (\varphi_j^{x}(x)\, \varphi_h^{y}(x) - \varphi_j^{y}(x)\, \varphi_h^{x}(\ell)\, dm \right.$$

$$\left. + M \{ \varphi_j^{x}(\ell)\, \varphi_i^{y}(\ell) - \varphi_j^{y}(\ell)\, \varphi_i^{x}(\ell) \} \right] + \dot{q}_h(t)\, M_h$$

$$\frac{d}{dt} \left[\frac{\partial T}{\partial \dot{q}_h} \right] = \ddot{\theta} \left[\int_0^{\ell} \{ R_x(x)\, \varphi_h^{y}(x) + R_y(x)\, \varphi_h^{x}(x))\, dm \right.$$

$$\left. + M (R_x(\ell)\, \varphi_h^{y}(\ell) - R_y(\ell)\, \varphi_h^{x}(\ell) \} \right]$$

$$+ \sum_j q_j(t) \{ \int_0^{\ell} (\varphi_j^x(x) \varphi_h^y(x) - \varphi_j^y(x) \varphi_h^x(\ell) \, dm$$

$$+ M \{ \varphi_j^x(\ell) \varphi_i^y(\ell) - \varphi_j^y(\ell) \varphi_i^x(\ell) \}] + q_h(t) M_h$$

$$+ \dot{\theta} \sum_i \dot{q}_j(t) [\int_0^{\ell} \{ \varphi_j^x(x) \varphi_h^y(x) - \varphi_j^y(x) \varphi_h^x(x) \} \, dm$$

$$+ M [\varphi_j^x(\ell) \varphi_h^y(\ell) - \varphi_j^y(\ell) \varphi_h^x(\ell)] + q_h(t) M_h$$

$$\frac{\partial U}{\partial q_h} = \omega^2_h M_h q_h(t)$$

$$\frac{\partial U}{\partial \dot{q}_h} = \frac{d}{dt} [\frac{\partial U}{\partial \dot{q}_h}] = 0$$

Plug these quantities in the equation A.1
then

$$\ddot{\theta} [\int_0^{\ell} R_0^2(x) \, dm + M R_0^2(\ell) + \sum_i q_i^2(t) M_i \qquad \text{(eqn A.28)}$$

$$+ 2 \sum_i q_i(t) \{ \int_0^{\ell} (R_x(x) \varphi_i^x(x) + R_y(x) \varphi_i^y(x)) \, dm$$

$$+ 2 M (R_x(\ell) \varphi_i^x(\ell) + R_y(\ell) \varphi_i^y(\ell)) \} + I_{r_{zz}}]$$

$$+ 2 \dot{\theta} \sum_i \dot{q}_i(t) q_i(t) M_i$$

$$+ 2 \theta \sum_i q_i(t) \int_0^{\ell} (R_x(x) \varphi_i^x(x) + R_y(x) \varphi_i^y(x)) \, dm$$

$$+ 2 M (R_x(\ell) \varphi_i^x(\ell) + R_y(\ell) \varphi_i^y(\ell)) \} + I_{r_{zz}} \theta^2]$$

$$+ \sum_j \ddot{q}_j(t) \{ \int_0^{\ell} \varphi_j^x(x) \varphi_j^y(x) - \varphi_j^y(x) \varphi_i^x(\ell) \} \, dm$$

$$+ M (\varphi_j^x(\ell) \varphi_i^y(\ell) - \varphi_j^y(\ell) \varphi_i^x(\ell)] = \tau$$

and the equation A.2 becomes

$$\ddot{\theta}\left[\int_0^{\ell}\{R_x(x)\,\varphi_h^{y}(x)+R_y(x)\,\varphi_h^{x}(x)\}\,dm\right. \qquad \text{(eqn A.29)}$$

$$+M\{R_x(\ell)\,\varphi_h^{y}(\ell)-R_y(\ell)\,\varphi_h^{x}(\ell)\}$$

$$+\sum_j q_j(t)\left\{\int_0^{\ell}(\varphi_j^{x}(x)\,\varphi_h^{y}(x)-\varphi_j^{y}(x)\,\varphi_h^{x}(\ell)\,dm\right.$$

$$\left.+M\{\varphi_j^{x}(\ell)\,\varphi_i^{y}(\ell)-\varphi_j^{y}(\ell)\,\varphi_i^{x}(\ell)\}\right]+\ddot{q}_h(t)\,M_h$$

$$-\dot{\theta}^2\left[q_h(t)\,M_h+\left\{\int_0^{\ell}(R_x(x)\,\varphi_h^{x}(x)+R_y(x)\,\varphi_h^{y}(x))\,dm\right.\right.$$

$$\left.+M\{R_x(\ell)\,\varphi_h^{x}(\ell)+R_y(\ell)\,\varphi_h^{y}(\ell))\}\right]$$

$$+2\dot{\theta}\sum_j\dot{q}_j(t)\left[\int_0^{\ell}(\varphi_j^{x}(x)\,\varphi_h^{y}(x)-\varphi_j^{y}(x)\,\varphi_h^{x}(x)\}\,dm\right.$$

$$\left.+M\{\varphi_j^{x}(\ell)\,\varphi_h^{y}(\ell)-\varphi_j^{y}(\ell)\,\varphi_h^{x}(\ell)\}\right]+\omega^2{}_h\,M_h\,q_h(t)=-2\zeta\,\omega_h\,M_h\,\dot{q}_h(t)$$

$$(h=1,2,3,\ldots\ldots,n)$$

e. Results

Table 5 and 6 show the eigenvalues of Aluminum Alloy and Composite material boom from NASTRAN simulation results and Figure A.3 shows first two mode shape of the double link boom in planar motion. As shown in Figure A.4, applied torque to maintain 15 r.p.m of rotating speed increased to one hundred times of the torque that applied to the same boom in 3-dimensional motion because its mass center is far away from rotating center. Angular displacement change with time was almost same as 3-dimensional case. Displacement in x and y-direction was much bigger than that of 3-dimensional motion because tip position is far away from the rotating center and concentrated mass attached to the tip.

While rotating speed increases, boom deflects negative y-direction and positive x-direction until reaching its equilibrium position. After cutting off torque, boom remains equilibrium position and oscillates with some amplitude. Magnitude of

deflection at equilibrium position was about 6.2 inchs and slope at the tip position was 2.3 °. These values are much bigger than that of 3-dimensional motion but it is quite natural because of its big radius of rotation.

Figures A.5 - A.12 show angular displacement, angular velocity, generalized displacement, deflection in each direction, magnitude of deflection and slope at the tip position respectively.

TABLE 5

REAL EIGENVALUES OF ALUMINUM ALLOY (2 D)

mode no.	radians ω_i	cycles ω_i	generalized mass(M_i)	generalized stiffness(K_i)
1	3.568816E+00	5.679947E−01	1.000000E+00	1.273645E+01
2	1.796733E+01	2.859589E+00	1.000000E+00	3.228248E+02

TABLE 6

REAL EIGENVALUES OF COMPOSITE MATERIAL (2 D)

mode no.	radians ω_i	cycles ω_i	generalized mass(M_i)	generalized stiffness(K_i)
1	4.461328E+00	7.100423E−01	1.000000E+00	1.990344E+01
2	2.246115E+01	3.574804E+00	1.000000E+00	5.045035E+02

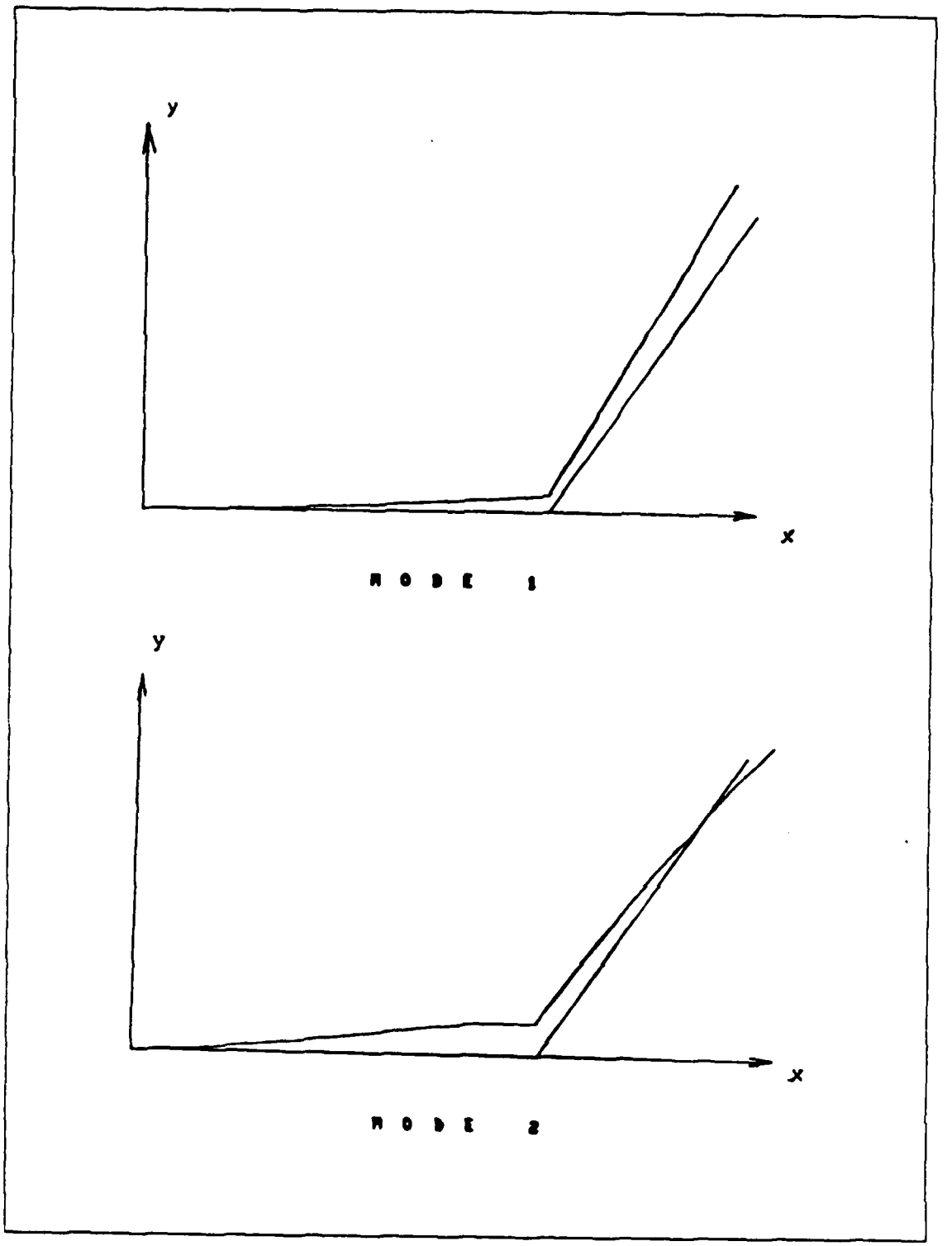

Figure A.3 First and second mode shape.

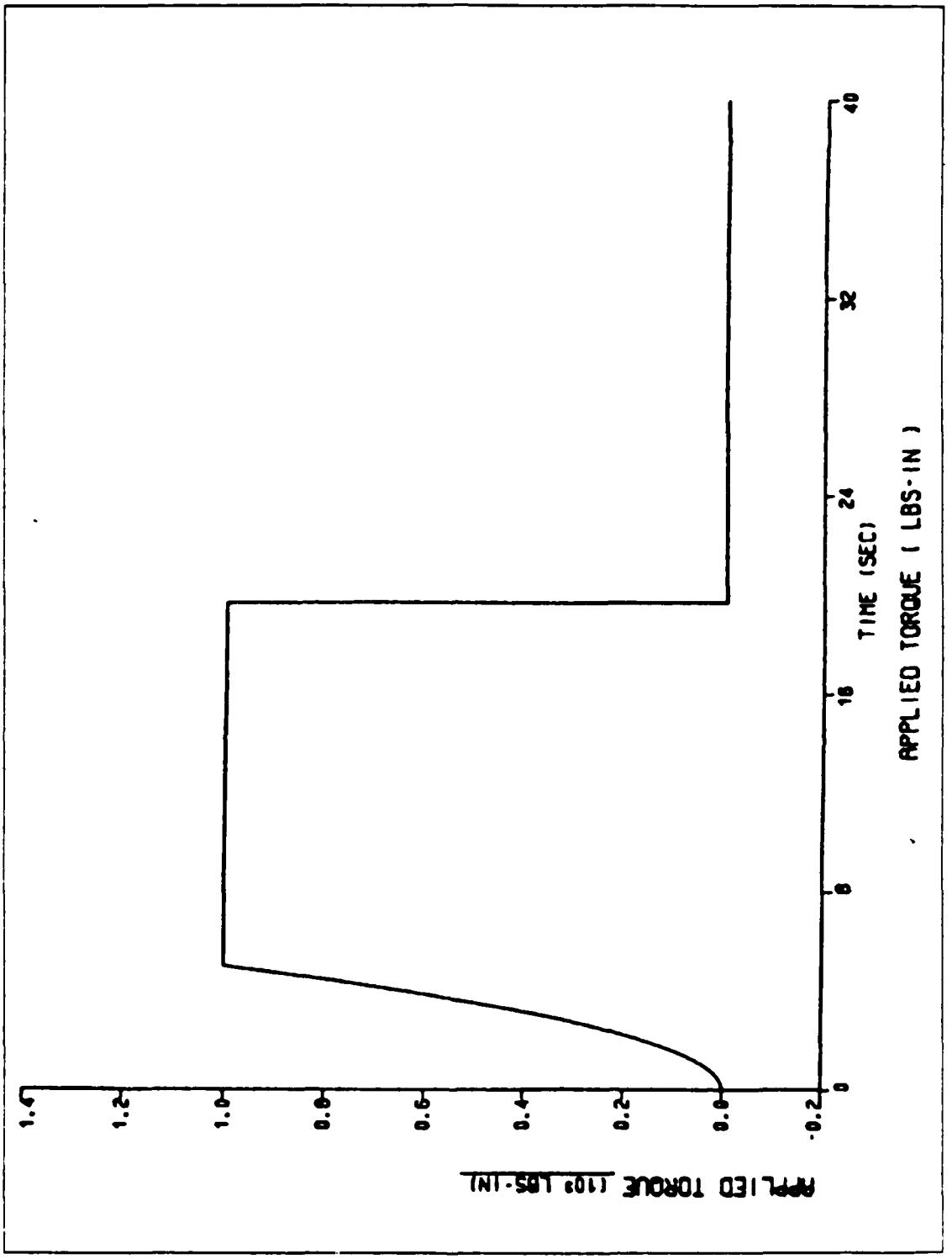

Figure A.4 Applied torque vs. time.

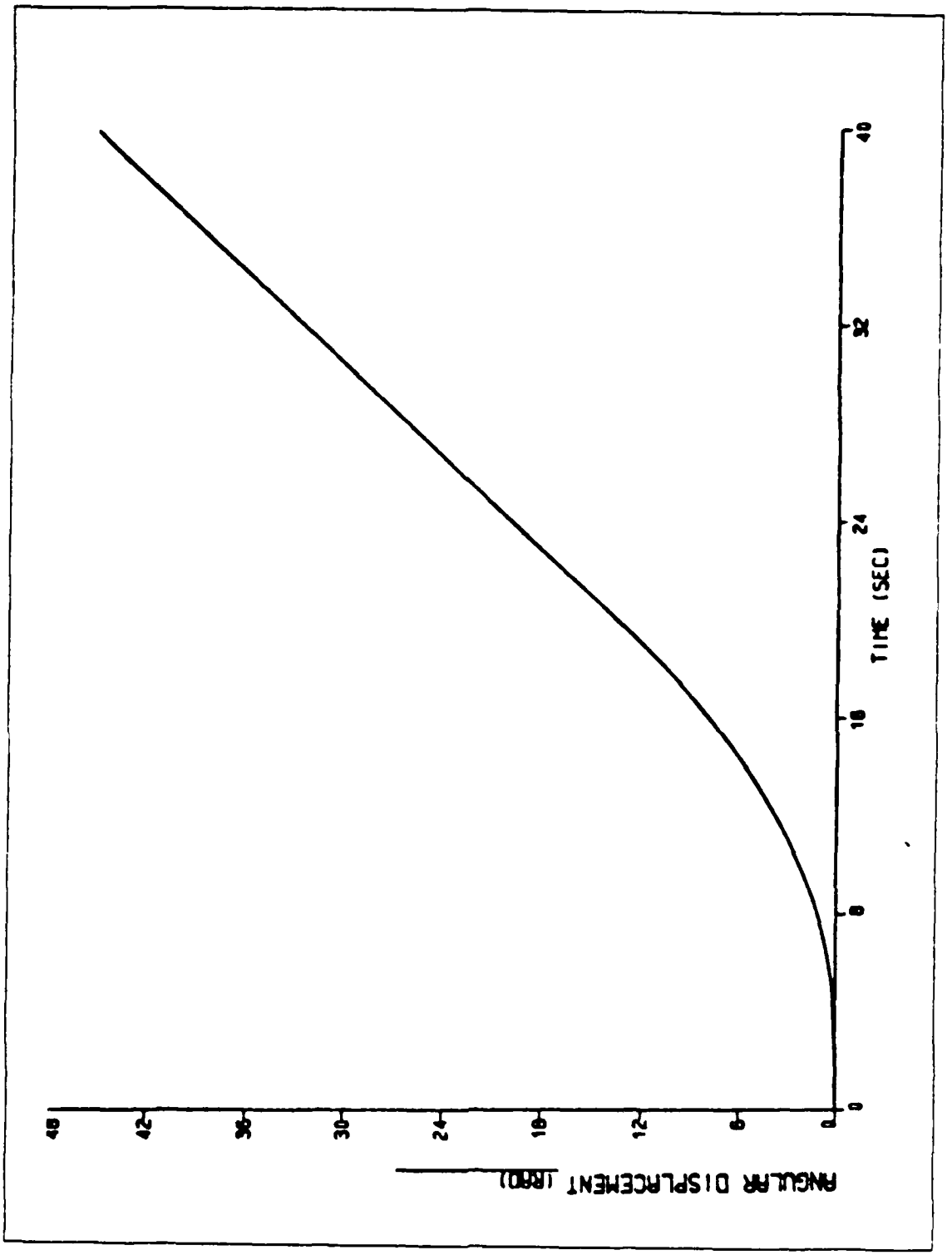

Figure A.5 Angular displacement vs. time.

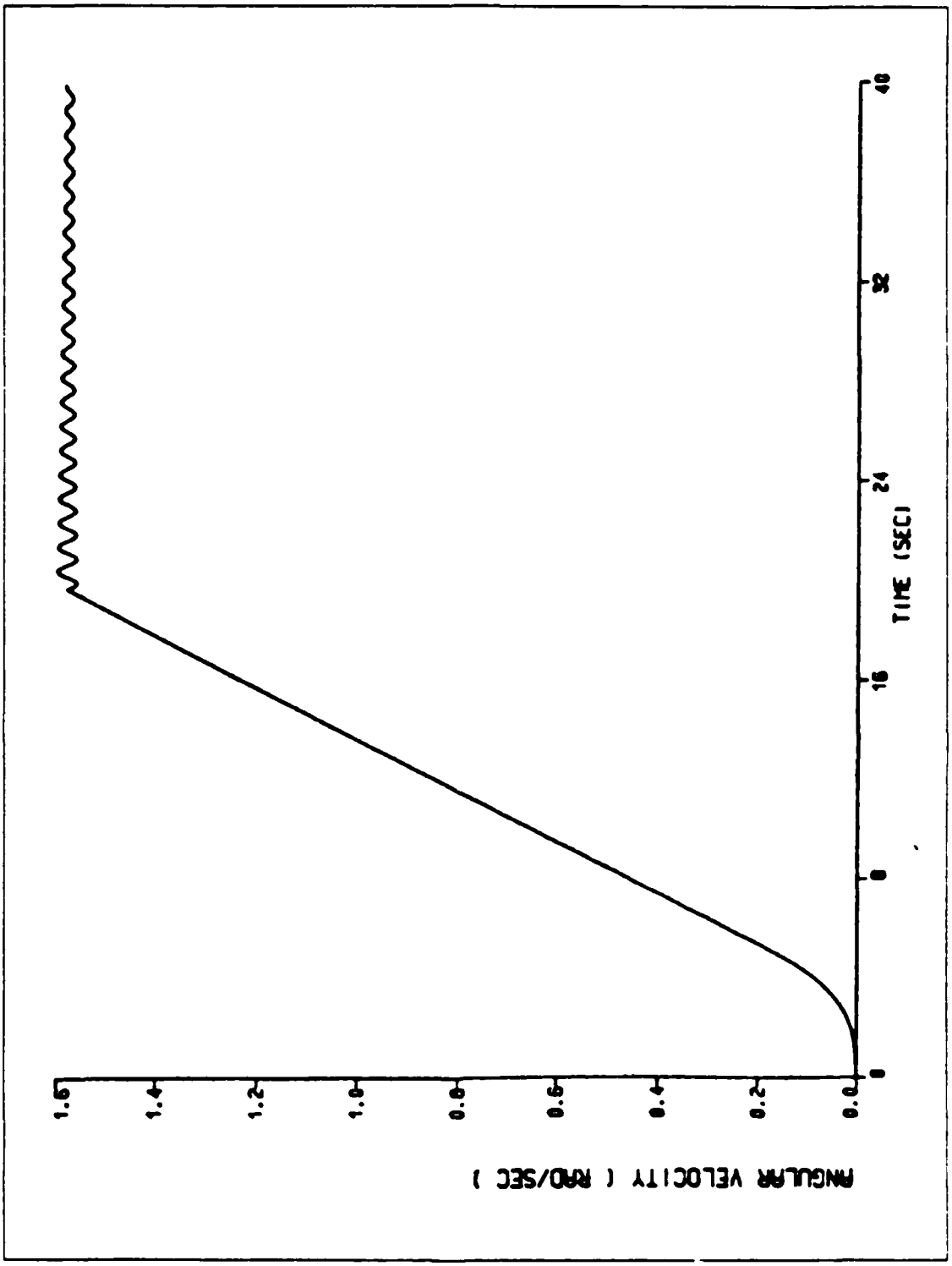

Figure A.6 Angular velocity vs. time.

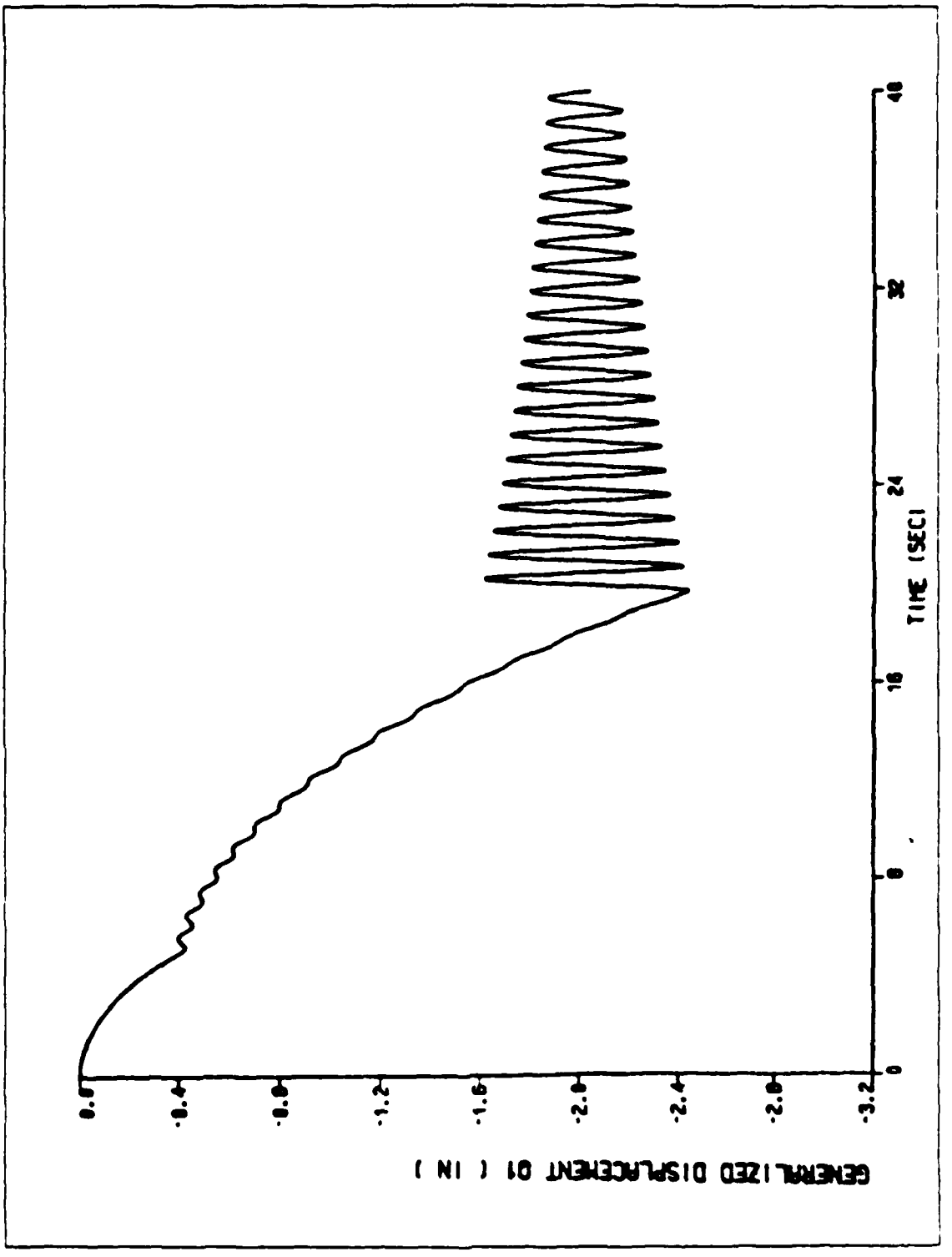

Figure A.7 First mode generalized displacement vs. time.

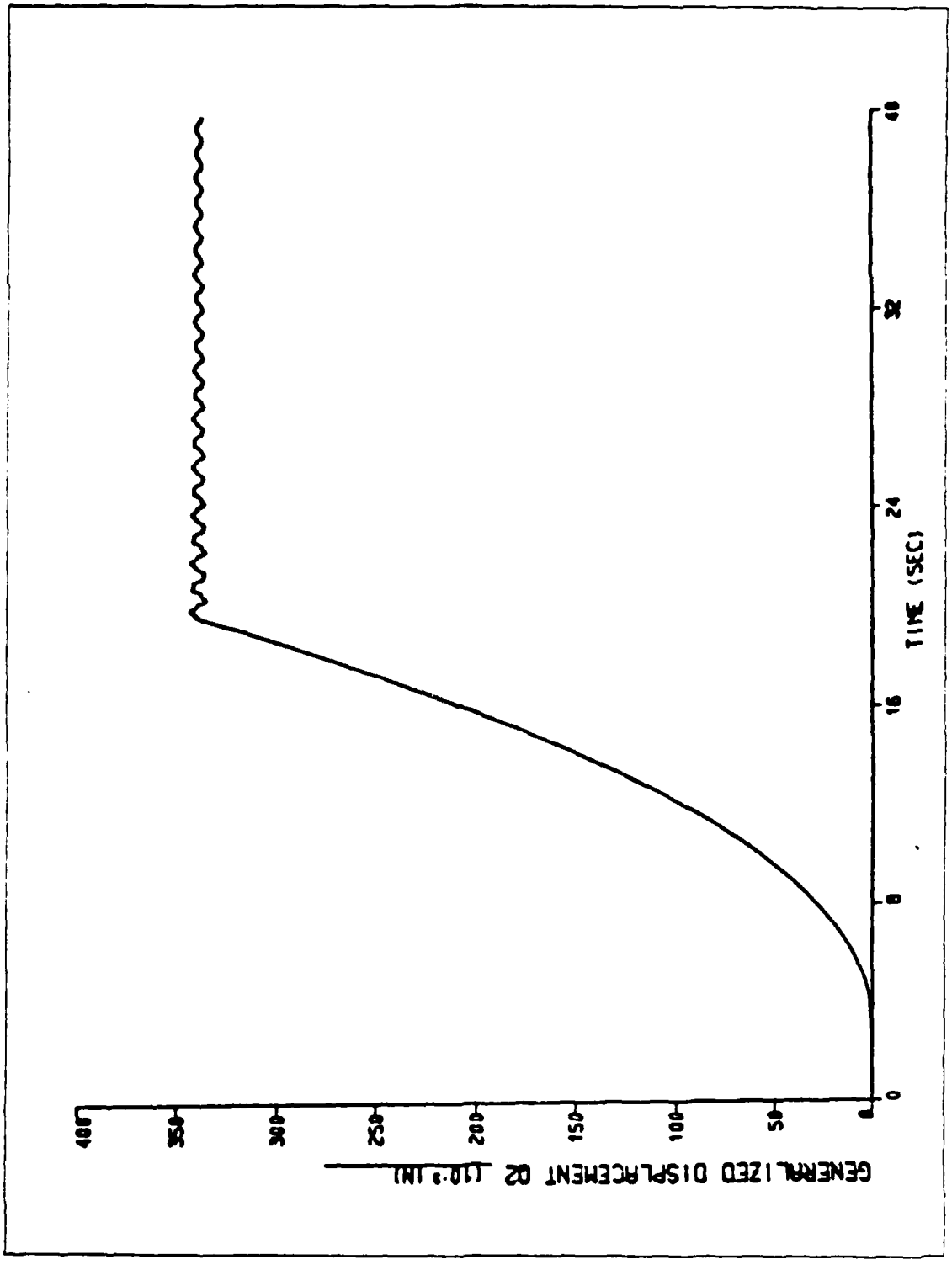

Figure A.8 Second mode generalized displacement vs. time.

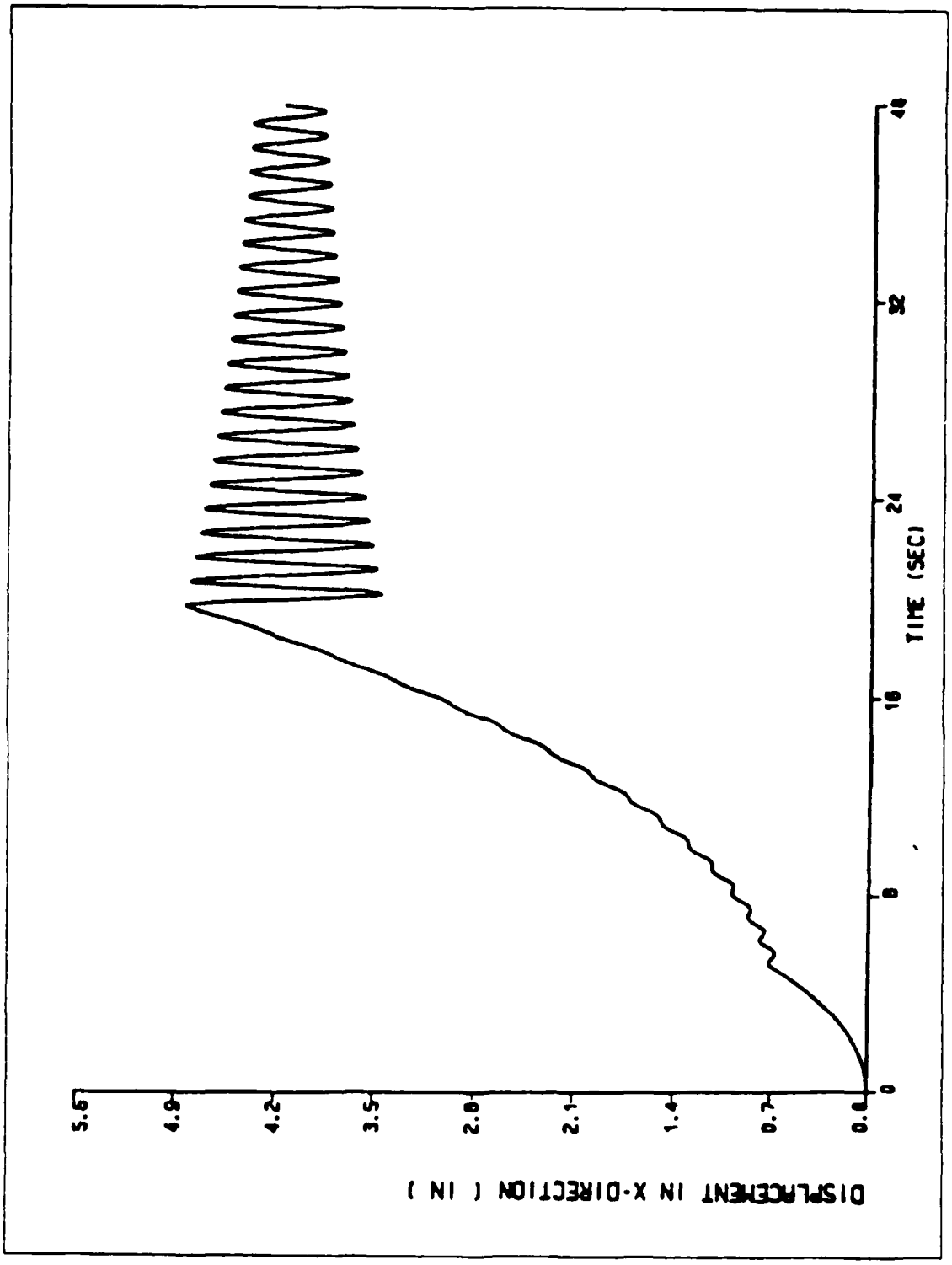

Figure A.9 Displacement in x-direction vs. time.

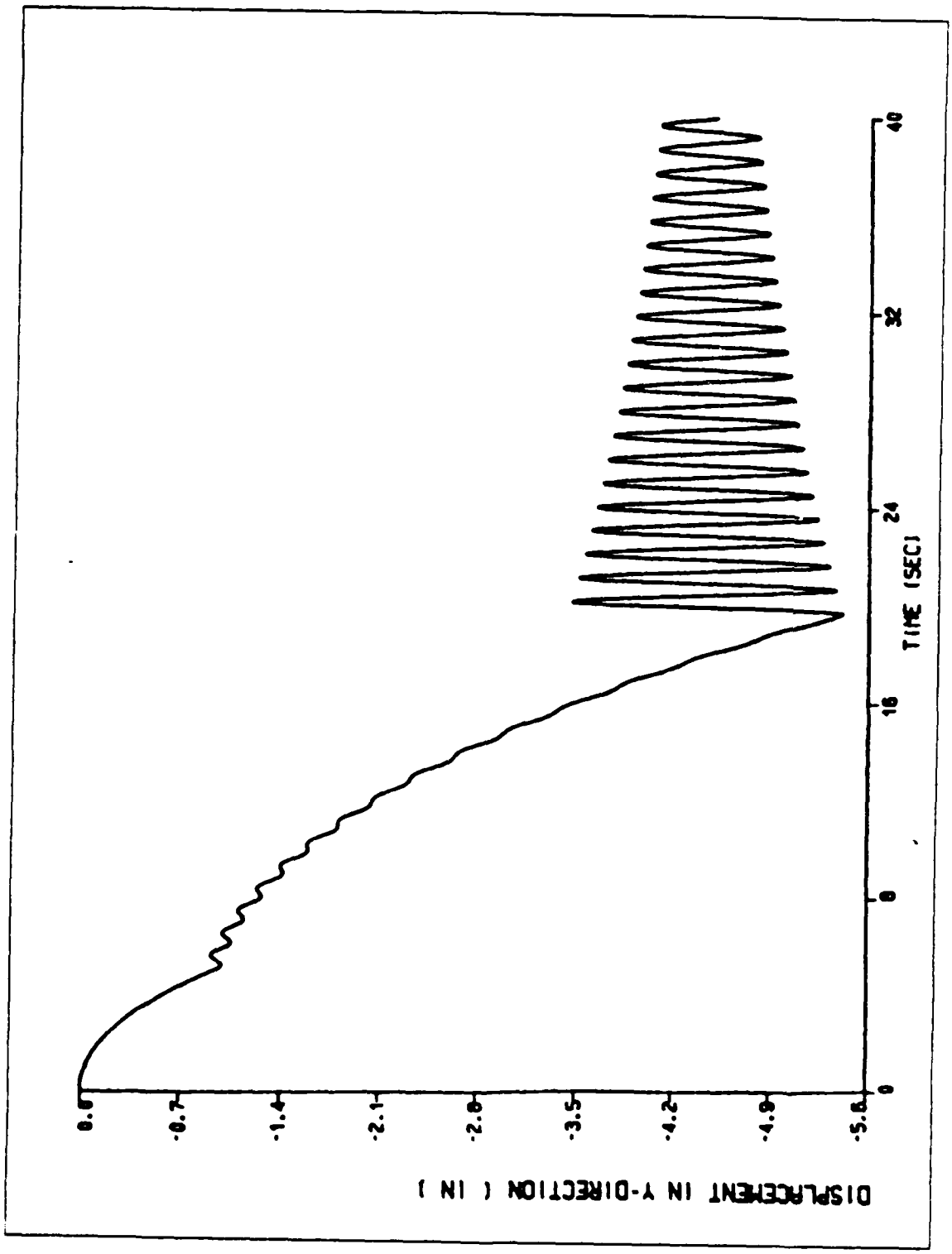

Figure A.10 Displacement in y-direction vs. time.

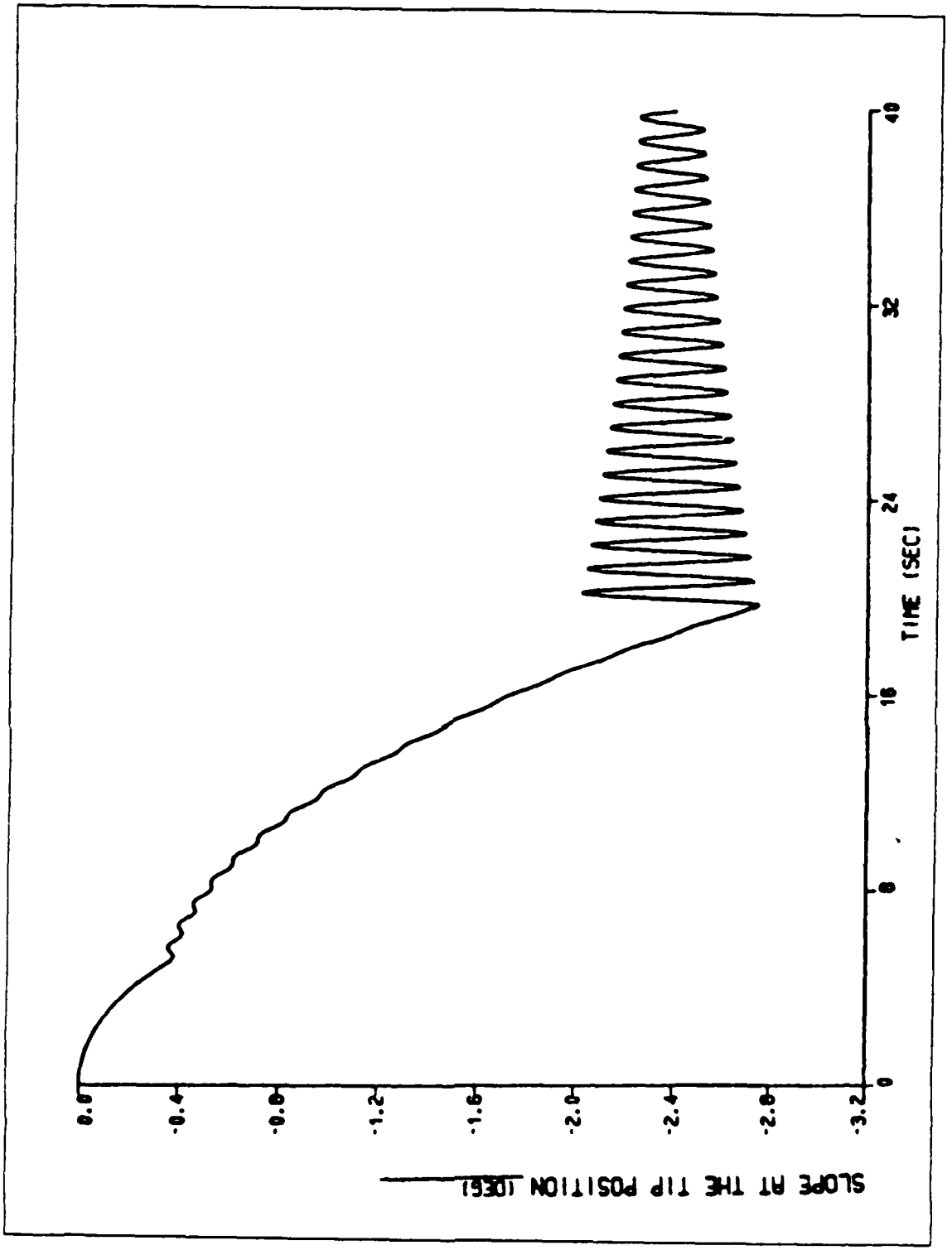

Figure A.11 Magnitude of deflection at tip position vs. time.

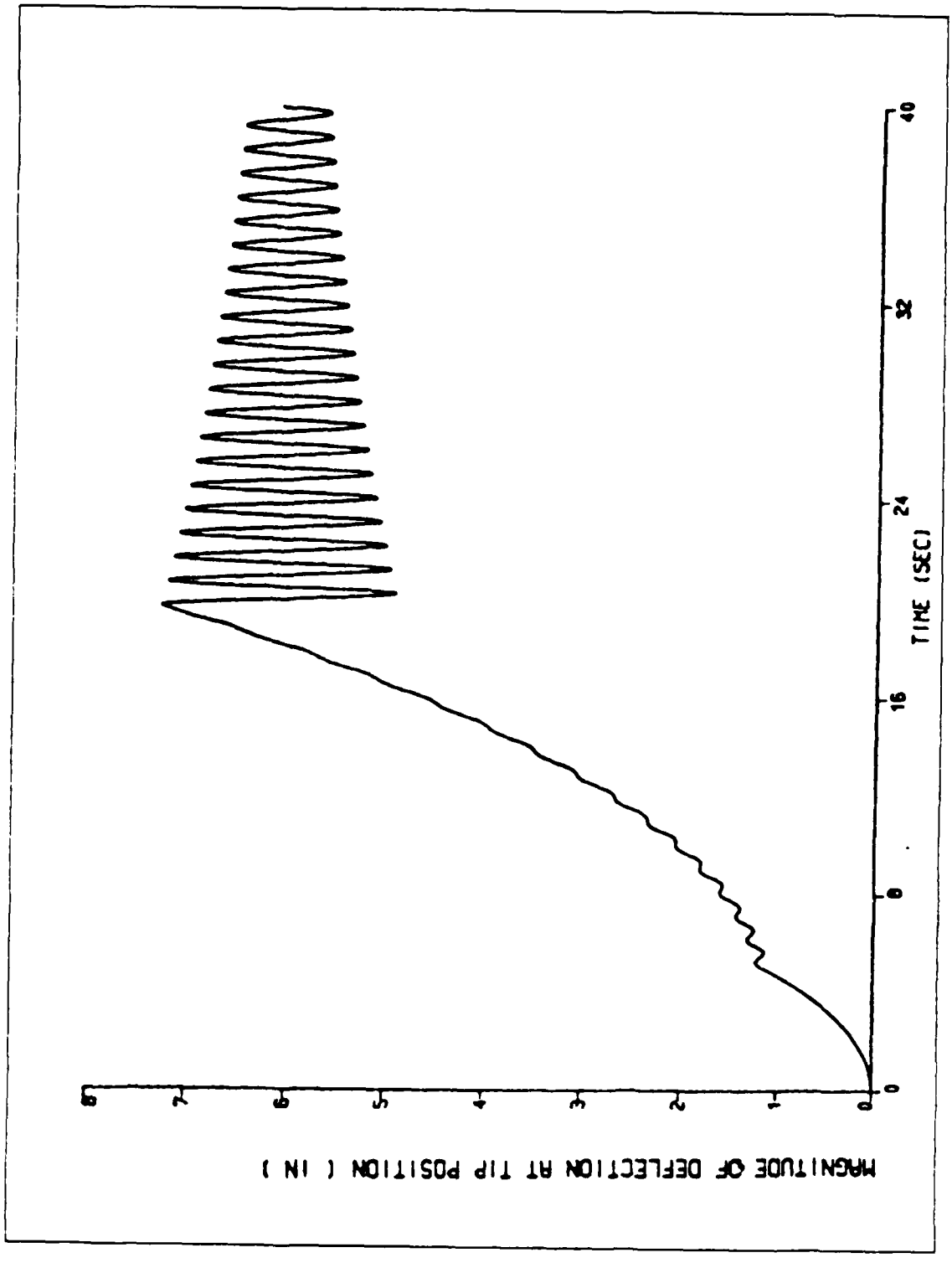

Figure A.12 Slope at tip position vs. time.

APPENDIX B

DETAILED DERIVATION OF LAGRANGE'S EQUATIONS FOR THREE DIMENSIONAL MOTION.

Apply Lagrange's equations 2.7 and 2.8 into equations 2.28 and 2.25 then

$$\frac{\partial T}{\partial \theta} = 0$$

$$\begin{aligned}\frac{\partial T}{\partial \dot{\theta}} = \dot{\theta} [& \sum_i q_i^2(t)\, M_i + \int_0^{\ell} R_x^2(x)\, dm + M\, R_x(\ell) \\ & + 2 \sum_i q_i(t) \{ \int_0^{\ell} R_x(x)\, \varphi_i^x(x)\, dm + M\, R_x(\ell)\, \varphi_i^x(\ell) \} \\ & - 2 \{ \int_0^{\ell} (\sum_i \varphi_i^z(x)\, q_i(t))^2 + M (\sum_i \varphi_i^z(\ell)\, q_i(t))^2 + I_{r_{zz}}] \\ & + \sum_i \sum_j \dot{q}_i(t)\, q_j(t) \{ \int_0^{\ell} \varphi_i^x(x)\, \varphi_j^y(x)\, dm + M\, \varphi_i^x(\ell)\, \varphi_j^y(\ell) \} \\ & + \sum_i \dot{q}_i(t) \{ \int_0^{\ell} R_x(x)\, \varphi_i^y(x)\, dm + M\, R_x(\ell)\, \varphi_i^y(\ell) \}\end{aligned}$$

$$\begin{aligned}\frac{d}{dt} [\frac{\partial T}{\partial \dot{\theta}}] = \ddot{\theta} [& \sum_i q_i^2(t)\, M_i + \int_0^{\ell} R_x^2(x)\, dm + M\, R_x^2(\ell) \\ & + 2 \sum_i q_i(t) \{ \int_0^{\ell} R_x(x)\, \varphi_i^x(x)\, dm + M\, R_x(\ell)\, \varphi_i^x(\ell) \} \\ & - 2 \{ \int_0^{\ell} (\sum_i \varphi_i^z(x)\, q_i(t))^2 + M (\sum_i \varphi_i^z(\ell)\, q_i(t))^2 + I_{r_{zz}}] \\ & + 2 \dot{\theta} \sum_i \dot{q}_i(t) [q_i(t)\, M_i + \int_0^{\ell} R_x(x)\, \varphi_i^x(x)\, dm + M\, R_x(\ell)\, \varphi_i^x(\ell) \} \\ & - 2 \sum_i q_j(t) \{ \int_0^{\ell} \varphi_i^z(x)\, \varphi_j^z(x)\, dm - M\, \varphi_i^z(\ell)\, \varphi_j^z(\ell) \}] \\ & - \sum_i \ddot{q}_i(t) [\sum q_j(t) \{ \int_0^{\ell} \varphi_i^x(x)\ \ \varphi_j^y(x)\, dm + M\, \varphi_i^x(\ell)\, \varphi_j^x(\ell)\end{aligned}$$

$$- \int_0^{\ell} \varphi_i^{y}(x)\, \varphi_j^{x}(x)\, dm - M\, \varphi_i^{y}(\ell)\, \varphi_j^{x}(\ell) \}$$

$$- \int_0^{\ell} R_x(x)\, \varphi_i^{y}(x)\, dm - M\, R_x(\ell)\, \varphi_i^{y}(\ell)]$$

$$\frac{\partial T}{\partial q_h} = \dot{\theta}^2 [\, q_i(t)\, M_i + \int_0^{\ell} R_x(x)\, \varphi_i^{x}(x)\, dm + M R_x(\ell)\, \varphi_i^{x}(\ell)$$

$$- 2 \sum_i q_i(t) \{ \int_0^{\ell} \varphi_i^{z}(x)\, \varphi_h^{x}(x)\, dm + M\, \varphi_i^{z}(\ell)\, \varphi_h^{z}(\ell) \}]$$

$$+ \dot{\theta} \sum_i \dot{q}_j(t) [\int_0^{\ell} \varphi_h^{x}(x)\, \varphi_j^{y}(x)\, dm + M\, \varphi_h^{x}(\ell)\, \varphi_j^{y}(\ell)$$

$$- \int_0^{\ell} \varphi_i^{y}(x)\, \varphi_j^{x}(x)\, dm - M\, \varphi_i^{y}(\ell)\, \varphi_j^{x}(\ell)]$$

$$\frac{\partial T}{\partial \dot{q}_h} = \dot{q}_h(t)\, M_h$$

$$+ \dot{\theta} \sum_i \dot{q}_i(t) [\int_0^{\ell} \varphi_i^{x}(x)\, \varphi_h^{y}(x)\, dm + M\, \varphi_i^{x}(\ell)\, \varphi_h^{y}(\ell)$$

$$- \int_0^{\ell} \varphi_i^{y}(x)\, \varphi_h^{x}(x)\, dm - M\, \varphi_i^{y}(\ell)\, \varphi_h^{x}(\ell)]$$

$$+ \dot{\theta} [\int_0^{\ell} R_x(x)\, \varphi_h^{y}(x)\, dm + M\, R_x(\ell)\, \varphi_h^{y}(\ell)]$$

$$\frac{d}{dt} [\frac{\partial T}{\partial \dot{q}_h}] = \ddot{q}_h(t)\, M_h$$

$$+ \ddot{\theta} [\sum_i q_i(t) \{ \int_0^{\ell} \varphi_i^{x}(x)\, \varphi_h^{y}(x)\, dm + M\, \varphi_i^{x}(\ell)\, \varphi_h^{y}(\ell)$$

$$- \int_0^{\ell} \varphi_i^{y}(x)\, \varphi_h^{x}(x)\, dm - M\, \varphi_i^{y}(\ell)\, \varphi_h^{x}(\ell) \}$$

$$+ \int_0^{\ell} R_x(x)\, \varphi_h^{y}(x)\, dm + M\, R_x(\ell)\, \varphi_h^{y}(\ell)]$$

$$+ \dot{\theta} \sum_i \dot{q}_i(t) [\int_0^{\ell} \varphi_i^{x}(x)\, \varphi_h^{y}(x)\, dm + M\, \varphi_i^{x}(\ell)\, \varphi_h^{y}(\ell)$$

$$- \int_0^{\ell} \varphi_i^{y}(x)\, \varphi_h^{x}(x)\, dm - M\, \varphi_i^{y}(\ell)\, \varphi_h^{x}(\ell)]$$

$$\frac{\partial U}{\partial \theta} = \frac{\partial U}{\partial \dot{\theta}} = \frac{d}{dt} [\frac{\partial U}{\partial \dot{\theta}}] = 0$$

$$\frac{\partial U}{\partial q_h} = \omega^2_h\, M_h\, q_h(t)$$

$$\frac{\partial U}{\partial \dot{q}_h} = \frac{d}{dt} [\frac{\partial U}{\partial \dot{q}_h}] = 0$$

Now plug all these quantities in equations 2.7 and 2.8

APPENDIX C

NASTRAN PROGRAM FOR DYNAMIC (MODAL) ANALYSIS

1. DYNAMIC ANALYSIS IN PLANAR MOTION

```
$
$ Double link flexible boom for dynamic analysis( 14 grid points )
$  in 2 dimension space  with tip mass (37.5 lb. ) link1:14 ft,link2:12 ft
$    Material:aluminum alloy
$
$**********************************
$
$     EXECUTIVE CONTROL DECK
$
$**********************************
$
id kang,dynamics SN-ROSS
sol 3
time 10
diag 8,13
cend
$
$**********************************
$
$        CASE CONTROL DECK
$
$**********************************
$
title = Modal analysis of double link flexible
title = boom in planar motion(Aluminum alloy)
echo = both
method = 120
spc = 101
disp = all
output(plot)
plotter nastran
axes z,x,y
cscale = 1.8
view 0.,0.,0.
paper size 14.0 by 10.0
set 1 = all
find scale, origin 1,set 1
plot modal deformation 0,set 1,origin 1,shape
maximum deformation 5
begin bulk
$
$**********************************
$
$        BULK DATA DECK
$
$**********************************
$
$ Define new coordinate system for convinience
$
$cord2c,1,,0.,0.,0.,0.,0.,1., + 23
$+ 23,1.,0.,,0
$-----------------
$ grid(node) data
$-----------------
grid,1,,0.,0.,0.
=,*(1),=,*(24.),= =
```

```
=6
grid,9,,182.1068,19.4164,0.
=,*(1),=,*(14.1068),*19.4164,=
=4
$----------------
$ element data
$----------------
cbar,21,102,1,2,0.,0.,1.
=,*(1),=,*(1),*(1),=,=
=11
$ Change these boom properties when material
$ changes AL. to COMPOSITE
$
$ --- DATA FOR ALUMINUM ALLOY ---
$
pbar,102,103,1.2101,1.2447,1.2447,2.4894
mat1,103,1.01+7,3.7+6,,2.5362-4
conm2,103,14,,9.7176-2
spc1,111,123456,1
spc1,112,345,2,thru,14
spcadd,101,111,112
eigr,120,mgiv,,,,7
$param,autospc,yes
$
$ --- DATA FOR COMPOSITE ---
$
pbar,102,103,2.0168,1.9451,1.9451,3.8902
mat1,103,1.01+7,,.25,2.5362-4
conm2,103,14,,9.7176-2
spc1,111,123456,1
spc1,112,345,2,thru,14
spcadd,101,111,112
eigr,120,mgiv,,,,7
$param,autospc,yes
enddata
```

2. DYNAMIC ANALYSIS IN 3 DIMENSION SPACE

```
$
$ Double link flexible boom for dynamic analysis( 14 grid points )
$  in 3 dimension space with tip mass (37.5 lb. )
$  link1:14 ft,link2:12 ft
$  angle between L1 and x-axes is 70,L1 and L2 is 126 degree
$  Material: Aluminum alloy
$
$**********************************
$
$     EXECUTIVE CONTROL DECK
$
$**********************************
$
id kang,dynamics Snross
sol 3
time 10
diag 8,13
cend
$**********************************
$
$       CASE CONTROL DECK
$
$**********************************
$
title = 2 link flexible boom in 3 dimension(Al,COM)
echo = both
method = 120
spc = 101
disp = all
output(plot)
plotter nastran
cscale = 1.8
view 0.,0.,0.
paper size 14.0 by 10.0
set 1 = all
find scale, origin 1,set 1
maximum deformation 10
axes my,x,z
plot modal deformation 0,set 1,origin 1,shape
axes x,y,z
plot modal deformation 0,set 1,origin 1,shape
begin bulk
$**********************************
$
$       BULK DATA DECK
$
$**********************************
$
$ Define new coordinate system for convinience
$
$cord2c,1,,0.,0.,0.,0.,0.,1.,+23
$+23,.5,0.,.5,.67
$
$-----------------------
$   grid(node) data
$-----------------------
$
grid,1,,0.,0.,0.
=,*(1),=,*(8.2085),=,*22.5526
=6
grid,9,,44.0388,0.,177.7653
=,*(1),=,*(-13.4206),=,*19.8969
=4
$
$-----------------------
$   element data
```

```
$----------------------
$
cbar,21,102,1,2,0.,0.,1.
=,*(1),=,*(1),*(1),=,=
=,11
$
$ Change following datas when the material
$ changes from AL. to COM.
$
$ --- DATA FOR ALUMINUM ALLOY ---
$
pbar,102,103,1.2101,1.2447,1.2447,2.4894
mat1,103,1.01+7,3.7+6,,2.5362-4
conm2,103,14,,9.7176-2
spc1,101,123456,1
$spc1,112,345,2,thru,13
$spcadd,101,111,112
eigr,120,mgiv,,,,7
$param,autospc,yes
$
$ --- DATA FOR COMPOSITE ---
$
pbar,102,103,1.2101,1.2447,1.2447,2.4894
mat1,103,1.01+7,3.7+6,,2.5362-4
conm2,103,14,,9.7176-2
spc1,101,123456,1
$spc1,112,345,2,thru,13
$spcadd,101,111,112
eigr,120,mgiv,,,,7
$param,autospc,yes
enddata
```

APPENDIX D
DSL PROGRAM SOLVING THE DYNAMIC EQUATIONS OF MOTION

1. PROGRAM OF DOUBLE LINK FLEXIBLE BOOM IN PLANAR MOTION

```
*   This program solves the dynamics of a dobule link flexible boom system
*   in planar motion. The applied torque ( τ ) was changed to see the effects
*   of the torque and also damping coefficient ( ζ ) was varied 0.0 to 0.5 %.
*   This program automatically calculates the slope and deflection of the tip
*   position in each direction ( local x, y, z ) from simulation results.
*
*-------------------------------------------------------------------------
*  THE FOLLOWING PARAMETERS ARE DEFINED
*-------------------------------------------------------------------------
*
*     N ;    number of discritized boom element
*     FL1 ;  length of lower boom
*     FL2 ;  length of uppper boom
*     TM ;   tip mass
*     RHO ;  mass per unit length
*     DX ;   differential length between each grid point
*     RX ;   local x distance from origin
*     TAO ;  applied torque
*     OMG1 ; 1st mode natural frequency
*     OMG2 ; 2nd mode natural frequency
*     PX1 ;  1st mode shape-displacement in local x direction
*     PY1 ;  1st mode shape-displacement in local y direction
*     PZ1 ;  1st mode shape-displacement in local z direction
*     PX2 ;  2nd mode shape-displacement in local x direction
*     PY2 ;  2nd mode shape-displacement in local y direction
*     PZ2 ;  2nd mode shape-displacement in local z direction
*     ALP ;  angle between upper boom and local x-axes
*     RX1L ; 1st mode shape-rotation at the tip position w.r.t x-axes
```

```
*     RZ1L ; 1st mode shape-rotation at the tip position w.r.t z-axes
*     RY2L ; 2nd mode shape-rotation at the tip position w.r.t y-axes
*     RZ2L ; 2nd mode shape-rotation at the tip position
*     TH ;  angular displacement
*     THD ; angular velocity
*     Q1 ;  1st mode generalized coordinatest
*     Q1D ; time derivative of 1st mode generalized coordinates
*     Q2 ;  2nd mode generalized coordinates
*     Q2D ; time derivative of 2nd mode generalized coordinates
*     ZETA ; damping coefficient
*     RIRZZ ;mass moment of inertia for R.F electronic box
*     RIBZZ ;mass moment of inertia for boom and tip n mass
*     C1 ;  starting up time coefficient
*     C2 ;  magnitude of applied torque
*     C3 ;  required time to reach required R.P.M
*
*********************************************************************************
*
*  SIMULATIOMS OF DOUBLE LINK FLEXIBLE BOOM IN PLANAR MOTION
*
*********************************************************************************
*
TITLE   SOLUTION OF SIMULTANEOUS DIFFERENTIAL EQUATIONS
TITLE   FOR DOUBLE LINK FLEXIBLE BOOM IN PLANAR MOTION
*
*
*
FIXED IER, IPVT, N, I
CONST FL1 = 168.,FL2 = 144.,RHO = 3.0690E-04,N = 13,DELT = .04
PARAM C1 = 40.  ,C2 = 1000. ,C3 = 19.65
*
INITIAL
*
        TM = 9.7176E-02
        ALP =  54.
        RIRZZ = 31.0559
        RZ1L = 1.527773E-02
        RZ2L = -3.149482E-02
*-------------------------------------------------------------------------------
*    BY CHANGING THE ZETA VALUE THE DAMPING FORCE
*    WILL BE CHANGED
*-------------------------------------------------------------------------------
*    ZETA = 0.
*    ZETA = 0.002
        ZETA = 0.005
*
*-------------------------------------------------------------------------------
*    DIMENSION SIZE SHOULD BE EXPRESSED BY NUMBER
*    INSTEAD OF CHARACTER
*-------------------------------------------------------------------------------
*
D    DIMENSION RX(13),RY(13),PX1(13),PX2(13),PY1(13),PY2(13),A(3,3)
ARRAY IPVT(3),B(3)
```

```
*
*-----------------------------------------------------------------------
* REMOVE THE ASTRICKS IN DATA STATEMENT FOR
* EXECUTION OF EACH MATERIAL
*-----------------------------------------------------------------------
D     DATA RX 24.,48.,72.,96.,120.,144.,168.,182.1068,196.214,210.321,
D    #224.428,238.535,252.642
D     DATA RY 7*0.0,19.4164,38.8328,58.2492,77.6656,97.082,116.498/
*
* = = = = = DATA FOR ALUMINUM ALLOY = = = = = =
*
D     DATA PX1/          -4.922269E-06,
D    #                  -9.844536E-06,
D    #                  -1.476680E-05,
D    #                  -1.968907E-05,
D    #                  -2.461132E-05,
D    #                  -2.953358E-05,
D    #                  -3.445583E-05,
D    #                  -2.457687E-01,
D    #                  -5.087806E-01,
D    #                  -7.853463E-01,
D    #          -1.071851E+00,-1.364817E+00,-1.660928E+00/
D     DATA PY1/                          2.800838E-02,
D    #                                 1.089855E-01,
D    #                                 2.383627E-01,
D    #                                 4.115835E-01,
D    #                                 6.241170E-01,
D    #                                 8.714750E-01,
D    #                                 1.149234E+00,
D    #                                 1.327774E+00,
D    #                                 1.518872E+00,
D    #                                 1.719815E+00,
D    #                  1.927978E+00,2.140836E+00,2.355983E+00/

D     DATA PX2/           1.657409E-04,
D    #                   3.314810E-04,
D    #                   4.972196E-04,
D    #                   6.629559E-04,
D    #                   8.286890E-04,
D    #                   9.944183E-04,
D    #                   1.160143E-03,
D    #                   4.385572E-02,
D    #                   2.710247E-01,
D    #                   6.487206E-01,
D    #                1.140457E+00,1.708180E+00,2.313523E+00/

D     DATA PY2/                          1.425431E-01,
D    #                                 5.101371E-01,
D    #                                 1.013169E+00,
D    #                                 1.563418E+00,
D    #                                 2.075334E+00,
D    #                                 2.467438E+00,
D    #                                 2.663624E+00,
D    #                                 2.632837E+00,
D    #                                 2.468005E+00,
D    #                                 2.193798E+00,
D    #                  1.836722E+00,1.424425E+00,9.847735E-01/

D     DATA OMG1/3.568816E+00/,OMG2/1.796733E+01/
*
* = = = = = DATA FOR COMPOSITE MATERIAL = = = = =
*

*     DATA PX1/-4.615325E-06,
*    #         -9.230651E-06,
*    #         -1.384597E-05,
```

```
*     #              -1.846129E-05,
*     #              -2.307661E-05,
*     #              -2.769193E-05,
*     #              -3.230723E-05,
*     #              -2.457675E-01,
*     #              -5.087805E-01,
*     #              -7.853472E-01,
*     #    -1.071853E+00,-1.364820E+00,-1.660932E+00/

*     DATA PY1/               2.800845E-02
*     #                      1.089857E-01
*     #                      2.383633E-01
*     #                      4.115847E-01
*     #                      6.241187E-01
*     #                      8.714775E-01
*     #                      1.149238E+00
*     #                      1.327778E+00
*     #                      1.518877E+00
*     #                      1.719820E+00
*     #             1.927984E+00,2.140842E+00,2.355990E+00/

*     DATA PX2/ 1.554086E-04,
*     #              3.108165E-04,
*     #              4.662230E-04,
*     #              6.216275E-04,
*     #              7.770293E-04,
*     #              9.324276E-04,
*     #              1.087822E-03,
*     #              4.377849E-02,
*     #              2.709504E-01,
*     #              6.486561E-01,
*     #    1.140408E+00,1.708149E+00,2.313514E+00/

*     DATA PY2/               1.425488E-01
*     #                      5.101575E-01
*     #                      1.013209E+00
*     #                      1.563480E+00
*     #                      2.075416E+00
*     #                      2.467535E+00
*     #                      2.663728E+00
*     #                      2.632930E+00
*     #                      2.468082E+00
*     #                      2.193855E+00
*     #             1.836756E+00,1.424434E+00,9.847565E-01/

D     DATA OMG1 4.461328E+00/,OMG2 2.246115E+01

*-----------------------------------------------------------------------
*   THESE CALL STATEMENTS CALCULATE ALL CONSTANT TERMS
*   AND COEFFICIENT INVOLVED IN THIS PROGRAM.
*-----------------------------------------------------------------------
*
      CALL FIBZZ(RHO,FL1,FL2,ALP,TM,RIBZZ)
      CALL ONE(RHO,RX,RY,PX1,PY1,DX,N,ST1)
      CALL TWO(RHO,RX,RY,PX2,PY2,DX,N,ST2)
      CALL THREE(N,RX,RY,PX1,PY1,PX2,PY2,TM,ST3,ST4,ST7,ST8,ST11, ...
                 ST12,ST16,ST18)
      CALL FOUR(N,RHO,DX,RX,RY,PX1,PY1,PX2,PY2,ST5,ST9)
      CALL FIVE(N,RHO,DX,RX,RY,PX1,PY1,PX2,PY2,ST6,ST10)
      CALL SIX(N,RHO,DX,TM,RX,RY,PX1,PY1,PX2,PY2,ST19,ST20,ST21,ST22)
*
DERIVATIVE
NOSORT
      T1 = 5.
      TAO1 = C1_*TIME**2
      TAO2 = C2*(1.-    STEP(C3_))
      TAO = SWITCH(TIME,LE,T1,TAO1,TAO2)
      A(1,1) = RIBZZ + RIRZZ + X2**2 + X3**2 + (ST1 + ST3)*X2 + (ST2 + ST4)*X3
      A(1,2) = ST5 + ST7 + (ST6 + ST8)*X3
```

```
            A(1,3) = ST9 + ST11 + (ST10 + ST12)*X2
            A(2,1) = ST5 + ST7 + (ST6 + ST8)*X3
            A(2,2) = 1.0
            A(2,3) = 0.0
            A(3,1) = ST9 + ST11 + (ST10 + ST12)*X2
            A(3,2) = 0.0
            A(3,3) = 1.0
            B(1) = TAO-X1D*(X2D*(2.*X2 + ST1 + ST3) + X3D*(2.*X3 + ST2 + ST4))
            B(2) = X1D**2*(X2 + ST20 + ST16)-2.*X1D*(X3D*(ST19 + ST8))-OMG1**2*X2 ...
                  -2.*ZETA*OMG1*X2D
            B(3) = X1D**2*(X3 + ST22 + ST18)-2.*X1D*(X2D*(ST21 + ST12))-OMG2**2*X3 ...
                  -2.*ZETA*OMG2*X3D
            CALL DGEFA (A, 3, 3, IPVT, IER)
            IF (IER.NE.0) GO TO 112
            CALL DGESL (A, 3, 3, IPVT, B, 0)
            X1D = INTGRL(0.,B(1))
            X2D = INTGRL(0.,B(2))
            X3D = INTGRL(0.,B(3))
            X1 = INTGRL(0.,X1D)
            X2 = INTGRL(0.,X2D)
            X3 = INTGRL(0.,X3D)
            TH = X1
            THD = X1D
            Q1 = X2
            Q1D = X2D
            Q2 = X3
            Q2D = X3D
            WX = PX1(N)*Q1 + PX2(N)*Q2
            WY = PY1(N)*Q1 + PY2(N)*Q2
            WXY = WX**2 + WY**2
            W = SQRT(WXY)
            SLOP = (RZ1L*Q1 + RZ2L*Q2)*57.2957
*     WRITE(6,120)RIBZZ,ST1,ST2,ST3,ST4,ST7,ST8,ST11,ST12,ST16,ST18, ...
*           ST5,ST9,ST10,ST19,ST20,ST21,ST22
*120  FORMAT(2X,18(F12.5,2X))
            RETURN
  112  WRITE(6,114) TIME,IER
  114  FORMAT(2X,'0 IER = ',I7)
*     CALL ENDJOB
*     WRITE(6,116)(Q(IF1),IF1 = 1,N)
*116  FORMAT(2X,3F8.3,2X)
PRINT TH,THD, Q1,Q2,WX,WY,W,SLOP
CONTRL FINTIM = 40.,DELPRT = .20
SAVE  0.025,TH,THD,Q1,Q2,WX,WY,W,SLOP,TAO
END
PARAM C1 = 80.  ,C2 = 2000. ,C3 = 11.50
END
PARAM C1 = 160. ,C2 = 4000. ,C3 = 7.4
GRAPH (G10,NI = 7,LO = -800.,DE = TEK618,SC = 800.) TIME(NI = 5,LE = 10.,UN =  ...
            'SEC'),TAO(UN = 'LBS-IN',RU = 1,LI = 1) ...
            ,TAO(PO = 0.,AX = OMIT,RU = 2,LI = 2) ...
            ,TAO(PO = 0.,AX = OMIT,RU = 3,LI = 3)
GRAPH (G1,NI = 7,LO = 0.,DE = TEK618,SC = 8. ) TIME(NI = 5,LE = 10.,UN = 'SEC') ...
            ,TH(UN = 'RAD',RU = 1,LI = 1) ...
            ,TH(PO = 0.,AX = OMIT,RU = 2,LI = 2) ...
            ,TH(PO = 0.,AX = OMIT,RU = 3,LI = 3)
GRAPH (G2,NI = 7,LO = 0.,DE = TEK618,SC = .3 ) TIME(NI = 5,LE = 10.,UN = 'SEC') ...
            ,THD(UN = 'RAD SEC',RU = 1,LI = 1) ...
            ,THD(PO = 0.,AX = OMIT,RU = 2,LI = 2) ...
            ,THD(PO = 0.,AX = OMIT,RU = 3,LI = 3)
GRAPH (G3,NI = 8,LO = -8.0   ,SC = 1.0 ,        DE = TEK618) ...
            TIME(NI = 5,LE = 10.,UN = 'SEC'),Q1(UN = 'IN',RU = 1,LI = 1), ...
            Q1(PO = 0.,AX = OMIT,RU = 2,LI = 2), ...
            Q1(PO = 0.,AX = OMIT,RU = 3,LI = 3)
GRAPH (G4,NI = 8,LO =  0.0   ,SC = .075         ,DE = TEK618) ...
            TIME(NI = 5,LE = 10.,UN = 'SEC'),Q2(UN = 'IN',RU = 1,LI = 1), ...
            Q2(PO = 0.,AX = OMIT,RU = 2,LI = 2), ...
            Q2(PO = 0.,AX = OMIT,RU = 3,LI = 3)
*GRAPH (G4,NI = 8,LO = -1.2E-3,SC = 3.0E-04,       DE = TEK618) ...
```

```
*     TIME(NI=9,UN='SEC'),Q3(UN='IN'          )
GRAPH (G5,DE=TEK618,LO=-0.0,SC=1.5   ,NI=8  ) TIME(NI=5,UN='SEC' ...
        ,LE=10.),WX(UN='IN',RU=1,LI=1) ...
        ,WX(PO=0.,AX=OMIT,RU=2,LI=2) ...
        ,WX(PO=0.,AX=OMIT,RU=3,LI=3)
GRAPH (G6,DE=TEK618,LO=-16.,SC=2.0   ,NI=8   ) TIME(NI=5,UN='SEC' ...
        ,LE=10.),WY(UN='IN',RU=1,LI=1) ...
        ,WY(PO=0.,AX=OMIT,RU=2,LI=2) ...
        ,WY(PO=0.,AX=OMIT,RU=3,LI=3)
*GRAPH (G7,DE=TEK618,LO=-.5,SC=.13     ) TIME(NI=5,UN='SEC',LE=10.) ...
*       UN='IN SEC',NI=8)
GRAPH (G8,DE=TEK618,LO=0.0,SC=2.5,NI=8       )TIME(NI=5,UN='SEC' ...
        ,LE=10.),W(UN='IN',RU=1,LI=1) ...
        ,W(PO=0.,AX=OMIT,RU=2,LI=2) ...
        ,W(PO=0.,AX=OMIT,RU=3,LI=3)
GRAPH (G9,DE=TEK618,LO=-6.4,SC=.8,NI=8       ) TIME(NI=5,UN='SEC' ...
        ,LE=10.),SLOP(UN='DEG',RU=1,LI=1) ...
        ,SLOP(PO=0.,AX=OMIT,RU=2,LI=2) ...
        ,SLOP(PO=0.,AX=OMIT,RU=3,LI=3)
LABEL (G10) APPLIED TORQUE
LABEL (G1) ANGULAR DISPLACEMENT
LABEL (G2) ANGULAR VELOCITY
LABEL (G3) GENERALIZED DISPLACEMENT Q1
LABEL (G4) GENERALIZED DISPLACEMENT Q2
LABEL (G5) DISPLACEMENT IN EXTENSION
LABEL (G6) DISPLACEMENT IN TRANSLATION
*LABEL (G7) TIME DERIVATIVE OF Q3
LABEL (G8) MAGNITUDE OF DEFLECTION AT TIP POSITION
LABEL (G9) SLOPE AT THE TIP POSITION
END
STOP
FORTRAN
C
C*****************************************************************
      SUBROUTINE FIBZZ(RHO,FL1,FL2,ALP,TM,RIBZZ)
C*****************************************************************
C
      IMPLICIT REAL*8(A-H,O-Z)
          PI=ARCOS(-1.0)
          ANG=ALP*PI/180.
          D1SQ=(FL1+(FL2/2.)*COS(ANG))**2+((FL2/2.)*SIN(ANG))**2
          D2SQ=(FL1+FL2*COS(ANG))**2+(FL2*SIN(ANG))**2
          BM1=RHO*FL1
          BM2=RHO*FL2
          RIBZZ=BM1*FL1**2/3.+BM2*FL2**2/12.+BM2*D1SQ+TM*D2SQ
          WRITE(6,111)RIBZZ
  111   FORMAT(2X,'RIBZZ=',F12.5)
      PRINT*,'*****************************************************'
      RETURN
      END
C
C*****************************************************************
      SUBROUTINE ONE(RHO,RX,RY,PX1,PY1,DX,N,ST1)
C*****************************************************************
C
      IMPLICIT REAL*8(A-H,O-Z)
      DIMENSION RX(N),RY(N),PX1(N),PY1(N)
      SONE1=0.0
      SONE2=0.0
      DO 10 I=1,N-1
          ONE1=RX(I)*PX1(I)
          ONE2=RY(I)*PY1(I)
          SONE1=SONE1+ONE1
          SONE2=SONE2+ONE2
   10 CONTINUE
      T11=(SONE1+RX(N)*PX1(N)/2.)*DX*RHO*2.0
      T12=(SONE2+RY(N)*PY1(N)/2.)*DX*RHO*2.0
      ST1=T11+T12
      WRITE(6,112)ST1
```

```
  112  FORMAT(2X,'ST1 = ',F12.5)
       PRINT*,'*****************************************************'
       RETURN
       END
C
C*****************************************************************
       SUBROUTINE TWO(RHO,RX,RY,PX2,PY2,DX,N,ST2)
C*****************************************************************
C
       IMPLICIT REAL*8(A-H,O-Z)
       DIMENSION RX(N),RY(N),PX2(N),PY2(N)
       STWO1 = 0.0
       STWO2 = 0.0
       DO 20 I = 1,N-1
            TWO1 = RX(I)*PX2(I)
            TWO2 = RY(I)*PY2(I)
            STWO1 = STWO1 + TWO1
            STWO2 = STWO2 + TWO2
   20  CONTINUE
       T21 = (STWO1 + RX(N)*PX2(N)/2.)*DX*RHO*2.0
       T22 = (STWO2 + RY(N)*PY2(N)/2.)*DX*RHO*2.0
       ST2 = T21 + T22
       WRITE(6,113)ST2
  113  FORMAT(2X,'ST2 = ',F12.5)
       PRINT*,'*****************************************************'
       RETURN
       END
C
C*****************************************************************************
       SUBROUTINE THREE(N,RX,RY,PX1,PY1,PX2,PY2,TM,ST3,ST4,ST7,
      1                 ST8,ST11,ST12,ST16,ST18)
C*****************************************************************************
C
       IMPLICIT REAL*8(A-H,O-Z)
       DIMENSION PX1(N),PY1(N),PX2(N),PY2(N),RX(N),RY(N)
       ST3 = (RX(N)*PX1(N) + RY(N)*PY1(N))*TM*2.
       ST4 = (RX(N)*PX2(N) + RY(N)*PY2(N))*TM*2.
       ST7 = (RX(N)*PY1(N)-RY(N)*PX1(N))*TM
       ST8 = (PX2(N)*PY1(N)-PY2(N)*PX1(N))*TM
       ST11 = (RX(N)*PY2(N)-RY(N)*PX2(N))*TM
       ST12 = (PX1(N)*PY2(N)-PY1(N)*PX2(N))*TM
       ST16 = (RX(N)*PX1(N) + RY(N)*PY1(N))*TM
       ST18 = (RX(N)*PX2(N) + RY(N)*PY2(N))*TM
       WRITE(6,114)ST3,ST4,ST7,ST8,ST11,ST12,ST16
  114  FORMAT(2X,'ST3 = ',F12.5,2X,'ST4 = ',F12.5,2X,'ST7 = ',F12.5,2X,'ST8 = ',
      1F12.5,2X,'ST11 = ',F12.5,2X,'ST12 = ',F12.5,2X,'ST16 = ',F12.5,2X)
       WRITE(6,118)ST18
  118  FORMAT(2X,'ST18 = ',F12.5)
       PRINT*,'*****************************************************'
       RETURN
       END
C
C*****************************************************************************
       SUBROUTINE FOUR(N,RHO,DX,RX,RY,PX1,PY1,PX2,PY2,ST5,ST9)
C*****************************************************************************
C
       IMPLICIT REAL*8(A-H,O-Z)
       DIMENSION RX(N),RY(N),PX1(N),PY1(N),PX2(N),PY2(N)
            SFOU1 = 0.0
            SFOU2 = 0.0
            SFOU3 = 0.0
            SFOU4 = 0.0
            DO 30 I = 1,N-1
                 FOU1 = RX(I)*PY1(I)
                 FOU2 = RY(I)*PX1(I)
                 SFOU1 = SFOU1 + FOU1
                 SFOU2 = SFOU2 + FOU2
                 FOU3 = RX(I)*PY2(I)
                 FOU4 = RY(I)*PX2(I)
```

```
                SFOU3 = SFOU3 + FOU3
                SFOU4 = SFOU4 + FOU4
   30   CONTINUE
            T41 = (SFOU1 + RX(N)*PY1(N)/2.)*DX*RHO
            T42 = (SFOU2 + RY(N)*PX1(N)/2.)*DX*RHO
            T43 = (SFOU3 + RX(N)*PY2(N)/2.)*DX*RHO
            T44 = (SFOU4 + RY(N)*PX2(N)/2.)*DX*RHO
            ST5 = T41-T42
            ST9 = T43-T44
            WRITE(6,115)ST5,ST9
  115   FORMAT(2X,'ST5 = ',F12.5,2X,'ST9 = ',F12.5)
        PRINT*,'*****************************************************'
        RETURN
        END
C
C*************************************************************************
        SUBROUTINE FIVE(N,RHO,DX,RX,RY,PX1,PY1,PX2,PY2,ST6,ST10)
C*************************************************************************
C
        IMPLICIT REAL*8(A-H,O-Z)
        DIMENSION RX(N),RY(N),PX2(N),PY2(N),PX1(N),PY1(N)
            SFIV1 = 0.0
            SFIV2 = 0.0
            SFIV3 = 0.0
            SFIV4 = 0.0
            DO 40 I = 1,N-1
                FIV11 = PX2(I)*PY1(I)
                FIV12 = PY2(I)*PX1(I)
                FIV21 = PX1(I)*PY2(I)
                FIV22 = PY1(I)*PX2(I)
                SFIV1 = SFIV1 + FIV11
                SFIV2 = SFIV2 + FIV12
                SFIV3 = SFIV3 + FIV21
                SFIV4 = SFIV4 + FIV22
   40   CONTINUE
            T51 = (SFIV1 + PX2(N)*PY1(N)/2.)*DX*RHO
            T52 = (SFIV2 + PY2(N)*PX1(N)/2.)*DX*RHO
            T53 = (SFIV3 + PX1(N)*PY2(N)/2.)*DX*RHO
            T54 = (SFIV4 + PY1(N)*PX2(N)/2.)*DX*RHO
            ST6 = T51-T52
            ST10 = T53-T54
            WRITE(6,116)ST6,ST10
  116   FORMAT(2X,'ST6 = ',F12.5,2X,'ST10 = ',F12.5)
        PRINT*,'*****************************************************'
        RETURN
        END
C
C*************************************************************************
        SUBROUTINE SIX(N,RHO,DX,TM,RX,RY,PX1,PY1,PX2,PY2,ST19,
       1          ST20,ST21,ST22)
C*************************************************************************
C
        IMPLICIT REAL*8(A-H,O-Z)
        DIMENSION RX(N),RY(N),PX1(N),PY1(N),PX2(N),PY2(N)
            SSIX11 = 0.0
            SSIX12 = 0.0
            SSIX21 = 0.0
            SSIX22 = 0.0
            SSIX31 = 0.0
            SSIX32 = 0.0
            SSIX41 = 0.0
            SSIX42 = 0.0
            DO 50 I = 1,N-1
                SIX11 = PX2(I)*PY1(I)
                SIX12 = PY2(I)*PX1(I)
                SIX21 = RX(I)*PX1(I)
                SIX22 = RY(I)*PY1(I)
                SIX31 = PX1(I)*PY2(I)
                SIX32 = PY1(I)*PX2(I)
```

```
                SIX41 = RX(1)*PX2(1)
                SIX42 = RY(1)*PY2(1)
                SSIX11 = SSIX11 + SIX11
                SSIX12 = SSIX12 + SIX12
                SSIX21 = SSIX21 + SIX21
                SSIX22 = SSIX22 + SIX22
                SSIX31 = SSIX31 + SIX31
                SSIX32 = SSIX32 + SIX32
                SSIX41 = SSIX41 + SIX41
                SSIX42 = SSIX42 + SIX42
 50     CONTINUE
        T61 = (SSIX11 + PX2(N)*PY1(N) 2.)*DX*RHO
        T62 = (SSIX12 + PY2(N)*PX1(N) 2.)*DX*RHO
        T63 = (SSIX21 + RX(N)*PX1(N) 2.)*DX*RHO
        T64 = (SSIX22 + RY(N)*PY1(N) 2.)*DX*RHO
        T65 = (SSIX31 + PX1(N)*PY2(N) 2.)*DX*RHO
        T66 = (SSIX32 + PY1(N)*PX2(N) 2.)*DX*RHO
        T67 = (SSIX41 + RX(N)*PX2(N) 2.)*DX*RHO
        T68 = (SSIX42 + RY(N)*PY2(N) 2.)*DX*RHO
        ST19 = T61-T62
        ST20 = T63 + T64
        ST21 = T65-T66
        ST22 = T67 + T68
        WRITE(6,117)ST19,ST20,ST21,ST22
 117    FORMAT(2X,'ST19 = ',F12.5,2X,'ST20 = ',F12.5,2X,'ST21 = ',F12.5,
       12X,'ST22 = ',F12.5)
        PRINT*,'*************************************************************'
        RETURN
        END
```

2. PROGRAM OF DOUBLE LINK FLEXIBLE BOOM IN 3 DIMENSIONAL MOTION WITH TWO MODES

```
*****************************************************************************
*
*  SIMULATIOMS OF DOUBLE LINK FLEXIBLE BOOM
*  IN 3 DIMENSIONAL MOTION WITH 2 MODES
*
*****************************************************************************
*
TITLE   SOLUTION OF SIMULTANEOUS DIFFERENTIAL EQUATIONS FOR
TITLE   DOUBLE LINK FLEXIBLE BOOM IN 3 DIMENSIONAL MOTION
TITLE           WITH TWO MODES
*
* THIS PROGRAM USES 2 MODE SHAPES FOR 3D AL. AND COM.
*
FIXED IER, IPVT, N, I
CONST DX = 24.,DELT = .04  ,RHO = 3.0690E-04,N = 13
PARAM C1 = .4 ,C2 = 10. ,C3 = 24.65
*INCON X0 =  3.1416
*
INITIAL
*
        TM = 9.7176E-02
        RIBZZ = 145.39
        RIRZZ = 7.764
*
*-------------------------------------------------------------------
*   THE DAMPING FORCE WILL BE CHANGED
*   BY VARYING THE DAMPING COEFFIENT ZETA
*-------------------------------------------------------------------
```

```
          ZETA = 0.0
*     ZETA = 0.002
*     ZETA = 0.005

* THIS VALUES ARE FOR ALUMINUM ALLOY

*     RX1L =  1.381823E-02
*     RZ1L = -6.144172E-03
*     RY2L = 1.527773E-02

* THIS VALUES ARE FOR COMPOSITE MATERIAL

          RX1L = -1.395893E-02
          RZ1L = -5.647870E-03
          RY2L = 1.527779E-02
*
*-------------------------------------------------------------------------------
*     DIMENSION SIZE SHOULD BE EXPRESSED BY NUMBER
*     INSTEAD OF CHARACTER
*-------------------------------------------------------------------------------
*
D     DIMENSION A(3,3),RX(13),PY1(13),PX2(13),PZ2(13)
ARRAY IPVT(3),B(3)
*
*-------------------------------------------------------------------------------
*  REMOVE ASTRICKS IN DATA STATEMENT FOR
*  EXECUTION OF EACH MATERIAL
*-------------------------------------------------------------------------------

D     DATA RX 8.2085,16.417,24.6255,32.834,41.0425,49.251,57.4595,
D    #        44.0388,30.6182,17.1976,3.777,-9.6436,-23.0642/

*     DATA RY 22.5526,45.1052,67.6578,90.2104,112.764,135.316,157.869,
*    #        177.7653,197.662,217.559,237.456,257.353,277.25/
*
* = = = = = DATA FOR ALUMINUM ALLOY = = = = = =
*
*     DATA OMG1/3.384515/,OMG2/3.568821/

*     DATA PY1/-2.320288E-02,
*    #             -8.960620E-02,
*    #             -1.944046E-01,
*    #             -3.328017E-01,
*    #             -5.000194E-01,
*    #             -6.913154E-01,
*    #             -9.019864E-01,
*    #             -1.199010E+00,
*    #             -1.516552E+00,
*    #             -1.850174E+00,
*    #             -2.195575E+00,-2.548629,-2.905414/

*     DATA PX2/2.632094E-02,
*    #                  1.024161E-01,
*    #                  2.239926E-01,
*    #                  3.867686E-01,
*    #                  5.864863E-01,
*    #                  8.189327E-01,
*    #                  1.079948E+00,
*    #                  1.331760E+00,
*    #                  1.601282E+00,
*    #                  1.884697E+00,
*    #                  2.178297E+00,2.478518,2.781967/

*     DATA PZ2/           -9.574829E-03,
*    #                        -3.726606E-02,
*    #                        -8.151116E-02,
*    #                        -1.401517E-01,
*    #                        -2.134380E-01,
*    #                        -2.980351E-01,
```

```
*   #                          -3.930303E-01,
*   #                          -2.231787E-01,
*   #                          -4.138608E-02,
*   #                           1.497749E-01,
*   #              3.478057E-01,5.503027E-01,7.549778E-01
*
*
* = = = = = DATA FOR COMPOSITE MATERIAL = = = = =
*
D    DATA OMG1 4.287485 ,OMG2 4.461334
D    DATA PY1      2.384356E-02,
D   #           9.207751E-02,
D   #           1.997595E-01,
D   #           3.419566E-01,
D   #           5.137555E-01,
D   #           7.102798E-01,
D   #           9.266955E-01,
D   #           1.218125E+00,
D   #           1.530611E+00,
D   #           1.859596E+00,
D   #           2.200665E+00,2.549586,2.902334/

D    DATA PX2/          2.632090E-02 ,
D   #                1.024162E-01,
D   #                2.239929E-01,
D   #                3.867693E-01,
D   #                5.864875E-01,
D   #                8.189344E-01,
D   #                1.079951E+00,
D   #                1.331764E+00,
D   #                1.601286E+00,
D   #                1.884702E+00,
D   #                2.178303E+00,2.478525,2.781976/
D    DATA PZ2/                          -9.575142E-03,
D   #                          -3.726674E-02,
D   #                          -8.151225E-02,
D   #                          -1.407533E-01,
D   #                          -2.134401E-01,
D   #                          -2.980377E-01,
D   #                          -3.930335E-01,
D   #                          -2.231811E-01,
D   #                          -4.138775E-02,
D   #                           1.497741E-01,
D   #              3.478057E-01,5.503036E-01,7.549797E-01/
*
        CALL CONST (N,DX,RHO,TM,RX,PY1,PX2,PZ2,SST1,SST2,SST3,SST4, ...
                    SST5,SST6,SST7,SST8)
*
DERIVATIVE
NOSORT
*   TAO=10.-10.*STEP(6.85)
        T1=5.
        TAO1=C1*TIME**2
        TAO2=C2*(1.-STEP(C3))
        TAO=SWITCH(TIME.LE.T1,TAO1,TAO2)
*   TAO=0.
        A(1,1)=RIBZZ+RIRZZ+X2**2+X3**2*(1.-2.*SST3-2.*SST4) ...
               +2.*X3*(SST1+SST2)
        A(1,2)=SST7+SST8+(SST5+SST6)*X3
        A(1,3)=-X2*(SST5+SST6)
        A(2,1)=A(1,2)
        A(2,2)=1.0
        A(2,3)=0.0
        A(3,1)=A(1,3)
        A(3,2)=0.0
        A(3,3)=1.0
        B(1)=TAO-2.*X1D*(X2D*X2+X3D*(X3+SST1+SST2-2.*X3*(SST3+SST4)))
        B(2)=X1D**2*X2-2.*X1D*X3D*(SST5+SST6)-OMG1**2*X2 ...
             -2.*ZETA*OMG1*X2D
```

```
          B(3) = X1D**2*(X3-SST1-SST2 + 2.*X3*(SST3 + SST4) + 2.*X1D*X2D*(SST5 ...
                + SST6))-OMG2**2*X3-2.*ZETA*OMG2*X3D
          CALL DGEFA (A, 3, 3, IPVT, IER)
          IF (IER.NE.0) GO TO 112
          CALL DGESL (A, 3, 3, IPVT, B, 0)
          X1D = INTGRL(X0,B(1))
          X2D = INTGRL(0.,B(2))
          X3D = INTGRL(0.,B(3))
          X1 = INTGRL(0.,X1D)
          X2 = INTGRL(0.,X2D)
          X3 = INTGRL(0.,X3D)
          TH = X1
          THD = X1D
          Q1 = X2
          Q1D = X2D
          Q2 = X3
          Q2D = X3D
          WX = PX2(N)*Q2
          WY = PY1(N)*Q1
          WZ = PZ2(N)*Q2
          WXYZ = WX**2 + WY**2 + WZ**2
          W = SQRT(WXYZ)
          XSLOP = RX1L*Q1*57.2957
          YSLOP = RY2L*Q2*57.2957
          ZSLOP = RZ1L*Q1*57.2957
*     WRITE(6,120)RIBZZ,ST1,ST2,ST3,ST4,ST7,ST8,ST11,ST12,ST16,ST18, ...
*               ST5,ST9,ST10,ST19,ST20,ST21,ST22
*120  FORMAT(2X,18(F12.5,2X))
          RETURN
  112  WRITE(6,114) TIME,IER
  114  FORMAT(2X,'0 IER = ',I7)
*     CALL ENDJOB
*     WRITE(6,116)(Q(IF1),IF1 = 1,N)
*116  FORMAT(2X,3F8.3,2X)
PRINT TH,THD, Q1,Q2,WX,WY,WZ,W,XSLOP,YSLOP,ZSLOP,TAO
CONTRL FINTIM = 40.,DELPRT = .80
SAVE  0.025,TH,THD,Q1,Q2,TAO,WX,WY,WZ,W,XSLOP,YSLOP,ZSLOP
*END
*PARAM C1 = .8 ,C2 = 20. ,C3 = 14.0
*END
*PARAM C1 = 1.6 ,C2 = 40. ,C3 = 8.7
GRAPH (G11,NI = 7,LO = -8.00,DE = TEK618,SC = 8.0 ) TIME(NI = 5,LE = 10.,UN = ...
          'SEC'),TAO(UN = 'LBS-IN', RU = 1,LI = 1) ...
          ,TAO(AX = OMIT,RU = 2,LI = 2),TAO(AX = OMIT,RU = 3,LI = 3)
GRAPH (G12,NI = 7,LO = 0.,DE = TEK618,SC = 8.0) TIME(NI = 5,LE = 10.,UN = ...
          'SEC'),TH(UN = 'RAD',RU = 1,LI = 1) ...
          ,TH(AX = OMIT,PO = 0. ,RU = 2,LI = 2) ...
          ,TH(AX = OMIT,PO = 0. ,RU = 3,LI = 3)
GRAPH (G1,NI = 7,LO = 0.,DE = TEK618,SC = .3 ) TIME(NI = 5,LE = 10.,UN = ...
          'SEC'),THD(PO = .0, UN = 'RAD SEC',RU = 1,LI = 1) ...
          ,THD(PO = .0,AX = OMIT ,RU = 2,LI = 2) ...
          ,THD(PO = .0,AX = OMIT ,RU = 3,LI = 3)
GRAPH (G2,NI = 8,LO = -.80   ,SC = .200,  DE = TEK618) ...
          TIME(NI = 5,LE = 10.,UN = 'SEC'),Q1(UN = 'IN',RU = 1,LI = 1), ...
          Q1(PO = 0.,  AX = OMIT,RU = 2,LI = 2), ...
          Q1(PO = 0.,  AX = OMIT,RU = 3,LI = 3)
GRAPH (G3,NI = 8,LO = 0.00   ,SC = .500  ,DE = TEK618) ...
          TIME(NI = 5,LE = 10.,UN = 'SEC'),Q2(UN = 'IN',RU = 1,LI = 1) ...
          ,Q2(PO = 0.,  AX = OMIT,RU = 2,LI = 2) ...
          ,Q2(PO = 0.,  AX = OMIT,RU = 3,LI = 3)
GRAPH (G5,DE = TEK618,LO = -0.0,SC = .60 ,NI = 8   ) TIME(NI = 5,UN = 'SEC' ...
          ,LE = 10.),WX(UN = 'IN' ,RU = 1,LI = 1) ...
          ,WX(PO = 0.,AX = OMIT,RU = 2,LI = 2) ...
          ,WX(PO = 0.,AX = OMIT,RU = 3,LI = 3)
GRAPH (G6,DE = TEK618,LO = -0.4,SC = .10 , NI = 8  ) TIME(NI = 5,UN = 'SEC' ...
          ,LE = 10.),WY(UN = 'IN'     ,RU = 1,LI = 1) ...
          ,WY(PO = 0.,AX = OMIT,RU = 2,LI = 2) ...
          ,WY(PO = 0.,AX = OMIT,RU = 3,LI = 3)
GRAPH (G7,DE = TEK618,LO = -.0,SC = .15    ) TIME(NI = 5,UN = 'SEC',LE = 10.) ...
```

```
     ,WZ(UN='IN',NI=8,RU=1,LI=1) ...
     ,WZ(PO=0.,AX=OMIT,RU=2,LI=2) ...
     ,WZ(PO=0.,AX=OMIT,RU=3,LI=3)
GRAPH (G8,DE=TEK618,LO=0.0,SC=.55,NI=8,RU=1,2)TIME(NI=5,UN='SEC' ...
     ,LE=10.),W(UN='IN',RU=1,LI=1) ...
     ,W(PO=0.,AX=OMIT,RU=2,LI=2) ...
     ,W(PO=0.,AX=OMIT,RU=3,LI=3)
GRAPH (G9,DE=TEK618,LO=-.4,SC=.1,NI=8,RU=1  ) TIME(NI=5,UN='SEC' ...
     ,LE=10.),XSLOP(UN='DEG',RU=1,LI=1), ...
     XSLOP(PO=0.,AX=OMIT,RU=2,LI=2) ...
     XSLOP(PO=0.,AX=OMIT,RU=3,LI=3)
GRAPH (G4,DE=TEK618,LO=-1.2,SC=.3,NI=8,RU=1  ) TIME(NI=5,UN='SEC' ...
     ,LE=10.),YSLOP(UN='DEG',RU=1,LI=1), ...
     YSLOP(PO=0.,AX=OMIT,RU=2,LI=2), ...
     YSLOP(PO=0.,AX=OMIT,RU=3,LI=3)
GRAPH (GZ,DE=TEK618,LO=-.40,SC=.1,NI=8,RU=1  ) TIME(NI=5,UN='SEC' ...
     ,LE=10.),ZSLOP(UN='DEG',RU=1,LI=1), ...
     ZSLOP(PO=0.,AX=OMIT,RU=2,LI=2), ...
     ZSLOP(PO=0.,AX=OMIT,RU=3,LI=3)
LABEL (G11) APPLIED TORQUE
LABEL (G12) ANGULAR DISPLACEMENT
LABEL (G1) ANGULAR VELOCITY
LABEL (G2) GENERALIZED DISPLACEMENT Q1
LABEL (G3) GENERALIZED DISPLACEMENT Q2
*LABEL (G4) GENERALIZED DISPLACEMENT Q3
LABEL (G5) DISPLACEMENT IN X-DIRECRION
LABEL (G6) DISPLACEMENT IN Y-DIRECTION
LABEL (G7) DISPLACEMENT IN Z-DIRECTION
LABEL (G8) MAGNITUDE OF DEFLECTION AT TIP POSITION
LABEL (G9) X-SLOPE AT THE TIP POSITION
LABEL (G4) Y-SLOPE AT THE TIP POSITION
LABEL (GZ) Z-SLOPE AT THE TIP POSITION
END
STOP
FORTRAN
C
C*****************************************************************************
      SUBROUTINE CONST (N,DX,RHO,TM,RX,PY1,PX2,PZ2,SST1,SST2,
     1                  SST3,SST4,SST5,SST6,SST7,SST8)
C*****************************************************************************
C
      IMPLICIT REAL*8(A-H,O-Z)
      DIMENSION RX(13),PY1(13),PX2(13),PZ2(13)
      ST1=0.0
      ST3=0.0
      ST5=0.0
      ST7=0.0
      DO 10 I=1,N-1
         T1=RX(I)*PX2(I)
         T3=PZ2(I)**2
         T5=PX2(I)*PY1(I)
         T7=RX(I)*PY1(I)
         ST1=ST1+T1
         ST3=ST3+T3
         ST5=ST5+T5
         ST7=ST7+T7
   10 CONTINUE
      PRINT*,ST1,ST3,ST5,ST7
      SST1=(ST1+RX(N)*PX2(N)/2.0)*RHO*DX
      SST3=(ST3+PZ2(N)**2/2.0)*RHO*DX
      SST5=(ST5+PX2(N)*PY1(N)/2.0)*RHO*DX
      SST7=(ST7+RX(N)*PY1(N)/2.0)*RHO*DX
      SST2=TM*RX(N)*PX2(N)
      SST4=TM*PZ2(N)**2
      SST6=TM*PX2(N)*PY1(N)
      SST8=TM*RX(N)*PY1(N)
      WRITE(6,20)SST1,SST2,SST3,SST4,SST5,SST6,SST7,SST8
   20 FORMAT(2X,8(F12.4,2X))
      RETURN
```

```
END
```

3. PROGRAM OF DOUBLE LINK FLEXIBLE BOOM IN 3 DIMENSIONAL MOTION WITH THREE MODES

```
*************************************************************************
*
*  SIMULATIOMS OF DOUBLE LINK FLEXIBLE BOOM
*  IN 3 DIMENSIONAL MOTION WITH 3 MODES
*
*************************************************************************
*
TITLE   SOLUTION OF SIMULTANEOUS DIFFERENTIAL EQUATIONS FOR
TITLE   DOUBLE LINK FLEXIBLE BOOM IN 3 DIMENSIONAL MOTION
TITLE           WITH THREE MODES
*
* THIS PROGRAM USES 3 MODE SHAPES FOR 3D ALUMINUM ALLOY
*
*
FIXED IER, IPVT, N, I
CONST DX = 24.,DELT = .04  ,RHO = 3.0690E-04,N = 13
PARAM C1 = .4 ,C2 = 10. ,C3 = 24.65
*INCON X0 = 1.5708
*
INITIAL
        TM = 9.7176E-02
        ZETA = 0.0
*   ZETA = 0.002
*   ZETA = 0.005
        RIBZZ = 145.39
        RIRZZ = 7.646
        RX1L =  1.381823E-02
        RZ1L = -6.144172E-03
        RY2L = 1.527773E-02
        RY3L = -3.149467E-02
*
*   DIMENSION SIZE SHOULD BE EXPRESSED BY NUMBER INSTEAD OF CHARACTER
*
D   DIMENSION A(4,4),RX(13),PY1(13),PX2(13),PZ2(13),PX3(13),PZ3(13)
ARRAY IPVT(4),B(4)
*
D   DATA OMG1/3.384515/,OMG2/3.568821/,OMG3/1.796723E+01/

D   DATA PY1     -2.320288E-02,
D  #            -8.960620E-02,
D  #            -1.944046E-01,
D  #            -3.328017E-01,
D  #            -5.000194E-01,
D  #            -6.913154E-01,
D  #            -9.019864E-01,
D  #            -1.199010E+00,
D  #            -1.516552E+00,
D  #            -1.850174E+00,
D  #            -2.195575E+00,-2.548629,-2.905414/

D   DATA PX2          2.632094E-02 ,
D  #                1.024161E-01,
D  #                2.239926E-01,
D  #                3.867686E-01,
D  #                5.864863E-01,
D  #                8.189327E-01,
```

```
D   #                1.079948E+00,
D   #                1.331760E+00,
D   #                1.601282E+00,
D   #                1.884697E+00,
D   #               2.178297E+00,2.478518,2.781967/

D    DATA PZ2/                    -9.574829E-03,
D   #                         -3.726606E-02,
D   #                         -8.151116E-02,
D   #                         -1.401517E-01,
D   #                         -2.134380E-01,
D   #                         -2.980351E-01,
D   #                         -3.930303E-01,
D   #                         -2.231787E-01,
D   #                         -4.138608E-02,
D   #                          1.497749E-01,
D   #                  3.478057E-01,5.503027E-01,7.549778E-01/

D    DATA PX3/      1.338891E-01,
D   #              4.792555E-01,
D   #              9.518909E-01,
D   #              1.468896E-01,
D   #              1.949881E-00,
D   #              2.318285E-00,
D   #              2.502583E-00,
D   #              2.459048E-00,
D   #              2.226467E+00,
D   #              1.839621E+00,
D   #              1.335901E+00,7.543012,1.341246/

D    DATA PZ3/        -4.890816E-02,
D   #                -1.747880E-01,
D   #                -3.469901E-01,
D   #                -5.353417E-01,
D   #                -7.105826E-01,
D   #                -8.448452E-01,
D   #                -9.120993E-01,
D   #                -9.414692E-01,
D   #                -1.098786E+00,
D   #                -1.359918E+00,
D   #                -1.699870E+00,-2.092339,-2.510817/

D    DATA RX/8.2085,16.417,24.6255,32.834,41.0425,49.251,57.4595,
D   #       44.0388,30.6182,17.1976,3.777,-9.6436,-23.0642/
*    DATA RY/ 22.5526,45.1052,67.6578,90.2104,112.764,135.316,157.869,
*   #        177.7653,197.662,217.559,237.456,257.353,277.25/
*
          CALL CONST (N,DX,RHO,TM,RX,PY1,PX2,PZ2,PX3,PZ3, ...
                              SST1,SST11,SST2, ...
                              SST21,SST3,SST31,SST4,SST41,SST5,SST51,SST6,SST61 ...
                             ,SST7,SST8,SST9,SST10,SST12,SST13)
*
DERIVATIVE
NOSORT
*       TAO=10.-10.*STEP(6.85)
          T1=5.
          TAO1=C1*TIME**2
          TAO2=C2*(1.-STEP(C3))
          TAO=SWITCH(TIME.LE.T1,TAO1,TAO2)
*       TAO=0.
          A(1,1)=RIBZZ+RIRZZ+X2**2+X3**2+X4**2+2.*X3*(SST1+SST2) ...
                      +2.*X4*(SST11+SST21)-2.*X3**2*SST3-2.*X4**2*SST31 ...
                     -4.*X3*X4*SST9-2.*(X3**2*SST4+X4**2*SST41) ...
                     -4.*X3*X4*SST10
          A(1,2)=SST7+SST8+(SST5+SST6)*X3+(SST51+SST61)*X4
          A(1,3)=-X2*(SST5+SST6)
          A(1,4)=-X2*(SST51+SST61)
          A(2,1)=A(1,2)
          A(2,2)=1.0
```

```
            A(2,3) = 0.0
            A(2,4) = 0.0
            A(3,1) = A(1,3)
            A(3,2) = 0.0
            A(3,3) = 1.0
            A(3,4) = 0.0
            A(4,1) = A(1,4)
            A(4,2) = 0.
            A(4,3) = 0.
            A(4,4) = 1.
            B(1) = TAO-2.*X1D*X2D*X2-2.*X1D*X3D*(X3 + SST1 + SST2-2.*(...
                  X3*(SST3 + SST4) + X4*(SST9 + SST10)))-2.*X1D*X4D*(X4 + ...
                  SST13 + SST12-2.*(X3*(SST9 + SST10) + X4*(SST31 + SST41)))
            B(2) = X1D**2*X2-2.*X1D*X3D*(SST5 + SST6)-2.*X1D*X4D*(SST51 + SST61) ...
                  -OMG1**2*X2-2.*ZETA*OMG1*X2D
            B(3) = X1D**2*(X3-SST1-SST2 + 2.*X3*(SST3 + SST4) + 2.*X4*(SST9 + SST10) ...
                  ) + 2.*X1D*X2D*(SST5 + SST6)-OMG2**2*X3-2.*ZETA*OMG2*X3D
            B(4) = X1D**2*(X4-SST11-SST21 + 2.*X3*(SST9 + SST10) + 2.*X4*(SST31 + ...
                  SST41)) + 2.*X1D*X2D*(SST51 + SST61)-OMG3**2*X4 ...
                  -2.*ZETA*OMG3*X4D
            CALL DGEFA (A, 4, 4, IPVT, IER)
            IF (IER.NE.0) GO TO 112
            CALL DGESL (A, 4, 4, IPVT, B, 0)
            X1D = INTGRL(0.,B(1))
            X2D = INTGRL(0.,B(2))
            X3D = INTGRL(0.,B(3))
            X4D = INTGRL(0.,B(4))
            X1 = INTGRL(0.,X1D)
            X2 = INTGRL(0.,X2D)
            X3 = INTGRL(0.,X3D)
            X4 = INTGRL(0.,X4D)
            TH = X1
            THD = X1D
            Q1 = X2
            Q1D = X2D
            Q2 = X3
            Q2D = X3D
            Q3 = X4
            Q3D = X4D
            WX = PX2(N)*Q2 + PX3(N)*Q3
            WY = PY1(N)*Q1
            WZ = PZ2(N)*Q2 + PZ3(N)*Q3
            WXYZ = WX**2 + WY**2 + WZ**2
            W = SQRT(WXYZ)
            XSLOP = RX1L*Q1*57.2957
            YSLOP = (RY2L*Q2 + RY3L*Q3)*57.2957
            ZSLOP = RZ1L*Q1*57.2957
*     WRITE(6,120)RIBZZ,ST1,ST2,ST3,ST4,ST7,ST8,ST11,ST12,ST16,ST18, ...
*           ST5,ST9,ST10,ST19,ST20,ST21,ST22
*120  FORMAT(2X,18(F12.5,2X))
            RETURN
  112  WRITE(6,114) TIME,IER
  114  FORMAT(2X,'0 IER = ',I7)
*     CALL ENDJOB
*     WRITE(6,116)(Q(IF1),IF1 = 1,N)
*116  FORMAT(2X,3F8.3,2X)
PRINT TH,THD, Q1,Q2,WX,WY,WZ,W,XSLOP,YSLOP,ZSLOP,TAO
CONTRL FINTIM = 40.,DELPRT = .80
SAVE  0.025,TH,THD,Q1,Q2,TAO,WX,WY,WZ,W,XSLOP,YSLOP,ZSLOP
*END
*PARAM C1 = .8 ,C2 = 20. ,C3 = 14.0
*END
*PARAM C1 = 1.6 ,C2 = 40. ,C3 = 8.7
GRAPH (G11,NI = 7,LO = -8.00,DE = TEK618,SC = 8.0 ) TIME(NI = 5,LE = 10.,UN = ...
          'SEC'),TAO(UN = 'LBS-IN',RU = 1,LI = 1          )
          ,TAO(AX = OMIT,RU = 2,LI = 2),TAO(AX = OMIT,RU = 3,LI = 3)
GRAPH (G12,NI = 7,LO = 0.,DE = TEK618,SC = 8.0) TIME(NI = 5,LE = 10.,UN = ...
          'SEC'),TH(UN = 'RAD',RU = 1,LI = 1) ...
          ,TH(AX = OMIT,PO = 0. ,RU = 2,LI = 2) ...
```

```
        ,TH(AX=OMIT,PO=0. ,RU=3,LI=3)
GRAPH (G1,NI=7,LO=0.,DE=TEK618,SC=.3 ) TIME(NI=5,LE=10.,UN= ...
        'SEC'),THD(PO=.0, N='RAD SEC',RU=1,LI=1) ...
        ,THD(PO=.0,AX=OMIT,RU=2,LI=2) ...
        ,THD(PO=.0,AX=OMIT,RU=3,LI=3)
GRAPH (G2,NI=8,LO=-.16   ,SC=.040, DE=TEK618) ...
        TIME(NI=5,LE=10.,UN='SEC'),Q1(UN='IN',RU=1,LI=1) ...
        ,Q1(PO=0.,  AX=OMIT,RU=2,LI=2) ...
        ,Q1(PO=0.,  AX=OMIT,RU=3,LI=3)
GRAPH (G3,NI=8,LO=0.00   ,SC=.200          ,DE=TEK618) ...
        ,TIME(NI=5,LE=10.,UN='SEC'),Q2(UN='IN',RU=1,LI=1) ...
        ,Q2(PO=0.,  AX=OMIT,RU=2,LI=2) ...
        ,Q2(PO=0.,  AX=OMIT,RU=3,LI=3)
GRAPH (G5,DE=TEK618,LO=-0.0,SC=.60 ,NI=8   ) TIME(NI=5,UN='SEC' ...
        ,LE=10.),WX(UN='IN'      ,RU=1,LI=1) ...
        ,WX(PO=0.,AX=OMIT,RU=2,LI=2) ...
        ,WX(PO=0.,AX=OMIT,RU=3,LI=3)
GRAPH (G6,DE=TEK618,LO=-0.4,SC=.10 ,NI=8   ) TIME(NI=5,UN='SEC' ...
        ,LE=10.),WY(UN='IN'      ,RU=1,LI=1) ...
        ,WY(PO=0.,AX=OMIT,RU=2,LI=2) ...
        ,WY(PO=0.,AX=OMIT,RU=3,LI=3)
GRAPH (G7,DE=TEK618,LO=-.0,SC=.15    ) TIME(NI=5,UN='SEC',LE=10.) ...
        ,WZ(UN='IN',NI=8,RU=1,LI=1) ...
        ,WZ(PO=0.,AX=OMIT,RU=2,LI=2) ...
        ,WZ(PO=0.,AX=OMIT,RU=3,LI=3)
GRAPH (G8,DE=TEK618,LO=0.0,SC=.55,NI=8,RU=1,2)TIME(NI=5,UN='SEC' ...
        ,LE=10.),W(UN='IN',RU=1,LI=1) ...
        ,W(PO=0.,AX=OMIT,RU=2,LI=2) ...
        ,W(PO=0.,AX=OMIT,RU=3,LI=3)
GRAPH (G9,DE=TEK618,LO=-.4,SC=.1,NI=8,RU=1   ) TIME(NI=5,UN='SEC' ...
        ,LE=10.),XSLOP(UN='DEG',RU=1,LI=1), ...
        XSLOP(PO=0.,AX=OMIT,RU=2,LI=2) ...
        ,XSLOP(PO=0.,AX=OMIT,RU=3,LI=3)
GRAPH (G4,DE=TEK618,LO=-1.2,SC=.3,NI=8,RU=1   ) TIME(NI=5,UN='SEC' ...
        ,LE=10.),YSLOP(UN='DEG',RU=1,LI=1), ...
        YSLOP(PO=0.,AX=OMIT,RU=2,LI=2), ...
        YSLOP(PO=0.,AX=OMIT,RU=3,LI=3)
GRAPH (GZ,DE=TEK618,LO=-.40,SC=.1,NI=8,RU=1   ) TIME(NI=5,UN='SEC' ...
        ,LE=10.),ZSLOP(UN='DEG',RU=1,LI=1), ...
        ZSLOP(PO=0.,AX=OMIT,RU=2,LI=2), ...
        ZSLOP(PO=0.,AX=OMIT,RU=3,LI=3)
LABEL (G11) APPLIED TORQUE
LABEL (G12) ANGULAR DISPLACEMENT
LABEL (G1) ANGULAR VELOCITY
LABEL (G2) GENERALIZED DISPLACEMENT Q1
LABEL (G3) GENERALIZED DISPLACEMENT Q2
*LABEL (G4) GENERALIZED DISPLACEMENT Q3
LABEL (G5) DISPLACEMENT IN X-DIRECRION
LABEL (G6) DISPLACEMENT IN Y-DIRECTION
LABEL (G7) DISPLACEMENT IN Z-DIRECTION
LABEL (G8) MAGNITUDE OF DEFLECTION AT TIP POSITION
LABEL (G9) X-SLOPE AT THE TIP POSITION
LABEL (G4) Y-SLOPE AT THE TIP POSITION
LABEL (GZ) Z-SLOPE AT THE TIP POSITION
END
STOP
FORTRAN
      SUBROUTINE CONST (N,DX,RHO,TM,RX,PY1,PX2,PZ2,PX3,PZ3,
     1           SST1,SST11,SST2,
     1           SST21,SST3,SST31,SST4,SST41,SST5,SST51,SST6,SST61,
     1           SST7,SST8,SST9,SST10,SST12,SST13)
      IMPLICIT REAL*8(A-H,O-Z)
      DIMENSION RX(13),PY1(13),PX2(13),PZ2(13),PX3(13),PZ3(13)
      ST1=0.0
      ST11=0.0
      ST3=0.0
      ST31=0.0
      ST5=0.0
      ST51=0.0
```

```
      ST7=0.0
      DO 10 I=1,N-1
         T1=RX(I)*PX2(I)
         T11=RX(I)*PX3(I)
         T3=PZ2(I)**2
         T31=PZ3(I)**2
         T5=PX2(I)*PY1(I)
         T51=PX3(I)*PY1(I)
         T7=RX(I)*PY1(I)
         T9=PZ2(I)*PZ3(I)
         T13=RX(I)
         ST1=ST1+T1
         ST11=ST11+T11
         ST3=ST3+T3
         ST31=ST31+T31
         ST5=ST5+T5
         ST51=ST51+T51
         ST7=ST7+T7
         ST9=ST9+T9
         ST13=ST13+T13
   10 CONTINUE
      SST1=(ST1+RX(N)*PX2(N)/2.0)*RHO*DX
      SST11=(ST11+RX(N)*PX3(N)/2.0)*RHO*DX
      SST3=(ST3+PZ2(N)**2/2.0)*RHO*DX
      SST31=(ST31+PZ3(N)**2/2.0)*RHO*DX
      SST5=(ST5+PX2(N)*PY1(N)/2.0)*RHO*DX
      SST51=(ST51+PX3(N)*PY1(N)/2.0)*RHO*DX
      SST7=(ST7+RX(N)*PY1(N)/2.0)*RHO*DX
      SST9=(ST9+PZ2(N)*PZ3(N)/2.0)*RHO*DX
      SST13=(ST13+RX(N)*PX3(N)/2.0)*RHO*DX
      SST2=TM*RX(N)*PX2(N)
      SST21=TM*RX(N)*PX3(N)
      SST4=TM*PZ2(N)**2
      SST41=TM*PZ3(N)**2
      SST6=TM*PX2(N)*PY1(N)
      SST61=TM*PX3(N)*PY1(N)
      SST8=TM*RX(N)*PY1(N)
C     WRITE(6,20)SST1,SST2,SST3,SST4,SST5,SST6,SST7,SST8
C  20 FORMAT(2X,8(F12.4,2X))
      RETURN
      END
```

LIST OF REFERENCES

1. Defense Meteorological Satellite Program (DMSP), "Technical Operating Report System Engineering Task 0007-11 Preliminary Study for Navy Remote Ocean Sensing System (N-ROSS)", issued July 1985, Prerared by DMSP Program Office, RCA Aerospace and Defense, Astro-Electronics Division, Princeton, New Jersey

2. Defense Meteorological Satellite Program, "Technical Operating Report System Engineering Task 0007-11 Preliminary Study for Navy Remote Ocean Sensing System (N-ROSS)", issued April 1984 Prerared by DMSP Program Office, RCA Aerospace and Defense, Astro-Electronics Division, Princeton, New Jersey

3. "Structural Dynamics and Control of Large Space Srructures - 1982", Proceedings of a workshop held at NASA Langley Research Center Hampton, Virginia January 21-22, 1982

4. Turner, J. D. and Chun, H. M., *Optimal Distributed Control of a Flexible Spacecraft During a Large-Angle Maneuver*, Journal of Guidance, Control and Dynamics Vol. 7, No. 3, May-June, 1983

5. Dr. J. D. turner, Mr. H. m. Chun, Dr. K. Soosaar, "N - ROSS Satellite Dynamic Stability Analysis Final Technical Briefing", 7 March 1986, Cambridge Research A Division of PRA, Inc.

6. D. T. Greenwood, Classical Dynamics, 1977 by Prentice-Hall, Inc., Englewood Cliffs, N.J.

7. W. T. Thomson, Theory of Vibration with Application, 1981 by Prence-Hall, Inc., Englewood Cliffs, N.J., second edition

8. MSC NASTRAN User's Manual Vol. 1 & 2, The Macneal-Schwendler Corporation

9. Dynamic Simulation Language VS Program Description Operation Manual, Program Number:5798-PXJ, IBM Corporation second edition (September 1985)

10. S. W. Tsai & H. T. Hahn, Intoduction To Composite Materials, 1980 Technomic Publishing Co., Inc. Westport Connecticut

INITIAL DISTRIBUTION LIST

		No. Copies
1.	Defense Technical Information Center Cameron Station Alexandria, VA 22304-6145	2
2.	Library, Code 0142 Naval Postgraduate School Monterey, CA 93943-5002	2
3.	Professor Y. S. Shin, Code 69Sg Department of Mechanical Engineering Naval Postgraduate School Monterey, CA 93943	4
4.	Department Chariman Code 69 Department of Mechanical Engineering Naval Postgraduate School Monterey, CA 93943	1
5.	Dr Kilsoo Kim, Code 69Ki Department of Mechanical Engineering Naval Postgraduate School Monterey, CA 93943	2
6.	Professor L. W. Chang, Code 69Ck Department of Mechanical Engineering Naval Postgraduate School Monterey, CA 93943	1
7.	Lt. Scott. Palmer, USN, Code Pdw 106 - 7 Space & Naval Warfare System Command Washington D. C. 20363 - 5100	1
8.	Capt. N. E. Holben, USN, Code Pdw 106 - 7 Space & Naval Warfare System Command Washington D. C. 20363 - 5100	1
9.	Dr. Robert Lindberg Head of Advanced Concepts Section Space System & Technology Division Naval Research Laboratory Washington, D. C. 30275	1
10.	Air Force Central Library Sindaebang Dong, Kwanak Gu, Seoul, Republic of Korea	1
11.	Library of Air Force Academy Chongwon Gun, Chung Cheong Buk Do, Republic of Korea	1
12.	Department of Mechanical Engineering Air Force Academy Chongwon Gun, Chung Cheong Buk Do, Republic of Korea	3
13.	Park, Ki Soon Department of Mechanical Engineering Naval Postgraduate School Monterey, CA 93943	1

14. Kang, Choong soon — 7
P.O. Box 17
Kang Nam Gu, Ban Po 2 Dong
Kang Nam Won, Hyo Sung Villa 5-201
Seoul, Republic of Korea

15. Kim, Jin Mock — 1
P.O. Box 18
Jinhae, Ki Kyei Chang
Jinhae City, Republic of Korea

16. Lee, Ki Gon — 1
Department of Mechanical Engineering
Naval Postgraduate School
Monterey, CA 93943